

ALMA MATER STUDIORUM · UNIVERSITY OF BOLOGNA

School of Science
Department of Physics and Astronomy
Master Degree in Physics

**QED-induced decoherence in the Quantum
Gravity induced Entanglement of Masses
(QGEM) experiment**

Supervisor:
Prof. Anupam Mazumdar

Submitted by:
Paolo Fragolino

Co-supervisor:
Prof. Roberto Casadio

Academic Year 2022/2023

Abstract

Contemporary research in physics focuses on unraveling the mysteries of quantum gravity, which has posed challenges due to the absence of empirical evidence. The question of whether gravity exhibits quantum behavior has ignited a debate. Traditional tests and cosmological observations have failed to provide definitive proof, prompting a shift towards laboratory investigations. The Quantum Gravity induced Entanglement of Masses (QGEM) proposal proposes a novel approach to detect the quantum nature of gravitational interactions through entanglement between test masses in matter-wave interferometers. This study demonstrates that observable entanglement can be generated between masses in a superposition state by using the quantum phase induced by gravitational interactions. By analyzing the linearized quantized version of Einstein's theory of gravity, the importance of off-diagonal terms in the coherent state basis of gravitational field modes for entanglement generation is identified. The proposal assumes that gravitational interaction is mediated by a quantum mechanical gravitational field. However, before the implementation of interferometry with nanoparticles becomes feasible, several experimental challenges must be addressed. These include the creation of spatial quantum superpositions, ensuring long coherence times, and mitigating external disturbances. The primary goal of this master's thesis is to investigate Quantum Electrodynamics (QED) decoherence in matter-wave interferometry with nanoparticles. This channel of decoherence is inevitable and must be considered even when dealing with neutral nanocrystals. Starting from the QED Lagrangian, we will derive the evolution of the density matrix and study the dipole-dipole interaction in both short and long wavelength limits. The derived formulas will then be applied to impose constraints on the crystal and environmental parameters within the QGEM protocol.

Contents

Introduction	1
1 Decoherence	8
1.1 Entanglement	8
1.2 Decoherence	10
1.3 Scattering Model	13
1.3.1 Short-wavelength limit	18
1.3.2 Long-wavelength limit	19
1.3.3 Comparing short and long-wavelength limit	20
1.4 Born-Markov Master Equation	21
2 Gravity-induced Entanglement and QGEM setup	29
2.1 Mechanism for quantum interactions to entangle matter	29
2.2 The case for gravitational interaction	34
2.3 QGEM Experiment	38
2.3.1 LOCC Theorem	39
2.3.2 QGEM Setup	40
3 Decoherence due to Electromagnetic interaction	45
3.1 Hamiltonian construction	46
3.2 Born-Markov Master Equation for QED interactions	49
3.3 Dipole-Dipole interaction	54
3.3.1 Short-wavelength limit approximation	57
3.3.2 Long-wavelength approximation	63
3.3.3 Applications to the QGEM experiment	65
3.4 Application to others QED interactions	70
3.4.1 Charge-charge interaction in the short wavelength limit	70
3.4.2 Charge-charge interaction in the long wavelength limit	72
3.4.3 Charge-dipole interaction in the short wavelength limit	74
3.4.4 Charge-dipole interaction in the long wavelength limit	76
3.5 Decoherence due to acceleration	79

3.5.1	Charged case	79
3.5.2	Dipole case	82
Conclusion		84
A Appendix		87
A.1	Differential cross section for a $2 \rightarrow 2$ process	87
A.2	Number density factor	89
A.3	Validity for the approximation of the $Ci(z)$ function	90

Introduction

In the last century, theoretical physicists have developed two fundamental theories of our universe: the first one is General Relativity (GR), created by Albert Einstein in 1915 [1]. General Relativity is a theory of space and time, which for the first time in the history of science were treated as *dynamical* entities subjected to their own equations of motion. In particular, the Einstein's field equation $R_{\mu\nu} + \frac{1}{2}g_{\mu\nu}R = \frac{8\pi G_N}{c^4}T_{\mu\nu}$ describes how space and time are bent in presence of a source, just like the Maxwell equations describe how the electromagnetic field changes in presence of electric charges and currents. In the gravitational case, the sources are represented by matter and energy, which curve the spacetime fabric around them.

The main lesson that scientists have learned from the General Theory of Relativity is that space and time are not absolute concepts physically isolated from the rest of the world: instead, the notions of length and time duration can change in different points of the universe, depending on the *local* content of matter and energy. In summary, GR treats space and time as a *single* and dynamical entity, while matter has *well defined* properties (like energy, position, momentum,...) and is considered to have only local effects on the spacetime structure.

The other theory is Quantum Mechanics (QM), which was first developed mainly in the '30s of the twentieth century by many different scientists, like Heisenberg, Bohr, De Broglie, Born, Dirac and others [2, 3]. Quantum mechanics describes the behavior of particles at the microscopic scale. It is a mathematical framework that allows us to understand and predict the properties and interactions of particles such as electrons, photons, and atoms. One of the key principles of quantum mechanics is wave-particle duality, which states that particles can exhibit both wave-like and particle-like behavior. This means that particles can exist in multiple states or positions simultaneously, known as superposition. The behavior of particles is described by wave functions, which are mathematical representations that capture the probabilities of different outcomes when measurements are made.

Quantum mechanics also introduces the concept of uncertainty, expressed through Heisenberg's uncertainty principle. This principle states that certain pairs of physical properties, such as position and momentum, cannot be precisely measured simultane-

ously. There is an inherent limit to the precision with which these properties can be known. Another intriguing aspect of quantum mechanics is entanglement. When particles become entangled, their states become correlated in such a way that the state of one particle is instantly connected to the state of another, regardless of the distance between them. Therefore, QM treats matter as *not* having sharply defined properties for the observables because of the superposition principle and the Heisenberg uncertainty principle, while entanglement tells us that physical systems can also have intrinsic *non-local* properties. Moreover, in such framework, space and time are treated *separately* and are absolute: they are *not* dynamical entities that in some way are influenced by their matter content and can be completely separate to all the other systems of the universe.

From this very brief analysis, it is clear how QM and GR are fundamentally different from each other. They both bring something completely new to our knowledge of the world if compared to classical mechanics, but their respective lessons are distinct at the foundations. In fact, GR tells us something completely new about space and time: they are a single and dynamical entity, besides being observer dependent. In more formal terms, GR is a *background independent* theory, where coordinates does not have any physical meaning; the only physically meaningful elements in the universe are *fields*, which can be described as to evolve not in terms of coordinates, but one in relation to each other and spacetime is a dynamical field itself [4].

Regarding matter, GR does not tell us anything particularly new: the only extra contribute on the concept of energy and matter comes from the famous mass-shell relation $E^2 = m^2c^4 + p^2c^2$, but it does not tell us anything *ontologically* different with respect to classical mechanics. In principle, for GR we could know the evolution of the entire universe given the initial conditions, particle by particle, and each piece of matter would have well defined physical properties with their own ontological value.

On the other hand, QM gives us something completely unexpected about matter: we cannot know at the same time all the value for all the physical observables of some system, but only their probability. It does not make sense to talk about trajectories anymore and the concept of reality itself struggles to explain all the quantum phenomena: particles can be created or destroyed [5] and non-local effects arise [6]. The ontology of the theory is not clear anymore, we don't know if the wavefunction represents a real physical variable of the system or simply encodes the observer's ignorance about the world [7].

Regarding space and time, instead, QM does not give us extra information compared to classical mechanics: space and time are absolute entities inside which matter evolves according to their own equations of motion, which are completely separate from the dynamics of space and time. Quantum Field Theory (QFT) is a useful framework through which one can relate the concept of quantum particles with spacetime symmetries [5], but QFT is still a background *dependent* theory. In particular, the concept of particle strictly depends on the Poincaré symmetries of Minkowski spacetime and as soon as one tries to generalize such concept to curved spacetimes through new definition of creation

and destruction operators it is impossible to define unambiguously what a particle actually is [8].

It should be clear at this point where is the main struggle of contemporary theoretical physics: we have two fundamental theories of the universe, both revolutionary in their own respective fields but deeply disconnected at the foundations. The need for a unification is self evident. Such a unification is important both from a theoretical and conceptual point of view for the reasons just exposed and from a more practical point of view: in fact, in theoretical physics there is the concrete need sometimes to analyze situations where both QM and GR are needed, such as Black Holes [9] and high energy density regions of the universe [10].

Starting from the '70s, many different theories have been proposed that try to unify QM and GR. One important theory is Loop Quantum Gravity (LQG) [4], which is based on the canonical quantization of general relativity. According to LQG, spacetime is quantized and described by interconnected loops, representing the fundamental building blocks of space. The goal is to obtain a quantum description of gravity at a fundamental level. Another prominent theory is String Theory[11], which postulates that elementary particles are not point-like but are instead tiny vibrating strings. These strings exist in a higher-dimensional spacetime, and the different vibrational patterns give rise to various particles and their interactions. String Theory attempts to reconcile gravity with the other fundamental forces in a unified framework. Causal Set Theory [12] proposes that spacetime is fundamentally discrete and constructed from discrete causal relations. It suggests that the geometry of spacetime arises from the relationships between events, and it aims to provide a discrete and causal foundation for quantum gravity. Emergent Gravity [13] is an alternative approach that suggests gravity may emerge as an effective description of a more fundamental theory. It explores the idea that spacetime and gravity could arise from the collective behavior of quantum degrees of freedom, potentially shedding light on the quantum nature of gravity. These are just a few examples of the diverse theories and approaches to quantum gravity that have been proposed.

Besides all the beautiful theoretical developments made by some of the proposal listed above, none of them has for the moment succeeded in giving concrete predictions on new physical phenomena that can be actually observed. Either the predictions are not clear or they are simply impossible to verify in real experiment, at least in a not so far future. This means that the physics community is still very far from communicating to the world an actual revolutionary discovery on our universe. We cannot claim yet that particles are made of strings, that spacetime is discrete at the fundamental level or that we know what happens inside a black hole. But behind all these (purely) theoretical predictions and speculations lies the most fundamental questions of all in quantum gravity: is gravity actually quantum? Can gravity truly be quantized? How do we know if a field is

quantum? How can we *prove* this basic yet fundamental assumption of all the quantum theories of gravity proposed so far?

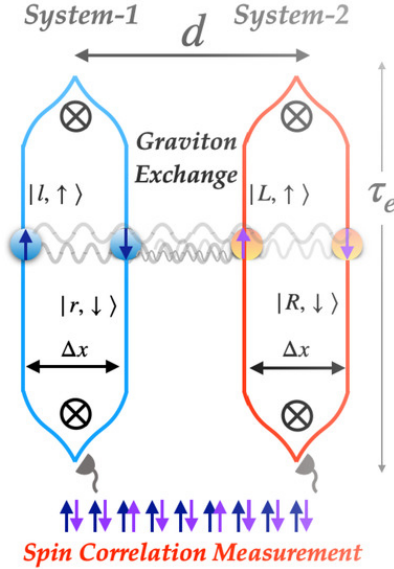


Figure 1: Schematic representation of the QGEM proposal

In 2017 two very similar proposals [14, 15] were officially presented. In these works, the main goal was to create the theoretical and experimental foundations for a tabletop experiment that could prove the quantum nature of the gravitational field. The key scheme is the following: two massive particles are posed in spatial superposition, one next to each other and it is supposed that they can interact exclusively via gravitational interaction. After a sufficient interaction time during which both the masses are kept in spatial superposition, they are brought back together (for example by a reversed Stern-Gerlach apparatus) and measurement are made on each of them. What should be the final result? How is the final quantum state modified after the interaction?

Observe figure 1: we can notice how the right branch R_1 of the system-1 is very close to the left L_2 branch of system-2; this means that the interaction between these two branches is the stronger one compared to all the other branch's pair. Now, what happens when a massive particle feels a gravitational field? General relativity tells us that gravity basically slows the time down as it is perceived some point far from the source. The stronger the gravitational field, the bigger will be the effect on the clocks around the massive object. This means in our case that, if we compute the quantum time evolution of the system-1 when the massive particle is in the right branch R_1 , the time will pass slower compared to the branch L_1 , because of the presence of the other massive object in L_2 . Therefore, the quantum time evolution dictated by the Hamiltonian H_0 of the system-1 will be different in L_1 and R_1 . What is the consequence of such effect? In

terms of equations, as will be shown in Section (2.3.2), the state of the composite system of the two massive particles will be:

$$\begin{aligned} |\Psi_0\rangle &= \frac{1}{2} \left(|L_1\rangle + |R_1\rangle \right) \otimes \left(|L_2\rangle + |R_2\rangle \right) \longrightarrow \\ \longrightarrow |\Psi(\tau)\rangle &= \frac{e^{\frac{i}{\hbar}H_0\tau}}{2} \left(|L_1\rangle |L_2\rangle + |R_1\rangle |R_2\rangle + |L_1\rangle |R_2\rangle + e^{\frac{i}{\hbar}H_0(\tau'-\tau)} |R_1\rangle |L_2\rangle \right), \end{aligned} \quad (1)$$

where τ represents the total time in which the particles are kept in superposition as perceived in absence of gravitational field (we suppose that the interactions of the branches outside of $|R_1\rangle |L_2\rangle$ are negligible given the spatial distance) and τ' is the same time as perceived by the branches $|R_1\rangle |L_2\rangle$ in which there is gravitational interaction. It is easy to recognize that the final state is an *entangled* state: its $|R_1\rangle |L_2\rangle$ component has in fact a different phase from the others, which means that at this point is *not* possible anymore to *separate* the states of the two subsystems 1 and 2.

This is a key feature of the proposals [14] and [15]: **quantum interaction generates entanglement**. The most important part of this very last statement is the very first word, **quantum**. In this case, Quantum Information Theory comes to help us: in fact, one of its fundamental principle is the so-called **LOCC principle**, which states that entanglement *cannot* be either generated or increased by *classical* communication channels. Only quantum channels of communication, i.e. quantum interactions, are able to create entanglement between two quantum systems. This leads to the most important contribution of such proposal: **Quantum Gravity induces Entanglement of Masses**. That is also the reason why this proposal is often called in the scientific community as **QGEM** experiment.

The importance of the QGEM proposal is self-evident: in fact, such an experiment should be able to gives us an answer on whether gravity is quantum or not. It is worth mentioning that, after the first publication on this work, a few other paper were published in which the interpretation of the results of the QGEM experiment were either criticized or discussed [16, 17]: what are the quantum degrees of freedom of gravity that are involved on the experiment? What aspect of gravity is actually witnessed? Is a model for linearized gravity enough to state that gravity is quantum? These and other questions are still at the center of some debates in the scientific community and it is beyond the purpose of this thesis trying to answer and discuss them. Nonetheless it is worth mentioning them in order to show how from the QGEM proposal can arise important contributions on more foundational aspects related to the quantization of gravity.

Until now, we have outlined the importance of the QGEM experiment and mentioned its main consequences. Let us now discuss about the main goal of this thesis.

In particular, already from the description of the QGEM setup given above, it is clear the importance of keeping the two massive particles in spatial superposition, in order to let them interact via gravitational interaction and measuring the entanglement phase that appears in Eq.(1). But in a real life experiment, it can happen that the massive particles interacts through other forces with the environment: for example, it can happen that inside the experimental box there are air molecules [18, 19] that scatter off the massive superposed particle or neutrinos can pass through the lab and interact with the experimental setup [20]. What are the effects of such random noise events on the experiment?

The general theory of quantum interaction between a quantum system and a large environment is called **decoherence** [18, 19]. Roughly speaking, decoherence studies how an open systems loses its coherence properties through the interaction with other external systems, i.e. how the quantum interference terms inside the wavefunction are lost. We will discuss about decoherence more in detail in Section 1.2. Therefore, decoherence leads to a change in the quantum state of the quantum system. In particular, as we will see below, the off-diagonal elements of the density matrix are suppressed in time by a factor $e^{-\Gamma t}$ and it is clear that for a sufficient long time $t \rightarrow +\infty$ they will be sent to 0. Remember that the off-diagonal terms of the density matrix encodes the quantum properties of the system: in fact, they contain the quantum interference term that distinguish a classical system from a quantum one. In this terms are also present entanglement information about the system, as it is already clear from Eq.(1), where the off-diagonal term $|R_1\rangle |L_2\rangle$ is multiplied a phase $e^{\frac{i}{\hbar}H_0(\tau'-\tau)}$, which contains all the information about the gravitational interaction.

It is therefore very important to keep trace of all the possible interaction of the superposed object with the environment. In this work we will analyze one particular type of source of decoherence: QED interactions. In fact, these types of interaction are inevitably present in a QGEM setup: the massive object posed in spatial superposition is a nano-crystal [14] and such material can either possesses a permanent dipole [21] or and induced one, because of its dielectric properties. In particular, in this last case, the crystal's dipole can be induced by an external electromagnetic field, which can be itself generated by an environmental dipole, such the one possessed by an air molecule [22]. Besides from dipole-dipole interactions, in the setup there can be also ion-dipole or Coulombian forces, which is very important to control during the realization of the experiment.

This master thesis is organized as follows: in Chapter 1 it will be presented a more detailed introduction on decoherence phenomena, together with the analysis of the Scattering Model for decoherence (section 1.3) and the Born-Markov Master Equation in section 1.4. In Chapter 2 it will be analyzed the general model for the generation of entanglement through gravitational interaction (sections 2.1 and 2.2), while an explicit and

more detailed presentation of the QGEM proposal will be given in section 2.3. The final and most important chapter of this work is Chapter 3, in which the QED decoherence effects are studied in detail. In particular, in sections 3.1 and 3.2 the general formalism useful for treating the QED-induced decoherence will be introduced and discussed. In section 3.3 the formalism will be applied to the case of a dipole-dipole potential, in which an application of the results to the QGEM setup is made. This section represents the main result of this work. Finally, in sections 3.4 and 3.5 the decoherence model used will be applied to other interactions and sources of QED-induced decoherence, such as the Coulomb potential and the radiation emitted by an accelerated particle.

Chapter 1

Decoherence

In this chapter we are going to analyze the key phenomenon analyzed in this work: decoherence. Quantum decoherence refers to the phenomenon in which a quantum system loses its coherence and exhibits classical-like behavior due to interactions with its environment. When a quantum system interacts with its surroundings, such as through collisions or electromagnetic radiation, it becomes entangled with the environment, leading to a loss of phase relationships and the decay of quantum superpositions. As a result, the system behaves in a classical manner, with definite and predictable properties. Decoherence is a significant challenge in quantum computation, quantum information processing, and maintaining the stability of quantum states. Various techniques and approaches, such as error correction codes and quantum error correction, are employed to mitigate the effects of decoherence and preserve quantum coherence.

We will start with a brief introduction about entanglement [1.1](#) and a general conceptual framework for decoherence [1.2](#), in order to get an intuitive idea about this phenomenon. In section [1.3](#) we will analyze the first of the two models for the decoherence used in this work, the so-called Scattering Model, while in section [1.4](#) we will derive the Born-Markov master equation for decoherence, the most fundamental model used in the literature [[18](#), [19](#)].

1.1 Entanglement

Let's for the moment shift our focus to quantum entanglement, which plays a pivotal role in the phenomenon known as decoherence. Firstly, let's establish a definition of entanglement. Imagine we have a quantum system S , characterized by a state vector $|\Psi\rangle$, consisting of two subsystems, S_1 and S_2 . The state vector $|\Psi\rangle$ of S is considered entangled concerning S_1 and S_2 when it cannot be expressed as a tensor product of the state vectors of these two subsystems. In other words, there are no state vectors $|\Psi_1\rangle$ of S_1 and $|\Psi_2\rangle$ of S_2 that satisfy the equation $|\Psi\rangle = |\Psi_1\rangle \otimes |\Psi_2\rangle$.

More in detail, we can associate to the total system S an Hilbert space \mathcal{H} constituted by all the vector states $|\Psi\rangle$ associated to the total composite system. This space can be decomposed in the tensorial product of the Hilbert spaces of the two subsystems S_1 and S_2 , i.e. it can be written as $\mathcal{H} = \mathcal{H}_1 \otimes \mathcal{H}_2$. In particular, let us define a basis on \mathcal{H}_1 as $\{|i\rangle_1\}$ and a basis on \mathcal{H}_2 as $\{|j\rangle_2\}$. This allows us to write a generic vector in \mathcal{H} as:

$$|\Psi\rangle = \sum_{i,j} c_{ij} |i\rangle_1 \otimes |j\rangle_2 \equiv \sum_{i,j} c_{ij} |i\rangle_1 |j\rangle_2, \quad (1.1)$$

where in the very last line the tensorial product symbol " \otimes " has been omitted, which is the notation that will be used from now on.

This expression can be rearranged by defining new vectors on \mathcal{H}_2 ; in particular, using the fact that $\{|j\rangle_2\}$ is a basis, we define $|\tilde{i}\rangle_2 \equiv \sum_j c_{ij} |j\rangle_2$. In this way, $|\Psi\rangle$ becomes:

$$|\Psi\rangle = \sum_i |i\rangle_1 |\tilde{i}\rangle_2. \quad (1.2)$$

Let us now define the matrix element for the system S as $\hat{\rho} \equiv |\Psi\rangle \langle \Psi|$. From this operator, we can obtain the matrix element of the subsystem S_1 by simply tracing out the subsystem S_2 :

$$\hat{\rho}_1 = Tr_2 [|\Psi\rangle \langle \Psi|] = Tr_2 \left[\sum_{i,k} |i\rangle_1 |\tilde{i}\rangle_2 \langle k|_1 \langle \tilde{k}|_2 \right] = \sum_{i,k} |i\rangle_1 \langle k|_1 \sum_{\beta} \langle \beta|\tilde{i}\rangle_2 \langle \tilde{k}|\beta\rangle_2, \quad (1.3)$$

where $\{|\beta\rangle_2\}$ is another generic basis of \mathcal{H}_2 .

One of the properties of the matrix element associated to a system is that it is hermitian, i.e. $\hat{\rho}_1^\dagger = \hat{\rho}_1$. This means that $\hat{\rho}_1$ admits an orthonormal basis in which it is diagonalized. If, in our case, this orthonormal basis is exactly $\{|i\rangle_1\}$, this means that $\hat{\rho}_1$ can be decomposed as:

$$\hat{\rho}_1 = \sum_i \lambda_i |i\rangle_1 \langle k|_1. \quad (1.4)$$

Comparing 1.3 and 1.4, we obtain the following condition:

$$\sum_{\beta} \langle \beta|\tilde{i}\rangle_2 \langle \tilde{k}|\beta\rangle_2 = \sum_{\beta} \langle \tilde{k}|\beta\rangle_2 \langle \beta|\tilde{i}\rangle_2 = \langle \tilde{k}|\tilde{i}\rangle_2 = \delta_{i,k} \lambda_i. \quad (1.5)$$

This relation allows us to redefine the vectors $|\tilde{i}\rangle_2$ as $|i'\rangle_2 \equiv \frac{1}{\sqrt{\lambda_i}} |\tilde{i}\rangle_2$. In this way, we can rewrite 1.2 as:

$$|\Psi\rangle = \sum_i \sqrt{\lambda_i} |i\rangle_1 |i'\rangle_2, \quad (1.6)$$

which is the so called **Schmidt decomposition**.

One of the main properties of this decomposition is that it is the one with the smallest number of terms. This means that the state $|\Psi\rangle$ is separable iff $\lambda_i = \delta_{i,k}$, i.e. if the number N of non-null eigenvalues of $\hat{\rho}_1$ is $N = 1$. In the opposite case, if $N > 1$, then the state is said to be entangled.

1.2 Decoherence

After the introduction of the concept of entanglement, we can start to talk about decoherence.

Quantum decoherence is a fundamental phenomenon in quantum mechanics that describes the loss of coherence and the weakening of interference effects between quantum states due to the interaction of the system with its surrounding environment.

In quantum mechanics, the states of systems are described by wave functions that can exist in a superposition of different states. This means that a system can be in a "quantum superposition" state, where it can simultaneously be in multiple distinct states until a measurement is performed, collapsing it into a specific state. During this phase, the system undergoes interactions with particles and external forces present in its environment.

Quantum decoherence occurs when these interactions with the environment cause a loss of correlation and coherence between the quantum states of the system. This results in a reduction or disappearance of interference effects, leading the system to behave more and more like a classical system. In other words, decoherence drives the transition of the quantum system towards a state of "statistical mixtures" rather than a state of superposition.

The process of decoherence can be caused by various factors, such as the system's interaction with environmental particles (such as photons, atoms, or molecules), radioactive decay, thermal effects, and other scattering processes. These interactions cause a reduction in entanglement between the particles of the system, leading to a rapid loss of quantum coherence.

In order to talk about decoherence it is useful to start from the **Von Neumann Scheme for Ideal Quantum Measurement**. Let's study more in detail the act of measurement of a system S through an apparatus A . This scheme treats the apparatus as a quantum object too, independently of the fact that it is considered to be a macroscopic object or not. This means that, in this case, the act of observation is purely quantum mechanical, not classical. This is the main difference between this scheme and the Copenhagen interpretation, where the apparatus of observation (and the observer too) is treated classically.

This means that we can associate an Hilbert space to both S and A , i.e. \mathcal{H}_S and \mathcal{H}_A respectively. In general, we can treat the composite system " $S + A$ " as an *isolated*

quantum system, with Hilbert space $\mathcal{H} = \mathcal{H}_S \otimes \mathcal{H}_A$. The act of measurement is then seen as an **interaction** between the two quantum subsystems S and A , so S cannot be considered as an *isolated* quantum system. This interaction is supposed to be *ideal*, which means that the action of the apparatus A on S does not modify the quantum state $|s\rangle$ of the system, i.e. the act of measurement does not disturb drastically the system. What actually happens is the opposite, i.e. the interaction between S and A changes the state of A . Let us consider, for example, our system S to be a particle in superposition $|s\rangle = \frac{1}{\sqrt{2}}(|x_1\rangle + |x_2\rangle)$ of positions (e.g. either left or right). In this case, let us consider the apparatus to have a pointer that indicates if the particle has been registered to pass either left or right. Before the measurement, the pointer is in a neutral position, which we will call $|ready\rangle$. After the interaction with the particle, the pointer will be either left or right and the quantum state associate to A will be either $|L\rangle$ or $|R\rangle$. Let us consider now the composite system $S + A$. Before the measurement, the state will be given by $|s\rangle|ready\rangle$, which is a separable state. After the interaction, we cannot determine the quantum state of the apparatus, which depends on the result of the measurement. The final result will thus give:

$$|s\rangle|ready\rangle \longrightarrow \frac{1}{\sqrt{2}}(|x_1\rangle|L\rangle + |x_2\rangle|R\rangle). \quad (1.7)$$

This means that the final state of $S + A$ is an *entangled* state, is not separable anymore. The entanglement has been induced **dynamically**, through the interaction between the particle and the apparatus.

But what is the main consequence of this entanglement? The main point of the concept of entanglement is that the two entangled systems are not independent anymore; in particular, the information of one of the subsystems is now shared with the other one and strongly depends on it. The information of one system is "spread" all over the other systems that it interacted with. This means that, in order to extrapolate information from a system is not sufficient anymore to perform measurements on the system *alone*, but in order to gain a complete knowledge of it we have to consider also the other systems that it is entangled with.

Let's understand better this concept from a mathematical point of view. In order to do that, we will now consider the famous **Double Slit Experiment**, where a quantum particle has to go through a wall with two holes in it. We will first consider the case where the detection of the particle happens far from the holes, i.e. on a screen positioned far from the wall. It is known that it will be registered an interference figure on the screen: in fact, the particle is now in a spatial superposition $|\Psi\rangle = |x_1\rangle + |x_2\rangle$, x_1 and x_2 being the positions of the two holes. This means that the probability to find the particle on the screen is described by the modulus squared of its wave function $\Psi(x) = \langle x|\Psi\rangle$:

$$|\Psi(x)|^2 = |\Psi_1(x)|^2 + |\Psi_2(x)|^2 + 2 \cdot Re \{ \Psi_1(x)\Psi_2^*(x) \}. \quad (1.8)$$

It is exactly the last term that encodes the quantum properties of the particle, i.e. the interference term. In the absence of this term we come back to a classical case, where we randomly shot a classical particle through a wall, without knowing exactly what holes it passed; we can only know its probability to pass each wall, given by $|\Psi_i(x)|^2$. From classical probability theory, we thus know that the particle will pass *either* the first *or* the second hole, meaning that we simply have to sum the single probabilities:

$$|\Psi(x)|^2 = |\Psi_1(x)|^2 + |\Psi_2(x)|^2. \quad (1.9)$$

So, without the interference term, we just have a classical mixture and we lost the quantum behaviour of the system.

Let's analyze the same setup but with a different type of measurement. In fact, we will now consider the presence of an apparatus immediately after the two holes, in order to know which of the two possible paths the particle takes before it is registered on the screen. It is already known that, in this case, we will not register an interference pattern anymore.

Let us thus consider this case with using the Von Neumann's scheme. If the states associated to the apparatus are $|L\rangle$ and $|R\rangle$ as before, after the particle's passage of the wall the state of the composite system $S + A$ will be given by $|\Psi\rangle_{tot} = |x_1\rangle |L\rangle + |x_2\rangle |R\rangle$. Thus, its matrix density will be given by:

$$\hat{\rho} = |x_1\rangle \langle x_1| \otimes |L\rangle \langle L| + |x_2\rangle \langle x_2| \otimes |R\rangle \langle R| + |x_1\rangle \langle x_2| \otimes |L\rangle \langle R| + |x_2\rangle \langle x_1| \otimes |R\rangle \langle L|. \quad (1.10)$$

Tracing out the apparatus's basis, we obtain the matrix element for the particle:

$$\rho_{part}(x) \equiv \langle x | \hat{\rho}_{part} | x \rangle = |\Psi_1(x)|^2 + |\Psi_2(x)|^2 + 2 \cdot Re \{ \Psi_1(x) \Psi_2^*(x) \cdot \langle L | R \rangle \}. \quad (1.11)$$

From this equation it is clear that the interference term, which encodes the quantum properties of our system, depends on the scalar product of the apparatus's states $\langle L | R \rangle$. What is the meaning of this result? Equation 1.11 is telling us that, if the states $|L\rangle$ and $|R\rangle$ are completely orthogonal, there is no interference term anymore; otherwise, if for example $|L\rangle$ and $|R\rangle$ are the same state (i.e. if $\langle L | R \rangle = 1$), the full quantum behaviour of the particle is preserved. That is because, when two states are mutually orthogonal, they do not share any type of properties of the apparatus, they are completely distinguishable states. This means that, after the system-apparatus interaction, the two states $|L\rangle$ and $|R\rangle$ carry two completely different types of information about the particle. This means that all the knowable properties of the system are completely spread in the apparatus, i.e. each component of the apparatus carries a different knowledge of the system. In the case where $|L\rangle$ and $|R\rangle$ are instead indistinguishable, they share the same type of information about the particle. In this case, each component of the apparatus gains

the same type of knowledge about the system. This behaviour does not cause any loss of coherence in the system, because now its state is completely independent on the apparatus's state, i.e. they are completely separable.

It is clear now how the distinguishability of the apparatus's states, i.e. their scalar product $\langle L|R \rangle = 1$, encodes the decoherence effect to which the system is subjected. Another important characteristic of this scalar product is that it allows a *continuous* transition from a quantum mechanical behaviour to a classical one. In particular, if $\langle L|R \rangle \in (0, 1)$, it is possible to have cases where we can acquire knowledge on the system without destroying completely its quantum interference patterns.

1.3 Scattering Model

We are going now to analyze the first model of decoherence of this elaborate [18]. In this model we are going to consider the effect that a generic environment has on a quantum system, using standard quantum scattering theory.

The first hypothesis that we make is that, before any interaction, the system and the environment are completely separable. This means that, if $\hat{\rho}_S(t)$ is the matrix element associated to our quantum system and $\hat{\rho}_E(t)$ is the one associated to the environment, the density matrix of the composite system $S + E$ is given by:

$$\hat{\rho}(0) = \hat{\rho}_S(0) \otimes \hat{\rho}_E(0), \quad (1.12)$$

where we have set $t = 0$ as the starting time of interaction.

The situation that we are going to analyze is the following: imagine having a quantum particle (i.e. our system S) at some point \vec{x} in space; we can associate to it a quantum state $|\vec{x}\rangle$ encoding information about the particle's position in space. This system is embedded in an environment composed of a large (i.e. $N \gg 1$) number of particles that interact with S through a generic type of interaction. This very simple model represents many physical situation that happen in a laboratory, like for example an atom (our S) surrounded by a thermal bath of photons (our E). We can associate to each one of our environmental particles a quantum vector $|\chi\rangle$ representing a generic state, like its energy, momentum, position, etc.

Let us focus on just one of the environmental particles that scatters of S . For the Von Neumann scheme, we will have the following situation before and after the interaction:

$$|\vec{x}\rangle |\chi_i\rangle \longrightarrow |\vec{x}\rangle |\chi(\vec{x})\rangle, \quad (1.13)$$

where $|\chi_i\rangle$ represents the *initial* state of the environmental particle and $|\chi(\vec{x})\rangle$ its state *after* the scattering. In considering the Von Neumann scheme we are implicitly assuming that the environment does not influence the system's state. This means that this model is suitable in physical situations where, for example, S is much heavier than the

environmental particles or where the environmental particles are not energetic enough. We can thus represent this interaction process as the action of the \hat{S} matrix on the initial state, i.e. $|\vec{x}\rangle |\chi_i\rangle \longrightarrow \hat{S} |\vec{x}\rangle |\chi_i\rangle$. Because of the ideal measurement assumption of the Von Neumann scheme, the scattering matrix \hat{S} does not act on the system's state $|\vec{x}\rangle$. We can rewrite the action of the \hat{S} matrix in the following way:

$$\hat{S} |\vec{x}\rangle |\chi_i\rangle = \hat{S} |\vec{x}\rangle e^{-\frac{i}{\hbar} \hat{q} \cdot \vec{x}} e^{\frac{i}{\hbar} \hat{q} \cdot \vec{x}} |\chi_i\rangle = \hat{S} e^{-\frac{i}{\hbar} (\hat{q} + \hat{p}) \cdot \vec{x}} |\vec{0}\rangle e^{\frac{i}{\hbar} \hat{q} \cdot \vec{x}} |\chi_i\rangle, \quad (1.14)$$

where \hat{q} is the momentum operator of the environment, \hat{p} is the one related to the system S and $\hat{P} = \hat{q} + \hat{p}$ is the momentum of the composite system $S + \mathcal{E}$. We can now make another assumption: we can consider the scattering interaction to be invariant under spatial translations of the composite system generated by \hat{P} , i.e. $[\hat{P}, \hat{S}] = 0$. In this way, Eq.(1.14) becomes:

$$\hat{S} |\vec{x}\rangle |\chi_i\rangle = e^{-\frac{i}{\hbar} (\hat{q} + \hat{p}) \cdot \vec{x}} |\vec{0}\rangle \hat{S} e^{\frac{i}{\hbar} \hat{q} \cdot \vec{x}} |\chi_i\rangle = e^{-\frac{i}{\hbar} \hat{p} \cdot \vec{x}} |\vec{0}\rangle e^{-\frac{i}{\hbar} \hat{q} \cdot \vec{x}} \hat{S} e^{\frac{i}{\hbar} \hat{q} \cdot \vec{x}} |\chi_i\rangle = |\vec{x}\rangle \hat{S}_{\vec{x}} |\chi_i\rangle, \quad (1.15)$$

where in the very last line we have defined the spatial shifted scattering operator $\hat{S}_{\vec{x}} \equiv e^{-\frac{i}{\hbar} \hat{q} \cdot \vec{x}} \hat{S} e^{\frac{i}{\hbar} \hat{q} \cdot \vec{x}}$. This means that the relation between the initial and the final environmental particle's state is $\hat{S}_{\vec{x}} |\chi_i\rangle = |\chi(\vec{x})\rangle$. Let us now expand the matrix element of the $S + \mathcal{E}$ system in terms of the S basis $\{|\vec{x}\rangle\}$ and the environment one $\{|\chi\rangle\}$:

$$\hat{\rho}(0) = \int d\vec{x} d\vec{x}' \rho(\vec{x}, \vec{x}', 0) \cdot |\vec{x}\rangle \langle \vec{x}'| \otimes |\chi_i\rangle \langle \chi_i|. \quad (1.16)$$

Equation 1.16 represents the density matrix at $t = 0$. After the interaction, it becomes:

$$\hat{\rho} = \int d\vec{x} d\vec{x}' \rho(\vec{x}, \vec{x}', 0) \cdot |\vec{x}\rangle \langle \vec{x}'| \otimes |\chi(\vec{x})\rangle \langle \chi(\vec{x}')|. \quad (1.17)$$

Tracing out the $\{|\chi\rangle\}$ basis, we can obtain the density matrix for our system S :

$$\begin{aligned} \hat{\rho}_S &= \int d\vec{x} d\vec{x}' \rho(\vec{x}, \vec{x}', 0) \cdot |\vec{x}\rangle \langle \vec{x}'| \int d\vec{x}'' \langle \chi(\vec{x}'') | (|\chi(\vec{x})\rangle \langle \chi(\vec{x}')|) | \chi(\vec{x}'') \rangle \\ &= \int d\vec{x} d\vec{x}' \rho(\vec{x}, \vec{x}', 0) \cdot |\vec{x}\rangle \langle \vec{x}'| \langle \chi(\vec{x}') | \chi(\vec{x}) \rangle. \end{aligned} \quad (1.18)$$

From this equation, it is clear how any modifications in the density matrix of the system is fully encoded in the scalar product $\langle \chi(\vec{x}') | \chi(\vec{x}) \rangle$. Let's thus try to compute explicitly this scalar product:

$$\langle \chi(\vec{x}') | \chi(\vec{x}) \rangle = \langle \chi_i | \hat{S}_{\vec{x}'}^\dagger \hat{S}_{\vec{x}} | \chi_i \rangle = Tr_{\mathcal{E}} [\hat{\rho}_{\mathcal{E}}(0) \hat{S}_{\vec{x}'} \hat{S}_{\vec{x}}]. \quad (1.19)$$

We can now consider the environment to be a quantum ensemble:

$$\hat{\rho}_\varepsilon(0) = \int d\vec{q} \mu(\vec{q}) |\vec{q}\rangle \langle \vec{q}|, \quad (1.20)$$

where $\mu(\vec{q})$ represents the particle distribution in momentum space and the $|\vec{q}\rangle$ states form a complete basis $\mathbb{I} = \frac{(2\pi\hbar)^3}{V} \int d\vec{q} |\vec{q}\rangle \langle \vec{q}|$ normalized over the physical volume V . Plugging now Eq.(1.20) in Eq.(1.19) we obtain:

$$\begin{aligned} \int d\vec{q} \mu(\vec{q}) \langle \vec{q}| \hat{S}_x^\dagger \hat{S}_x |\vec{q}\rangle &= \int d\vec{q} \mu(\vec{q}) \langle \vec{q}| e^{-\frac{i}{\hbar} \hat{q} \cdot \vec{x}'} \hat{S}^\dagger e^{-\frac{i}{\hbar} \hat{q} \cdot (\vec{x} - \vec{x}')} \hat{S} e^{\frac{i}{\hbar} \hat{q} \cdot \vec{x}} |\vec{q}\rangle \\ &= \int d\vec{q} \mu(\vec{q}) e^{\frac{i}{\hbar} \hat{q} \cdot (\vec{x} - \vec{x}')} \langle \vec{q}| (\mathbb{I} - i\hat{T}^\dagger) e^{-\frac{i}{\hbar} \hat{q} \cdot (\vec{x} - \vec{x}')} (\mathbb{I} + i\hat{T}) |\vec{q}\rangle \\ &= \int d\vec{q} \mu(\vec{q}) \left[1 - \langle \vec{q}| \hat{T} \hat{T}^\dagger |\vec{q}\rangle + e^{\frac{i}{\hbar} \hat{q} \cdot (\vec{x} - \vec{x}')} \langle \vec{q}| \hat{T}^\dagger e^{-\frac{i}{\hbar} \hat{q} \cdot (\vec{x} - \vec{x}')} \hat{T} |\vec{q}\rangle \right], \end{aligned} \quad (1.21)$$

where we have used the expansion of the scattering matrix in terms of the T matrix $\hat{S} = \mathbb{I} + i\hat{T}$ and the fact that, from the unitarity of \hat{S} (i.e. $\hat{S}^\dagger \hat{S} = \mathbb{I}$), the following relation for \hat{T} holds: $\hat{T} \hat{T}^\dagger + i(\hat{T} - \hat{T}^\dagger) = 0$.

We can now rearrange Eq.(1.21) by inserting $\mathbb{I} = \frac{(2\pi\hbar)^3}{V} \int d\vec{q}' |\vec{q}'\rangle \langle \vec{q}'|$ inside the last two terms, i.e.:

$$\begin{aligned} &\int d\vec{q} \mu(\vec{q}) \left[1 - \frac{(2\pi\hbar)^3}{V} \int d\vec{q}' \left(\langle \vec{q}| \hat{T} |\vec{q}'\rangle \langle \vec{q}'| \hat{T}^\dagger |\vec{q}\rangle \right. \right. \\ &\quad \left. \left. + e^{\frac{i}{\hbar} \hat{q} \cdot (\vec{x} - \vec{x}')} \langle \vec{q}| \hat{T}^\dagger e^{-\frac{i}{\hbar} \hat{q} \cdot \vec{x}} |\vec{q}'\rangle \langle \vec{q}'| e^{\frac{i}{\hbar} \hat{q} \cdot \vec{x}'} \hat{T} |\vec{q}\rangle \right) \right] \\ &= \int d\vec{q} \mu(\vec{q}) \left[1 - \frac{(2\pi\hbar)^3}{V} \int d\vec{q}' |\langle \vec{q}| \hat{T} |\vec{q}'\rangle|^2 \cdot \left(1 - e^{\frac{i}{\hbar} (\vec{q} - \vec{q}') \cdot (\vec{x} - \vec{x}')} \right) \right], \end{aligned} \quad (1.22)$$

where in the very last line we have used the trivial relation $e^{-\frac{i}{\hbar} \hat{q} \cdot \vec{x}} |\vec{q}'\rangle = e^{-\frac{i}{\hbar} \vec{q}' \cdot \vec{x}} |\vec{q}'\rangle$. Using the fact that $\int d\vec{q} \mu(\vec{q}) = 1$ for a normalized momentum distribution density, we have that the difference between the density matrix before and after the scattering process is:

$$\begin{aligned} &\rho_S(\vec{x}, \vec{x}', 0) \langle \chi(\vec{x}') | \chi(\vec{x}) \rangle - \rho_S(\vec{x}, \vec{x}', 0) = \\ &= -\rho_S(\vec{x}, \vec{x}', 0) \int d\vec{q} \mu(\vec{q}) \frac{(2\pi\hbar)^3}{V} \int d\vec{q}' |\langle \vec{q}| \hat{T} |\vec{q}'\rangle|^2 \cdot \left(1 - e^{\frac{i}{\hbar} (\vec{q} - \vec{q}') \cdot (\vec{x} - \vec{x}')} \right), \end{aligned} \quad (1.23)$$

Let us now expand the $\langle \vec{q}| \hat{T} |\vec{q}'\rangle$ term. It is usually expressed as:

$$\langle \vec{q}| \hat{T} |\vec{q}'\rangle = \frac{i}{2\pi\hbar m} \delta(E - E') f(\vec{q}, \vec{q}'), \quad (1.24)$$

where $f(\vec{q}, \vec{q}')$ is related to the differential cross section, i.e. $|f(\vec{q}, \vec{q}')|^2 = \frac{d\sigma}{d\Omega}$, while E and E' indicate the environmental particle's energy before and after the scattering process (this means also that $\delta(E - E')$ takes into account the energy conservation during the process).

If we now consider the $|\langle \vec{q} | \hat{T} | \vec{q}' \rangle|^2$ term, we have to face the problem of defining the action of a squared of a Dirac's delta $\delta^2(E - E')$. This can be done by considering the Fourier expansion of the Dirac's delta:

$$\delta^2(E - E') = \delta(E - E') \lim_{T \rightarrow +\infty} \frac{1}{2\pi\hbar} \int_{-T/2}^{T/2} dt e^{\frac{i}{\hbar}(E-E')t} = \delta(E - E') \lim_{T \rightarrow +\infty} \frac{T}{2\pi\hbar}, \quad (1.25)$$

where in the very last line we have set $E = E'$ inside the exponential phase because of the presence of the other Dirac's delta outside the integral. If now the time T appearing in 1.25 is much bigger then the time elapsed during the scattering process, we can simply write $\delta^2(E - E') = \delta(E - E') \frac{T}{2\pi\hbar} = \delta(q - q') \frac{dq}{dE} \frac{T}{2\pi\hbar} = \delta(q - q') \frac{m}{q} \frac{T}{2\pi\hbar}$, with $q \equiv |\vec{q}|$ and $E = \frac{q^2}{2m}$.

Thus, substituting this expression for $\delta^2(E - E')$ inside $|\langle \vec{q} | \hat{T} | \vec{q}' \rangle|^2$, Eq.(1.23) becomes:

$$\begin{aligned} \rho_S(\vec{x}, \vec{x}', 0) \langle \chi(\vec{x}') | \chi(\vec{x}) \rangle - \rho_S(\vec{x}, \vec{x}', 0) &= -\rho_S(\vec{x}, \vec{x}', 0) \int d\vec{q} \mu(\vec{q}) \frac{(2\pi\hbar)^3}{V} \times \\ &\times \int d\Omega' dq q^2 \left(1 - e^{\frac{i}{\hbar}(\vec{q}-\vec{q}') \cdot (\vec{x}-\vec{x}')} \right) \frac{|f(\vec{q}, \vec{q}')|^2}{m^2(2\pi\hbar)^2} \delta(q - q') \frac{m}{q} \frac{T}{2\pi\hbar} = \\ &= -\rho_S(\vec{x}, \vec{x}', 0) \frac{T}{V} \int d\vec{q} \mu(\vec{q}) \frac{q}{m} \int d\Omega' \left(1 - e^{\frac{i}{\hbar}(\vec{q}-q\vec{n}') \cdot (\vec{x}-\vec{x}')} \right) |f(\vec{q}, q\vec{n}')|^2. \end{aligned} \quad (1.26)$$

where now, because of $\delta(q - q')$, $|\vec{q}'| = |\vec{q}|$ and \vec{n}' is a unitary vector that specifies the direction of the environmental particle *after* the interaction. This means that we are considering a physical situation in which the scattered environmental particle has initial momentum $\vec{q} = q\vec{n}$ and final one like $\vec{q}' = q\vec{n}'$, i.e. same modulus but different direction.

We can also generalize the $\frac{q}{m}$ term inside 1.26 with a generic velocity function $\frac{q}{m} \rightarrow v(q)$ (e.g. for a massive classical particle we have $v(q) = \frac{q}{m}$, while for a photon we will have $v(q) = c$). This allows us to apply formula 1.26 to many different physical situations.

It is possible to go even further if we make the assumption that the environment is composed of particles that are *isotropically* distributed:

$$\mu(\vec{q}) = \frac{1}{4\pi} \frac{V}{N} \rho(q) dq d\Omega, \quad (1.27)$$

where $\int dq \rho(q) = \frac{N}{V}$, in order to have $\int d\vec{q} \mu(\vec{q}) = 1$. Eq.(1.26) will thus become:

$$\begin{aligned} & \rho_S(\vec{x}, \vec{x}', 0) \langle \chi(\vec{x}') | \chi(\vec{x}) \rangle - \rho_S(\vec{x}, \vec{x}', 0) = \\ & -\rho_S(\vec{x}, \vec{x}', 0) \frac{T}{N} \int dq \rho(q) v(q) \int \frac{d\Omega d\Omega'}{4\pi} \left(1 - e^{\frac{i}{\hbar}(\vec{q}-q \vec{n}') \cdot (\vec{x}-\vec{x}')} \right) |f(\vec{q}, q \vec{n}')|^2. \end{aligned} \quad (1.28)$$

This formula represents the decoherence caused by only *one* scattering event. If we want to generalize it to the case with an environment of N particles, we have to multiply everything for N in order to take into account of the decoherence effect due to *all* the particles in the environment.

Finally, we can consider the differential form of Eq.(1.28) by dividing it for T and taking the infinitesimal limit $T \rightarrow 0$:

$$\frac{\rho_S(\vec{x}, \vec{x}', 0) \langle \chi(\vec{x}') | \chi(\vec{x}) \rangle - \rho_S(\vec{x}, \vec{x}', 0)}{T} \longrightarrow \frac{d\rho_S(\vec{x}, \vec{x}', t)}{dt}, \quad (1.29)$$

which, from Eq.(1.28), leads to:

$$\begin{aligned} \frac{d\rho_S(\vec{x}, \vec{x}', t)}{dt} &= -\rho_S(\vec{x}, \vec{x}', t) \int dq \rho(q) v(q) \\ &\times \int \frac{d\Omega d\Omega'}{4\pi} \left(1 - e^{\frac{i}{\hbar}(\vec{q}-q \vec{n}') \cdot (\vec{x}-\vec{x}')} \right) |f(\vec{q}, q \vec{n}')|^2. \end{aligned} \quad (1.30)$$

Eq.(1.30) is the final equation for the decoherence rate of the Scattering Model. It will be used often in the next chapters. In particular, Eq.(1.30) has the following structure:

$$\frac{d\rho_S(\vec{x}, \vec{x}', t)}{dt} = -\rho_S(\vec{x}, \vec{x}', t) F(\vec{x} - \vec{x}'), \quad (1.31)$$

which can be solved integrating in the time variable t :

$$\rho_S(\vec{x}, \vec{x}', t) = \rho_S(\vec{x}, \vec{x}', 0) e^{-F(\vec{x}-\vec{x}')t}. \quad (1.32)$$

This formula shows the role played by the function $F(\vec{x} - \vec{x}')$: it suppresses the off diagonal density matrix elements. In fact, for the elements on the diagonal, we have that $\vec{x} = \vec{x}'$; this means that the element $\left(1 - e^{\frac{i}{\hbar}(\vec{q}-q \vec{n}') \cdot (\vec{x}-\vec{x}')} \right)$ inside the integral of Eq.(1.30) is 0, resulting in:

$$\frac{d\rho_S(\vec{x}, \vec{x}, t)}{dt} = 0 \longrightarrow \rho_S(\vec{x}, \vec{x}, t) = \text{const.} \quad (1.33)$$

This last equation shows that the diagonal elements of ρ_S are not influenced by the environmental interaction, they remain constant over time evolution.

Instead, the non diagonal elements are suppressed because of $F(\vec{x} - \vec{x}')$ and, in the limit $t \rightarrow +\infty$, they are completely suppressed, i.e. they become asymptotically 0. This means

that asymptotically the density matrix ρ_S will have a diagonal form, representing thus a mixture. This is a consequence that we have already discussed in the past section, where we have explained that, after the interaction, the information of the system is spread all over the environment.

1.3.1 Short-wavelength limit

We have seen in the previous section that it is possible to find a decoherence rate for the density matrix elements of a generic quantum system S , which is given by:

$$F(\vec{x} - \vec{x}') = \int dq \rho(q)v(q) \int \frac{d\Omega d\Omega'}{4\pi} \left(1 - e^{\frac{i}{\hbar}(\vec{q}-q \vec{n}') \cdot (\vec{x}-\vec{x}')} \right) |f(\vec{q}, q \vec{n}')|^2. \quad (1.34)$$

Presented in this form, Eq.(1.34) does not have any practical purposes. In particular, the second integral in the RHS can be very hard to compute, especially for the presence of the $\left(1 - e^{\frac{i}{\hbar}(\vec{q}-q \vec{n}') \cdot (\vec{x}-\vec{x}')} \right)$ factor. It is thus useful to start making some approximation which can be applied to many different physical situations.

In this subsection, we will explore the so-called **Short-wavelength limit**, while in the next one we will study the other extremal behaviour of Eq.(1.34), i.e. the so-called *long-wavelength* limit.

Let us start by analyzing the phase's argument in RHS:

$$\frac{i}{\hbar} (\vec{q} - q \vec{n}') \cdot (\vec{x} - \vec{x}') = \frac{i}{\hbar} q (\vec{n} - \vec{n}') \cdot \Delta\vec{x}, \quad (1.35)$$

where $\Delta\vec{x}$ can represent the spatial superposition size of the system S . In particular, we are interested in the product $\frac{q}{\hbar} |\Delta\vec{x}| \equiv \frac{q}{\hbar} \Delta x$.

We define the Short-wavelength limit through the following condition:

$$\lambda_{part} \ll \Delta x, \quad (1.36)$$

i.e. when the wavelength associated to the scattered environmental particle is much smaller than the superposition size of the quantum object S . The QGEM experiment exemplifies a scenario where this limit is upheld: in fact, as we will see in the next chapters, the QGEM setup allows the temperature to be of the order of $T \sim 1 \text{ K}$. If we now suppose that the environmental particles are in thermal equilibrium, their average energy will be $\bar{E} = k_B T$. This means that, considering these particles to have a mass $m \sim 10^{-27} \text{ kg}$ (as, for example, an Helium molecule), their resulting average momentum will be $\bar{p} = \sqrt{2mk_B T} \sim 10^{-25} \text{ kg} \frac{m}{s}$. The average wavelength associated to an environmental particle will be thus given by:

$$\lambda_{part} = \frac{2\pi\hbar}{\bar{p}} = \frac{2\pi\hbar}{\sqrt{2mk_B T}} \sim 4.7 \times 10^{-9} m. \quad (1.37)$$

Considering now that in the QGEM setup the superposition size of the crystal is of the order of $\Delta x \sim 10^{-5}m$, we have satisfied the short-wavelength limit condition, i.e. $\lambda_{part} \ll \Delta x$.

In this limit, we have that the phase given by Eq.(1.35) results to be much bigger than 1, i.e. $\frac{i}{\hbar}(\vec{q} - q \vec{n}') \cdot (\vec{x} - \vec{x}') \gg 1$. That is because $\lambda \sim \frac{\hbar}{q}$ and, if $\lambda \ll \Delta x$, then $\frac{q}{\hbar} \gg \Delta x$. This means that the exponential $e^{\frac{i}{\hbar}(\vec{q} - q \vec{n}') \cdot (\vec{x} - \vec{x}')}$, when integrated over the all possible q 's (see Eq.(1.34)), oscillates very rapidly. Therefore, its contribution to the integral in Eq.(1.34) will be negligible compared to the one given by the 1 factor inside $(1 - e^{\frac{i}{\hbar}(\vec{q} - q \vec{n}') \cdot (\vec{x} - \vec{x}')})$.

This leads to the following form for the decoherence rate:

$$F_{short}(\vec{x} - \vec{x}') \equiv \Gamma = \int dq \rho(q)v(q) \int \frac{d\Omega d\Omega'}{4\pi} |f(\vec{q}, q \vec{n}')|^2. \quad (1.38)$$

Now, it is known in Quantum Scattering Theory, the function $|f(\vec{q}, q \vec{n}')|^2$ represents exactly the **differential cross section** $\frac{d\sigma}{d\Omega}$. Thus, when it is integrated over all the possible scattering angles $d\Omega$ and $d\Omega'$, it will give back the **total cross section** $\sigma_{tot}(p)$. The final result is:

$$\Gamma = \int dq \rho(q)v(q)\sigma_{tot}(q). \quad (1.39)$$

It is interesting to notice that Eq.(1.39) represents exactly the so-called *interaction rate*, a well known variable in Quantum scattering theory which gives the number of interactions (or decay) per second (its units are $[\Gamma] = \frac{1}{s} = Hz$). In fact, considering that $\rho(q)$ inside Eq.(1.39) is a probability distribution, Γ can be also rewritten as:

$$\Gamma = \langle v \sigma_{tot} \rangle_{\rho}, \quad (1.40)$$

which is the usual form in which the interaction rate is presented in scattering theory. This analysis thus shows the strong connection between the concepts of decoherence (or entanglement) and interactions. Such a connection will be analyzed in the next chapters (see 2).

1.3.2 Long-wavelength limit

Let us now study the opposite limit case of Eq.(1.34). In particular, we will consider the case where the wavelength associated to the environmental particle is much bigger than the superposition size, i.e. $\lambda_{part} \gg \Delta x$. This means that, because $\lambda_{part} \sim \frac{\hbar}{q}$, we have that $\frac{i}{\hbar}(\vec{q} - q \vec{n}') \cdot (\vec{x} - \vec{x}') \ll 1$.

In this way, we can expand the exponential that appears in the RHS of Eq.(1.34) to obtain:

$$\frac{i}{\hbar}q(\hat{n}' - \hat{n}) \cdot (\vec{x} - \vec{x}') + \frac{1}{2\hbar^2}q^2[(\hat{n}' - \hat{n}) \cdot (\vec{x} - \vec{x}')]^2. \quad (1.41)$$

The first term gives an integral of an odd function, due to the fact that $\hat{n}' - \hat{n}$ is antisymmetric in the exchange of \hat{n} and \hat{n}' , while $\frac{d\sigma}{d\Omega}(\hat{n}, \hat{n}')$ is symmetric, giving a total odd function.

The second term gives instead a non-null contribution. Moreover, it can be further simplified: in fact, we can assume that the particular direction $\vec{x} - \vec{x}' = |\vec{x} - \vec{x}'| \hat{i} = \Delta x \hat{i}$ of the scattering center (i.e. of the crystal) does not depend on the direction \hat{i} .

We can thus average this term over all possible directions \hat{i} , obtaining:

$$\begin{aligned} (\Delta x)^2 \frac{1}{3} \sum_{i=x,y,z} [\hat{i} \cdot (\hat{n}' - \hat{n})]^2 &= \frac{1}{3} (\Delta x)^2 |\hat{n}' - \hat{n}|^2 \\ &= \frac{2}{3} (\Delta x)^2 |1 - \hat{n}' \cdot \hat{n}| = \frac{2}{3} (\Delta x)^2 (1 - \cos(\theta)). \end{aligned} \quad (1.42)$$

where θ is the scattering angle.

This means that, in the expression for Γ , the angular integral will become:

$$\int d\Omega \frac{d\sigma}{d\Omega}(\hat{n}, \hat{n}') \frac{2}{3} (1 - \cos(\theta)) = \frac{2\pi}{3} \int d(\cos(\theta)) (1 - \cos(\theta)) \frac{d\sigma}{d\Omega}(\hat{n}, \hat{n}') \equiv \sigma_{eff}, \quad (1.43)$$

where we have integrated over the azimuthal angle $\int_0^{2\pi} d\phi = 2\pi$ and we have defined the effective cross section σ_{eff} .

This leads to the final form of the decoherence rate in the long-wavelength limit:

$$F_{long}(\vec{x} - \vec{x}') \equiv \Delta x^2 \Lambda = \Delta x^2 \int dq \rho(q) v(q) \frac{q^2}{\hbar^2} \sigma_{eff}(q). \quad (1.44)$$

1.3.3 Comparing short and long-wavelength limit

Let us now compare the two limit behaviours of the decoherence rate, given by Eq.(1.39) and Eq.(1.44). It is important to distinguish two different physical situations: one in which the *physical* limit is the short-wavelength limit, i.e. when the particle has a wavelength λ_{part} such that $\lambda_{part} \ll \Delta x$, and the other where $\lambda_{part} \gg \Delta x$.

Let us start from the first case, i.e. with $\lambda_{part} \ll \Delta x$. In this context, it is obvious that Eq.(1.39) gives the *exact* expression for the decoherence rate. What is the role of Eq.(1.44) in this case? Is there any information that we can extrapolate from this equation?

Comparing Eq.(1.39) and Eq.(1.44) we notice that we can obtain the long-wavelength limit expression by substituting $\sigma_{tot} \rightarrow \sigma_{eff}$ inside the short-wavelength limit formula

and by multiplying it by the term $\Delta x^2 \frac{q^2}{\hbar^2}$. In particular, we can notice that σ_{eff} will be numerically of the same order of σ_{tot} , given that the only difference between the two is a purely geometrical factor $(1 - \cos(\theta))$ inside Eq.(1.43). Therefore, the main difference between the two expressions is entirely encoded inside the term $\Delta x^2 \frac{q^2}{\hbar^2}$.

Now, when the *physical* situation is the short-wavelength limit, this term will be $\Delta x^2 \frac{q^2}{\hbar^2} \gg 1$, given that $\lambda_{part} \sim \frac{\hbar}{q} \ll \Delta x$. This means that, when we have physically a short wavelength for the environmental particle compared to the superposition size, the following inequality holds:

$$\frac{F_{short}(\vec{x} - \vec{x}')}{F_{long}(\vec{x} - \vec{x}')} \equiv \frac{\Gamma}{\Delta x^2 \Lambda} \sim \frac{1}{\Delta x^2 \frac{q^2}{\hbar^2}} \ll 1, \quad (1.45)$$

which leads to:

$$F_{short}(\vec{x} - \vec{x}') \ll F_{long}(\vec{x} - \vec{x}'). \quad (1.46)$$

This means that, in the short-wavelength limit, Eq.(1.44) will thus be an **upper bound** to the decoherence rate. Therefore, if we use Eq.(1.44) to compute the decoherence rate when $\lambda_{part} \ll \Delta x$, we will obtain a superior limit which will be never exceeded by the physical decoherence rate given by Eq.(1.39).

Finally, considering the case where the physical situation is $\lambda_{part} \gg \Delta x$, we have that:

$$\frac{F_{short}(\vec{x} - \vec{x}')}{F_{long}(\vec{x} - \vec{x}')} \sim \frac{1}{\Delta x^2 \frac{q^2}{\hbar^2}} \gg 1, \quad (1.47)$$

because now we have that $\Delta x^2 \frac{q^2}{\hbar^2} \ll 1$. This leads to:

$$F_{long}(\vec{x} - \vec{x}') \ll F_{short}(\vec{x} - \vec{x}'), \quad (1.48)$$

which means that when the short-wavelength limit is the *physical* limit, Eq.(1.39) will be an upper bound for the physical decoherence rate given by Eq.(1.44).

1.4 Born-Markov Master Equation

Let us now analyze another method used to compute the decoherence effects on an open system. In this method, the approach to the problem is slightly different from what we have seen in the previous chapter. In fact, roughly speaking, in the Scattering Model the dynamics of the system S was determined by starting from the composite system $S + \mathcal{E}$, which is a *closed* system and for this reason its density matrix $\hat{\rho}_{S+\mathcal{E}}(t)$ is subjected to a *unitary* evolution:

$$\hat{\rho}_{S+\mathcal{E}}(t) = \hat{U}(t)\hat{\rho}_{S+\mathcal{E}}(0)\hat{U}^\dagger(t). \quad (1.49)$$

In order to compute the effects of the environment on the system, we can thus simply tracing out the environment:

$$\hat{\rho}_S(t) = \text{Tr}_{\mathcal{E}} [\hat{\rho}_{S+\mathcal{E}}(t)] = \text{Tr}_{\mathcal{E}} [\hat{U}(t)\hat{\rho}_{S+\mathcal{E}}(0)\hat{U}^\dagger(t)]. \quad (1.50)$$

In this chapter, instead, we will consider a different approach to the problem. In particular, we will focus on the generic form that the time evolution for the system S can have:

$$\hat{\rho}_S(t) = \hat{V}(t)\hat{\rho}_S(0), \quad (1.51)$$

where $\hat{V}(t)$ is a generic *non-unitary* evolution operator. Of course, the non-unitarity of $\hat{V}(t)$ is a consequence of the fact that the system S is not isolated but is constantly influenced by the interaction with the environment. In particular, we will see how we are able to compute explicitly $\hat{V}(t)$ starting from a few physically reasonable approximations. In particular, with these approximations, we will be able to express the time evolution of $\hat{\rho}_S(t)$ in terms of a *first order* and *local* differential equation:

$$\frac{d\hat{\rho}_S(t)}{dt} = \hat{\mathcal{L}}[\hat{\rho}_S(t)] = -\frac{i}{\hbar} [\hat{H}'_S, \hat{\rho}_S(t)] + \hat{\mathcal{D}}\hat{\rho}_S(t), \quad (1.52)$$

where the first term in the last equality represents the ordinary *unitary* evolution of the system, while the non-unitary part is taken care by $\hat{\mathcal{D}}\hat{\rho}_S(t)$, which represents the effects of the decoherence on the system S . It is also important to specify that, in the unitary part, \hat{H}'_S is *not* the unperturbed free Hamiltonian of the system S (which will be indicated by \hat{H}_S) but it is instead the *perturbed* Hamiltonian modified by the mere presence of the environment \mathcal{E} , i.e. it takes into account a general type of **Lamb-shift** effect on, for example, the energy levels of the system S . This does not mean that \hat{H}'_S takes into account the decoherence effects, which are taken care only by the non-unitary part $\hat{\mathcal{D}}\hat{\rho}_S(t)$ in the time evolution of $\hat{\rho}_S(t)$.

Let us now discuss the approximations the we will make in the derivation for the Born-Markov Master Equation:

- **Born approximation:** The environment is much larger than the system and the coupling between S and \mathcal{E} is weak enough that it is possible at all times to write the composite $S + \mathcal{E}$ system as a tensorial product:

$$\hat{\rho}_{S+\mathcal{E}}(t) \approx \hat{\rho}_S(t) \otimes \hat{\rho}_{\mathcal{E}}, \quad (1.53)$$

where $\hat{\rho}_{\mathcal{E}}$ is approximately constant at all times.

- **Markov approximation:** Memory effects in the environment are negligible, i.e. any effect that the system has on the environment decays rapidly compared to the evolution of the environment \mathcal{E} itself.

Considering these approximation to hold, another assumption that we will use in the derivation of the Master Equation is to consider the Hamiltonian interaction \hat{H}_{int} to be *separable* in terms of system-operators \hat{S}_α and environment-operators \hat{E}_α :

$$\hat{H}_{int} = \sum_{\alpha} \hat{S}_{\alpha} \otimes \hat{E}_{\alpha}. \quad (1.54)$$

It is time now to derive the Born-Markov Master Equation. The derivation will be obtained by considering all the observable to be expressed in the **Interaction picture**. In particular, let us start to express the explicit form of the Hamiltonian \hat{H} of the composite system $S + \mathcal{E}$:

$$\hat{H} = \hat{H}_S + \hat{H}_{\mathcal{E}} + \hat{H}_{int}. \quad (1.55)$$

It is clear that $\hat{H}_0 = \hat{H}_S + \hat{H}_{\mathcal{E}}$ is the *total* free Hamiltonian of the composite system, while \hat{H}_{int} represents the interaction Hamiltonian, which will be treated perturbatively. Thus, with a total Hamiltonian of this form, the interaction Hamiltonian \hat{H}_{int} will evolve as:

$$\hat{H}_{int}(t) = e^{\frac{i}{\hbar}\hat{H}_0 t} \hat{H}_{int} e^{-\frac{i}{\hbar}\hat{H}_0 t}, \quad (1.56)$$

while the density matrix operator will transform in the following way:

$$\hat{\rho}_{int}^{(I)}(t) = e^{\frac{i}{\hbar}\hat{H}_0 t} e^{-\frac{i}{\hbar}\hat{H} t} \hat{\rho} e^{\frac{i}{\hbar}\hat{H} t} e^{-\frac{i}{\hbar}\hat{H}_0 t} = e^{\frac{i}{\hbar}\hat{H}_0 t} \hat{\rho} e^{-\frac{i}{\hbar}\hat{H}_0 t}, \quad (1.57)$$

where the label (I) specifies in what picture we are considering the time evolution. In the interaction picture it is also possible to define a Liouville equation:

$$\frac{d\hat{\rho}^{(I)}(t)}{dt} = -\frac{i}{\hbar} [\hat{H}_{int}(t), \hat{\rho}^{(I)}(t)], \quad (1.58)$$

in complete analogy with the Heisenberg picture.

Eq.(1.58) is the starting point of our derivation of the Master Equation. In fact, we can solve it by integrating one time over t :

$$\hat{\rho}^{(I)}(t) = \hat{\rho}(0) - \frac{i}{\hbar} \int_0^t dt' [\hat{H}_{int}(t'), \hat{\rho}^{(I)}(t')]. \quad (1.59)$$

We can thus plug this equation back in Eq.(1.58), obtaining:

$$\begin{aligned} \frac{d\hat{\rho}^{(I)}(t)}{dt} &= -\frac{i}{\hbar} \left[\hat{H}_{int}(t), \hat{\rho}(0) - \frac{i}{\hbar} \int_0^t dt' [\hat{H}_{int}(t'), \hat{\rho}^{(I)}(t')] \right] \\ &= -\frac{i}{\hbar} [\hat{H}_{int}(t), \hat{\rho}(0)] - \frac{1}{\hbar^2} \int_0^t dt' [\hat{H}_{int}(t'), [\hat{H}_{int}(t'), \hat{\rho}^{(I)}(t')]]. \end{aligned} \quad (1.60)$$

It is easy to show that, also in the interaction picture, in order to obtain the density matrix $\hat{\rho}_S^{(I)}(t)$ of the system S it is sufficient to trace out the environmental degrees of freedom, i.e. $\hat{\rho}_S^{(I)}(t) = \text{Tr}_{\mathcal{E}} [\hat{\rho}^{(I)}(t)]$. Thus, tracing out Eq.(1.60), we obtain:

$$\begin{aligned} \frac{d\hat{\rho}_S^{(I)}(t)}{dt} &= -\frac{i}{\hbar} \text{Tr}_{\mathcal{E}} \left\{ \left[\hat{H}_{int}(t), \hat{\rho}(0) \right] \right\} \\ &- \frac{1}{\hbar^2} \int_0^t dt' \text{Tr}_{\mathcal{E}} \left\{ \left[\hat{H}_{int}(t'), \left[\hat{H}_{int}(t'), \hat{\rho}^{(I)}(t') \right] \right] \right\}. \end{aligned} \quad (1.61)$$

Now it is always possible to set the first term of this equation to 0 by simply defining a suitable initial condition for $\hat{\rho}(0)$, i.e. $\text{Tr}_{\mathcal{E}} \left\{ \left[\hat{H}_{int}(t), \hat{\rho}(0) \right] \right\} \equiv 0$.

At this point, we did not make any approximation, neither on the composite system $S + \mathcal{E}$ or on the interaction between the system and the environment. The first assumption that we will make is the Born Approximation explained above. We can understand why we need such an approximation by looking at the structure of Eq.(1.61): in particular, we can notice how the time evolution $\frac{d\hat{\rho}_S^{(I)}(t)}{dt}$ of the system's density matrix is for the moment a function of the *total* density matrix $\hat{\rho}^{(I)}(t)$, as it is clear from the last term in the RHS of Eq.(1.61). This is not a convenient expression, because we would like to write the time evolution $\frac{d\hat{\rho}_S^{(I)}(t)}{dt}$ only in terms of $\hat{\rho}_S^{(I)}(t)$ itself, in order to obtain a differential equation of the type of Eq.(1.52).

However, it is possible to have such result by imposing the Born Approximation $\hat{\rho}^{(I)}(t) \approx \hat{\rho}_S^{(I)}(t) \otimes \hat{\rho}_{\mathcal{E}}$. Plugging this approximation inside Eq.(1.61), we obtain:

$$\frac{d\hat{\rho}_S^{(I)}(t)}{dt} = -\frac{1}{\hbar^2} \int_0^t dt' \text{Tr}_{\mathcal{E}} \left\{ \left[\hat{H}_{int}(t'), \left[\hat{H}_{int}(t'), \hat{\rho}_S^{(I)}(t') \otimes \hat{\rho}_{\mathcal{E}} \right] \right] \right\}. \quad (1.62)$$

In this expression, the RHS now contains $\hat{\rho}_S^{(I)}(t')$ explicitly, as desired. However, the missing property of this equation, in order to have a first order and *local* differential equation (see Eq.(1.52)), is having the RHS to be a function of $\hat{\rho}_S^{(I)}(t)$ only, and not a dependence from all times $t' \in [0, t]$, as in Eq.(1.62). Thus, let us see how can we obtain such a result.

Using the explicit form for \hat{H}_{int} as in Eq.(1.54), we have that:

$$\begin{aligned}
\frac{d\hat{\rho}_S^{(I)}(t)}{dt} &= -\frac{1}{\hbar^2} \int_0^t dt' \sum_{\alpha,\beta} Tr_{\mathcal{E}} \left\{ \left[\hat{S}_\alpha(t) \otimes \hat{E}_\alpha(t), \left[\hat{S}_\beta(t') \otimes \hat{E}_\beta(t'), \hat{\rho}_S^{(I)}(t') \otimes \hat{\rho}_{\mathcal{E}} \right] \right] \right\} \\
&= -\frac{1}{\hbar^2} \int_0^t dt' \sum_{\alpha,\beta} Tr_{\mathcal{E}} \left\{ \hat{S}_\alpha(t) \hat{S}_\beta(t') \hat{\rho}_S^{(I)}(t') \otimes \hat{E}_\alpha(t) \hat{E}_\beta(t') \hat{\rho}_{\mathcal{E}} \right. \\
&\quad \left. - \hat{S}_\beta(t') \hat{\rho}_S^{(I)}(t') \hat{S}_\alpha(t) \otimes \hat{E}_\beta(t') \hat{\rho}_{\mathcal{E}} \hat{E}_\alpha(t) \right\} \\
&\quad - \frac{1}{\hbar^2} \int_0^t dt' \sum_{\alpha,\beta} Tr_{\mathcal{E}} \left\{ -\hat{S}_\alpha(t) \hat{\rho}_S^{(I)}(t') \hat{S}_\beta(t') \otimes \hat{E}_\alpha(t) \hat{\rho}_{\mathcal{E}} \hat{E}_\beta(t') \right. \\
&\quad \left. + \hat{\rho}_S^{(I)}(t') \hat{S}_\beta(t') \hat{S}_\alpha(t) \otimes \hat{\rho}_{\mathcal{E}} \hat{E}_\beta(t') \hat{E}_\alpha(t) \right\} \\
&= -\frac{1}{\hbar^2} \int_0^t dt' \sum_{\alpha,\beta} \left[\hat{S}_\alpha(t) \hat{S}_\beta(t') \hat{\rho}_S^{(I)}(t') Tr_{\mathcal{E}} \left\{ \hat{E}_\alpha(t) \hat{E}_\beta(t') \hat{\rho}_{\mathcal{E}} \right\}, \right. \\
&\quad \left. - \hat{S}_\beta(t') \hat{\rho}_S^{(I)}(t') \hat{S}_\alpha(t) Tr_{\mathcal{E}} \left\{ \hat{E}_\beta(t') \hat{\rho}_{\mathcal{E}} \hat{E}_\alpha(t) \right\} \right] \\
&\quad - \frac{1}{\hbar^2} \int_0^t dt' \sum_{\alpha,\beta} \left[-\hat{S}_\alpha(t) \hat{\rho}_S^{(I)}(t') \hat{S}_\beta(t') Tr_{\mathcal{E}} \left\{ \hat{E}_\alpha(t) \hat{\rho}_{\mathcal{E}} \hat{E}_\beta(t') \right\} \right. \\
&\quad \left. + \hat{\rho}_S^{(I)}(t') \hat{S}_\beta(t') \hat{S}_\alpha(t) Tr_{\mathcal{E}} \left\{ \hat{\rho}_{\mathcal{E}} \hat{E}_\beta(t') \hat{E}_\alpha(t) \right\} \right] \\
&= -\frac{1}{\hbar^2} \int_0^t dt' \sum_{\alpha,\beta} \langle \hat{E}_\alpha(t) \hat{E}_\beta(t') \rangle_{\hat{\rho}_{\mathcal{E}}} \left[\hat{S}_\alpha(t) \hat{S}_\beta(t') \hat{\rho}_S^{(I)}(t') - \hat{S}_\beta(t') \hat{\rho}_S^{(I)}(t') \hat{S}_\alpha(t) \right] \\
&\quad - \frac{1}{\hbar^2} \int_0^t dt' \sum_{\alpha,\beta} \langle \hat{E}_\beta(t') \hat{E}_\alpha(t) \rangle_{\hat{\rho}_{\mathcal{E}}} \left[-\hat{S}_\alpha(t) \hat{\rho}_S^{(I)}(t') \hat{S}_\beta(t') + \hat{\rho}_S^{(I)}(t') \hat{S}_\beta(t') \hat{S}_\alpha(t) \right]
\end{aligned} \tag{1.63}$$

where in the very last line we have used the cyclic property of the trace:

$$Tr_{\mathcal{E}} \left\{ \hat{E}_\alpha(t) \hat{\rho}_{\mathcal{E}} \hat{E}_\beta(t') \right\} = Tr_{\mathcal{E}} \left\{ \hat{E}_\beta(t') \hat{E}_\alpha(t) \hat{\rho}_{\mathcal{E}} \right\} \tag{1.64}$$

and defined the so-called **Environment Self-correlation Functions**:

$$\mathcal{C}_{\alpha\beta}(t, t') \equiv \langle \hat{E}_\alpha(t) \hat{E}_\beta(t') \rangle_{\hat{\rho}_{\mathcal{E}}} = Tr_{\mathcal{E}} \left\{ \hat{E}_\alpha(t) \hat{E}_\beta(t') \hat{\rho}_{\mathcal{E}} \right\}. \tag{1.65}$$

It is now useful to consider the fact that $\hat{\rho}_{\mathcal{E}}$ is time independent, as required by the Born approximation already applied above. In particular, we can consider $\hat{\rho}_{\mathcal{E}}$ to be a *stationary state*, i.e. $[\hat{H}_{\mathcal{E}}, \hat{\rho}_{\mathcal{E}}] = 0$. This implies also that $[e^{\pm \frac{i}{\hbar} \hat{H}_{\mathcal{E}} t}, \hat{\rho}_{\mathcal{E}}] = 0$, which leads to:

$$\begin{aligned}
\mathcal{C}_{\alpha\beta}(t, t') &\equiv \text{Tr}_{\mathcal{E}} \left\{ \hat{E}_{\alpha}(t) \hat{E}_{\beta}(t) \hat{\rho}_{\mathcal{E}} \right\} = \text{Tr}_{\mathcal{E}} \left\{ \hat{E}_{\alpha}(t) e^{\frac{i}{\hbar} \hat{H}_{\mathcal{E}} t} \hat{E}_{\beta} e^{-\frac{i}{\hbar} \hat{H}_{\mathcal{E}} t} \hat{\rho}_{\mathcal{E}} \right\} = \\
&\text{Tr}_{\mathcal{E}} \left\{ \hat{E}_{\alpha}(t) e^{\frac{i}{\hbar} \hat{H}_{\mathcal{E}} t} \hat{E}_{\beta} \hat{\rho}_{\mathcal{E}} e^{-\frac{i}{\hbar} \hat{H}_{\mathcal{E}} t} \right\} = \text{Tr}_{\mathcal{E}} \left\{ e^{-\frac{i}{\hbar} \hat{H}_{\mathcal{E}} t} \hat{E}_{\alpha}(t) e^{\frac{i}{\hbar} \hat{H}_{\mathcal{E}} t} \hat{E}_{\beta} \hat{\rho}_{\mathcal{E}} \right\} \\
&= \text{Tr}_{\mathcal{E}} \left\{ \hat{E}_{\alpha}(t - t') \hat{E}_{\beta} \hat{\rho}_{\mathcal{E}} \right\} \equiv \mathcal{C}_{\alpha\beta}(t - t').
\end{aligned} \tag{1.66}$$

It is now clear what is the physical interpretation of the environment self-correlation functions $\mathcal{C}_{\alpha\beta}(t, t') = \mathcal{C}_{\alpha\beta}(t - t') \equiv \langle \hat{E}_{\alpha}(t - t') \hat{E}_{\beta} \rangle_{\hat{\rho}_{\mathcal{E}}}$: in fact, they indicate the degree of correlation between the measurement of a specific observable \hat{E}_{β} at one time and the measurement of the same observable $\hat{E}_{\alpha}(t - t')$ carried out at a later time $\tau \equiv t - t'$. Essentially, these functions quantify how much information the environment retains over time regarding its interaction with the system.

This allows us to finally use the Markov approximation: in fact, it assumes that the environment's self-correlation functions decay rapidly compared to the timescale determined by the system's evolution. The Markov approximation simplifies equation (1.63) by assuming that the environment quickly forgets any internal self-correlations established during its interaction with the system. This means that the environment does not keep track of its history, and any quantum correlations between parts of the environment decay on a timescale τ_{corr} much shorter than the characteristic timescale over which the system's density operator changes noticeably. This assumption is valid when the environment is weakly coupled to the system and at a sufficiently high temperature.

In classical probability theory, a stochastic process is considered Markovian if the probability of an event is independent of all earlier events. This implies that each step in the process is independent of previous steps, and the system retains no memory of its past.

The consequences of the Markov approximation for obtaining a time-local master equation in differential form are as follows: the environment self-correlation functions sharply peak around $(t - t') = 0$ and decay much faster than the timescale determined by the rate of change of the system's density operator. This allows us to replace the retarded-time density operator with the current-time density operator in the master equation. The Markov assumption further simplifies the master equation by extending the integration limit to $-\infty$ for t greater than or equal to τ_{corr} , as the self-correlation functions vanish beyond that timescale.

This means that Eq.(1.63) becomes:

$$\begin{aligned}
\frac{d\hat{\rho}_S^{(I)}(t)}{dt} &= -\frac{1}{\hbar^2} \int_0^{+\infty} d\tau \sum_{\alpha, \beta} \mathcal{C}_{\alpha\beta}(\tau) \left[\hat{S}_{\alpha}(t) \hat{S}_{\beta}(t - \tau) \hat{\rho}_S^{(I)}(t) - \hat{S}_{\beta}(t - \tau) \hat{\rho}_S^{(I)}(t) \hat{S}_{\alpha}(t) \right] \\
&\quad - \frac{1}{\hbar^2} \int_0^{+\infty} d\tau \sum_{\alpha, \beta} \mathcal{C}_{\beta\alpha}(-\tau) \left[-\hat{S}_{\alpha}(t) \hat{\rho}_S^{(I)}(t) \hat{S}_{\beta}(t - \tau) + \hat{\rho}_S^{(I)}(t) \hat{S}_{\beta}(t - \tau) \hat{S}_{\alpha}(t) \right],
\end{aligned} \tag{1.67}$$

which is the Born-Markov Master Equation in the interaction picture.

We can finally transform Eq.(1.67) back to the Schrodinger picture. In fact, using the relation between $\hat{\rho}_S^{(I)}(t)$ and $\hat{\rho}_S(t)$:

$$\hat{\rho}_S^{(I)}(t) = e^{\frac{i}{\hbar}\hat{H}_S t} \hat{\rho}_S(t) e^{-\frac{i}{\hbar}\hat{H}_S t} \quad (1.68)$$

we have that:

$$\begin{aligned} \frac{d\hat{\rho}_S^{(I)}(t)}{dt} &= \frac{i}{\hbar} \hat{H}_S e^{\frac{i}{\hbar}\hat{H}_S t} \hat{\rho}_S(t) e^{-\frac{i}{\hbar}\hat{H}_S t} + e^{\frac{i}{\hbar}\hat{H}_S t} \hat{\rho}_S(t) e^{-\frac{i}{\hbar}\hat{H}_S t} \left(-\frac{i}{\hbar}\right) \hat{H}_S \\ + e^{\frac{i}{\hbar}\hat{H}_S t} \frac{d\hat{\rho}_S(t)}{dt} e^{-\frac{i}{\hbar}\hat{H}_S t} &= \frac{i}{\hbar} \hat{H}_S \hat{\rho}_S^{(I)}(t) - \frac{i}{\hbar} \hat{\rho}_S^{(I)}(t) \hat{H}_S + e^{\frac{i}{\hbar}\hat{H}_S t} \frac{d\hat{\rho}_S(t)}{dt} e^{-\frac{i}{\hbar}\hat{H}_S t} \\ &= \frac{i}{\hbar} \left[\hat{H}_S, \hat{\rho}_S^{(I)}(t) \right] + e^{\frac{i}{\hbar}\hat{H}_S t} \frac{d\hat{\rho}_S(t)}{dt} e^{-\frac{i}{\hbar}\hat{H}_S t} = \frac{d\hat{\rho}_S^{(I)}(t)}{dt}. \end{aligned} \quad (1.69)$$

Inverting Eq.(1.69) we find that:

$$\begin{aligned} \frac{d\hat{\rho}_S(t)}{dt} &= -\frac{i}{\hbar} e^{-\frac{i}{\hbar}\hat{H}_S t} \left[\hat{H}_S, \hat{\rho}_S^{(I)}(t) \right] e^{\frac{i}{\hbar}\hat{H}_S t} + e^{-\frac{i}{\hbar}\hat{H}_S t} \frac{d\hat{\rho}_S^{(I)}(t)}{dt} e^{\frac{i}{\hbar}\hat{H}_S t} \\ &= -\frac{i}{\hbar} \left[\hat{H}_S, e^{-\frac{i}{\hbar}\hat{H}_S t} \hat{\rho}_S^{(I)}(t) e^{\frac{i}{\hbar}\hat{H}_S t} \right] + e^{-\frac{i}{\hbar}\hat{H}_S t} \frac{d\hat{\rho}_S^{(I)}(t)}{dt} e^{\frac{i}{\hbar}\hat{H}_S t} \\ &= -\frac{i}{\hbar} \left[\hat{H}_S, \hat{\rho}_S(t) \right] + e^{-\frac{i}{\hbar}\hat{H}_S t} \frac{d\hat{\rho}_S^{(I)}(t)}{dt} e^{\frac{i}{\hbar}\hat{H}_S t} = \frac{d\hat{\rho}_S(t)}{dt}. \end{aligned} \quad (1.70)$$

The next step is to plug Eq.(1.67) into Eq.(1.70). In order to do that, let us first transform the following term into the Schrodinger picture:

$$\begin{aligned} &e^{-\frac{i}{\hbar}\hat{H}_S t} \hat{S}_\alpha(t) \hat{S}_\beta(t - \tau) \hat{\rho}_S^{(I)}(t) e^{\frac{i}{\hbar}\hat{H}_S t} = \\ = e^{-\frac{i}{\hbar}\hat{H}_S t} \hat{S}_\alpha(t) e^{\frac{i}{\hbar}\hat{H}_S t} e^{-\frac{i}{\hbar}\hat{H}_S t} \hat{S}_\beta(t - \tau) e^{\frac{i}{\hbar}\hat{H}_S t} e^{-\frac{i}{\hbar}\hat{H}_S t} \hat{\rho}_S^{(I)}(t) e^{\frac{i}{\hbar}\hat{H}_S t} &= \hat{S}_\alpha \hat{S}_\beta(-\tau) \hat{\rho}_S(t). \end{aligned} \quad (1.71)$$

The same computation can be easily done with the other terms that appear in the squared brackets in the of the RHS of Eq.(1.67). In the end, one obtains:

$$\begin{aligned} \frac{d\hat{\rho}_S(t)}{dt} &= -\frac{i}{\hbar} \left[\hat{H}_S, \hat{\rho}_S(t) \right] - \frac{1}{\hbar^2} \int_0^{+\infty} d\tau \sum_{\alpha, \beta} \mathcal{C}_{\alpha\beta}(\tau) \left[\hat{S}_\alpha, \hat{S}_\beta(-\tau) \hat{\rho}_S(t) \right] \\ &\quad - \frac{1}{\hbar^2} \int_0^{+\infty} d\tau \sum_{\alpha, \beta} \mathcal{C}_{\beta\alpha}(-\tau) \left[\hat{\rho}_S(t) \hat{S}_\beta(-\tau), \hat{S}_\alpha \right]. \end{aligned} \quad (1.72)$$

Finally, defining the following time-independent quantities:

$$\begin{cases} \hat{B}_\alpha = \int_0^{+\infty} d\tau \sum_\beta \mathcal{C}_{\alpha\beta}(\tau) \hat{S}_\beta(\tau) \\ \hat{C}_\alpha = \int_0^{+\infty} d\tau \sum_\beta \mathcal{C}_{\beta\alpha}(-\tau) \hat{S}_\beta(\tau) \end{cases}, \quad (1.73)$$

we find the final form for the **Born-Markov Master Equation**:

$$\frac{d\hat{\rho}_S(t)}{dt} = -\frac{i}{\hbar} [\hat{H}_S, \hat{\rho}_S(t)] - \frac{1}{\hbar^2} \sum_\alpha \{ [\hat{S}_\alpha, \hat{B}_\alpha \hat{\rho}_S(t)] + [\hat{\rho}_S(t) \hat{C}_\alpha, \hat{S}_\alpha] \}. \quad (1.74)$$

Chapter 2

Gravity-induced Entanglement and QGEM setup

New physics studies aim to understand quantum gravity, but the lack of empirical evidence has sparked a debate about whether gravity is a quantum entity. Traditional tests and cosmological observations have not provided conclusive evidence, leading to a shift towards laboratory probes. The Quantum Gravity induced Entanglement of Masses (QGEM) proposal [14, 23, 15, 24] suggests using entanglement between test masses in matter-wave interferometers as a way to detect the quantum nature of gravitational interactions. The study shows that observable entanglement can be generated between masses in superposition through the quantum phase induced by gravitational interaction. By analyzing the linearized quantized version of Einstein's theory of gravity, the study identifies the importance of off-diagonal terms in the coherent state basis of gravitational field modes for generating entanglement. The proposal assumes that gravitational interaction is mediated by a quantum mechanical gravitational field.

In this chapter, we will delve into the fundamental properties underlying the QGEM proposal and analyze its key features. In particular, in section 2.1 we are going to study the mechanics that lies behind the interaction between two massive quantum objects in superposition. In section 2.2 the discussion is applied for the specific case of gravity, where a model for linearized quantum gravity will be used. Finally in section 2.3.2 we are going to study the QGEM proposal, its main step, assumptions and its setup.

2.1 Mechanism for quantum interactions to entangle matter

Let us begin by analyzing a very simple model that could represent a generic physical situation in which two or more matter systems interact [23]. We know from Quantum Field Theory that to each matter particle/system it is possible to associate a continuous

field. This field comes out asymptotically from a collection of *Harmonic Oscillators*, in which the length of the links of the lattice is set to vanish smoothly.

To begin with, let's thus consider two Harmonic Oscillators A and B . Each of them has its own Hamiltonian, respectively \hat{H}_A and \hat{H}_B :

$$\begin{cases} \hat{H}_A = \frac{\hat{p}_A^2}{2m} + \frac{1}{2}m\omega^2\hat{x}_A^2 \\ \hat{H}_B = \frac{\hat{p}_B^2}{2m} + \frac{1}{2}m\omega^2\hat{x}_B^2 \end{cases} . \quad (2.1)$$

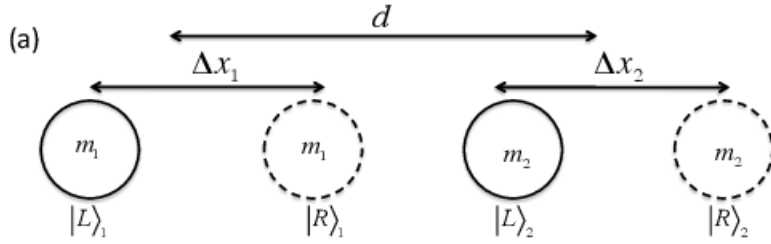


Figure 2.1: Schematic representation of two quantum harmonic oscillators located at distance d from one another.

We have considered them to have the same mass m and the same frequency ω . The only distinction between them is that they are spatially separated: their respective centers are located at distance d , as show in figure 2.1.

Using standard Quantum Mechanics, it is possible to introduce the so-called *creation* and *annihilation* operators, $\{\hat{a}, \hat{a}^\dagger\}$ for the system A and $\{\hat{b}, \hat{b}^\dagger\}$ for the system B :

$$\begin{cases} \hat{a} = \sqrt{\frac{m\omega}{2\hbar}}\hat{x}_A - \frac{i}{\sqrt{2\hbar m\omega}}\hat{p}_A \\ \hat{a}^\dagger = \sqrt{\frac{m\omega}{2\hbar}}\hat{x}_A + \frac{i}{\sqrt{2\hbar m\omega}}\hat{p}_A \end{cases} , \quad (2.2)$$

with analogue relations for B . In particular, the two Hamiltonians in terms of these operators become:

$$\begin{cases} \hat{H}_A = \hbar\omega\hat{a}^\dagger\hat{a} \\ \hat{H}_B = \hbar\omega\hat{b}^\dagger\hat{b} \end{cases} . \quad (2.3)$$

Each of them admit a set of eigenvectors, that we will call $\{|n\rangle_A\}$ for A and $\{|N\rangle_B\}$ for B . Their eigenvalues are given by $E_n^{(A)} = \hbar\omega n$ and $E_N^{(B)} = \hbar\omega N$ respectively, with $n, N \in \mathbb{N}$. In a QFT framework, these two sets of natural numbers represent the number of particles related to each quantum field.

It is now time to consider the composite system $A + B$. It will have a total free Hamiltonian $\hat{H}_0 = \hat{H}_A + \hat{H}_B$. Let us suppose now that there is an interaction between A and

B , driven by $\lambda\hat{H}_{int}$, where λ is a small (i.e. $\lambda \ll 1$) coupling constant that will allow us to treat the interaction perturbatively. The total Hamiltonian will thus be given by:

$$\hat{H} = \hat{H}_0 + \lambda\hat{H}_{int} = \hat{H}_A + \hat{H}_B + \lambda\hat{H}_{int}. \quad (2.4)$$

If the interaction is turned off, the free total Hamiltonian \hat{H}_0 will have the spectrum simply given by vectors that are tensorial products of the old separable basis, i.e. $\{|\Psi_m^{(0)}\rangle = |n\rangle_A |N\rangle_B\}$, with $m = n + N$. In particular, the eigenvalues are given by:

$$\hat{H}_0 |\Psi_m^{(0)}\rangle = \hbar\omega(n + N) |\Psi_m^{(0)}\rangle. \quad (2.5)$$

In the presence of interactions, the results are slightly different. In this situation, it is useful to use the basic concepts of Quantum Perturbation Theory. Let us thus study the eigenvalue problem for the total Hamiltonian \hat{H} :

$$\hat{H} |\Psi\rangle = E |\Psi\rangle. \quad (2.6)$$

We can thus expand the following variables in powers of λ :

$$\begin{cases} \hat{H} = \hat{H}_0 + \lambda\hat{H}_{int} \\ |\Psi\rangle = |\Psi_0\rangle + \lambda|\Psi_1\rangle + \dots \\ E = E_0^{tot} + \lambda E_1 + \dots \end{cases} \quad (2.7)$$

In this way, at the first order in λ Eq.(2.6) becomes:

$$\begin{aligned} (\hat{H}_0 + \lambda\hat{H}_{int})(|\Psi_0\rangle + \lambda|\Psi_1\rangle + \dots) &= (E_0^{tot} + \lambda E_1 + \dots)(|\Psi_0\rangle + \lambda|\Psi_1\rangle + \dots) \\ &= \hat{H}_0 |\Psi_0\rangle + \lambda\hat{H}_0 |\Psi_1\rangle + \lambda\hat{H}_{int} |\Psi_0\rangle = E_0^{tot} |\Psi_0\rangle + \lambda E_0^{tot} |\Psi_1\rangle + \lambda E_1 |\Psi_0\rangle. \end{aligned} \quad (2.8)$$

First of all, the first terms in the RHS and LHS of the very last line cancel each other out, because of $\hat{H}_0 |\Psi_0\rangle = E_0^{tot} |\Psi_0\rangle$. Knowing this, we can multiply Eq.(2.8) by $\langle\Psi_m^{(0)}|$, which is another eigenvector of the unperturbed Hamiltonian \hat{H}_0 such that $\hat{H}_0 |\Psi_m^{(0)}\rangle = E_m |\Psi_m^{(0)}\rangle$ and $\langle\Psi_m^{(0)}|\Psi_0\rangle = 0$. In this way, we obtain:

$$E_m \langle\Psi_m^{(0)}|\Psi_1\rangle + \langle\Psi_m^{(0)}|\hat{H}_{int}|\Psi_0\rangle = E_0^{tot} \langle\Psi_m^{(0)}|\Psi_1\rangle, \quad (2.9)$$

which leads to:

$$\langle\Psi_m^{(0)}|\Psi_1\rangle = \frac{\langle\Psi_m^{(0)}|\hat{H}_{int}|\Psi_0\rangle}{E_0^{tot} - E_m}. \quad (2.10)$$

In this way, we can write down the expansion for the perturbed quantum state $|\Psi\rangle$:

$$\begin{aligned}
|\Psi\rangle &= |\Psi_0\rangle + \lambda |\Psi_1\rangle + \dots \simeq |\Psi_0\rangle + \lambda \sum_m \langle \Psi_m^{(0)} | \Psi_1 \rangle |\Psi_m^{(0)}\rangle \\
&= |\Psi_0\rangle + \lambda \sum_m \frac{\langle \Psi_m^{(0)} | \hat{H}_{int} | \Psi_0 \rangle}{E_0^{tot} - E_m} |\Psi_m^{(0)}\rangle.
\end{aligned} \tag{2.11}$$

Let us now suppose that the initial state $|\Psi_0\rangle$ is separable, e.g. $|\Psi_0\rangle = |n\rangle_A |N\rangle_B$. This means that, before the interaction, the two systems A and B were completely separable. We want to understand what is the situation *after* the interaction, i.e. if the two systems get entangled or if they keep to be separate. In order to do that, we can study Eq.(2.11), which is the energy eigenstate after the interaction induced by \hat{H}_{int} . In particular, considering $\{|\Psi_m^{(0)}\rangle = |n\rangle_A |N\rangle_B\}$ with $m = n + N$ as before, Eq.(2.11) takes the form:

$$|\Psi\rangle = \frac{1}{\sqrt{\mathcal{N}}} \sum_{n,N} C_{nN} |n\rangle_A |N\rangle_B, \tag{2.12}$$

where $C_{00} = 1$ corresponds to the initial unperturbed state $|\Psi_0\rangle$, $\mathcal{N} = \sum_{n,N} |C_{nN}|^2$ and $C_{nN} = \lambda \frac{\langle n| \langle N | \hat{H}_{int} | 0 \rangle | 0 \rangle}{E_0^{tot} - E_m}$ for $n, N > 0$. Moreover, if the initial state is the vacuum for both A and B , we have that $E_0^{tot} = 2E_0$, with E_0 being the vacuum energy of the single system A or B , while E_m becomes $E_m = E_n + E_N$ if $\{|\Psi_m^{(0)}\rangle = |n\rangle_A |N\rangle_B\}$. In this way, the C_{nN} coefficients are:

$$C_{nN} = \begin{cases} \lambda \frac{\langle n| \langle N | \hat{H}_{int} | 0 \rangle | 0 \rangle}{2E_0 - E_n - E_N} & \text{for } n, N > 0 \\ 1 & \text{for } n, N = 0 \end{cases}. \tag{2.13}$$

We can thus now compute the entanglement of the state Eq.(2.12). In order to do that, we choose one of the two systems, e.g. A , and compute its density matrix $\hat{\rho}_A$ by simply tracing out the B basis $\{|N\rangle\}$ from the *total* density matrix $\hat{\rho} = |\Psi\rangle \langle \Psi|$:

$$\hat{\rho} = \frac{1}{\mathcal{N}} \sum_{n,N,n',N'} C_{nN} C_{n'N'}^* |n\rangle \langle n'| \otimes |N\rangle \langle N'| \longrightarrow \hat{\rho}_A = \frac{1}{\mathcal{N}} \sum_{n,N,n'} C_{nN} C_{n'N}^* |n\rangle \langle n'| \tag{2.14}$$

In this way, it is possible to compute the **Concurrence** of the state $\hat{\rho}_A$, which is defined as:

$$C \equiv \sqrt{2(1 - Tr[\hat{\rho}_A^2])}, \tag{2.15}$$

where now the trace is computed over the A basis $\{|n\rangle\}$. In particular, using Eq.(2.14), we have that:

$$C = \sqrt{2 \left(1 - \sum_{n,n',N,N'} C_{nN} C_{n'N}^* C_{n'N'} C_{nN'}^* / \mathcal{N}^2 \right)}. \quad (2.16)$$

It is known that the Concurrence C represents a separable state when $C = 0$, while $C = \sqrt{2}$ represents a *maximally entangled state*. This means that, in our case, if the only non-null coefficient C_{nN} is $C_{00} = 1$, the summation in Eq.(2.16) gives 1, resulting in a value for the Concurrence C of $C = 0$. This is a trivial case, because it corresponds to a final state $|\Psi\rangle = |\Psi_0\rangle$, which is separable by construction.

Another situation in which is possible to obtain $C = 0$ is, more in general, when $\sum_{n,n',N,N'} C_{nN} C_{n'N}^* C_{n'N'} C_{nN'}^* = \mathcal{N}^2 = \sum_{n,N} |C_{nN}|^2$. It is indeed possible to have such a case when:

$$C_{nN} = \delta_{0N} \quad \text{and} \quad C_{nN} = \delta_{n0}. \quad (2.17)$$

In fact, in this case we have that:

$$\begin{aligned} \sum_{n,n',N,N'} C_{nN} C_{n'N}^* C_{n'N'} C_{nN'}^* &= \sum_{n,n',N} C_{nN} C_{n'N}^* \sum_{N'} C_{n'N'} C_{nN'}^* \\ &= \sum_{n,n',N} C_{nN} C_{n'N}^* \delta_{n'0} \delta_{n0} = \sum_{n,N} C_{nN} C_{0N}^* \\ &\equiv \sum_{n,N} C_{nN} C_{nN}^* = \sum_{n,N} |C_{nN}|^2 = \mathcal{N}^2, \end{aligned} \quad (2.18)$$

where at the beginning of the very last line we have used the fact that the only non-null terms are now $C_{nN} = C_{0N}$. We have thus proved that in this situation, the concurrence is $C = 0$ and no entanglement is created by the interaction.

The only case in which $C > 0$ is when \exists at least one element $C_{nN} \neq 0$ for $n, N > 0$. Thus, in this situation, the interaction generates entanglement between the two systems A and B .

Therefore, the only significant coefficients for the creation of entanglement are the ones with $n, N > 0$. This means that, from Eq.(2.13), it is possible to generate entanglement only when transitions where *both* the systems A and B are in an **excited** state are allowed. If the only energy transitions allowed are the ones in which *at least* one of the two systems remains in the vacuum state $|0\rangle_A$ (or $|0\rangle_B$), the only non-null coefficients are either C_{n0} or C_{0N} and entanglement is *not* generated, as we have proved above.

We have thus just proved that it is possible to entangle two generic matter systems if there is an interaction between them. In particular, entanglement is already created at the **first order** in perturbation theory.

2.2 The case for gravitational interaction

In this section, we will consider the setup of two quantum harmonic oscillators (introduced in the previous section 2.1) in the presence of the gravitational field [23]. In particular, we will work in the regime of small perturbations $|h_{\mu\nu}| \ll 1$ about the Minkowski background $\eta_{\mu\nu}$. The metric is given by: $g_{\mu\nu} = \eta_{\mu\nu} + h_{\mu\nu}$ (where $\mu, \nu = 0, 1, 2, 3$ and we are using $(-, +, +, +)$ signature throughout). We will promote the fluctuations into the quantum operators:

$$\hat{h}_{\mu\nu} = A \int d^3\vec{k} \sqrt{\frac{\hbar}{(2\pi)^3 \omega_k}} (\hat{P}_{\mu\nu}^\dagger(k) e^{-i\vec{k}\cdot\vec{r}} + \text{H.c.}), \quad (2.19)$$

where \vec{k} is the three-vector. The prefactor is denoted by $A = \sqrt{\frac{16\pi G}{c^2}}$, where G is the Newton's constant, and $\hat{P}_{\mu\nu}$ and $\hat{P}_{\mu\nu}^\dagger$ denote the graviton annihilation and creation operator, respectively. We will discuss in detail the properties of the graviton and the relevant degrees of freedom below.

Around the Minkowski background, the graviton coupling to the stress-energy tensor $\hat{T}_{\mu\nu}$ is given by the following operator-valued interaction term:

$$\hat{H}_{\text{int}} = -\frac{1}{2} \int d^3\vec{r} \hat{h}_{\mu\nu}(\vec{r}) \hat{T}_{\mu\nu}(\vec{r}), \quad (2.20)$$

where \vec{r} denotes the three-vector.

Let us now consider two particles of mass m (which will form the two oscillating systems). The two particles are generating the following current in the static limit:

$$\hat{T}_{00}(\vec{r}) \equiv mc^2 (\delta(\vec{r} - \hat{r}_A) + \delta(\vec{r} - \hat{r}_B)), \quad (2.21)$$

where $\hat{r}_A = (\hat{x}_A, 0, 0)$, $\hat{r}_B = (\hat{x}_B, 0, 0)$ denote the positions of the two matter systems. The Fourier transform of the current is given by:

$$\hat{T}_{00}(\vec{k}) = mc^2 \sqrt{\frac{1}{(2\pi)^3}} (e^{i\vec{k}\cdot\hat{r}_A} + e^{i\vec{k}\cdot\hat{r}_B}). \quad (2.22)$$

After employing canonical quantization of the graviton within a weak field regime, we can decompose $\hat{h}^{\mu\nu} = \hat{\gamma}^{\mu\nu} - \frac{1}{2}\eta^{\mu\nu}\hat{\gamma}$ around a Minkowski background, adhering to the convention $\gamma \equiv \eta^{\mu\nu}\gamma_{\mu\nu}$. In this context, the two distinct modes, namely the spin-2 component, $\gamma_{\mu\nu}$, and the spin-0 component, γ , can be treated independently as variables. These components are treated as self-adjoint operators and can be decomposed as follows:

$$\hat{\gamma}^{\mu\nu} = A \int d^3\vec{k} \sqrt{\frac{\hbar}{(2\pi)^3 2\omega_k}} (\hat{P}^{\dagger\mu\nu}(\vec{k}) e^{-i\vec{k}\cdot\vec{r}} + \text{H.c.}), \quad (2.23)$$

$$\hat{\gamma} = 2A \int d^3\vec{k} \sqrt{\frac{\hbar}{(2\pi)^3 2\omega_k}} \left(\hat{P}^\dagger(\vec{k}) e^{-i\vec{k}\cdot\vec{r}} + \text{H.c.} \right), \quad (2.24)$$

where:

$$\begin{cases} [\hat{P}^{\mu\nu}(\vec{k}), \hat{P}^{\dagger\lambda\rho}(\vec{k}')] = [\eta^{\mu\lambda}\eta^{\nu\rho} + \eta^{\mu\rho}\eta^{\nu\lambda}] \delta(\vec{k} - \vec{k}') \\ [\hat{P}(\vec{k}), \hat{P}^\dagger(\vec{k}')] = -\delta(\vec{k} - \vec{k}'). \end{cases} \quad (2.25)$$

The expression for the graviton Hamiltonian is now given by:

$$\hat{H}_g = \int d^3\vec{k} \hbar\omega_k \left(\hat{P}^{\dagger\mu\nu}(\vec{k}) \hat{P}_{\mu\nu}(\vec{k}) - \frac{1}{2} \hat{P}^\dagger(\vec{k}) \hat{P}(\vec{k}) \right). \quad (2.26)$$

Our objective is to calculate the change in energy, denoted as $\Delta\hat{H}_g$, which represents the shift in the graviton vacuum energy due to its interaction with matter. In the static limit, where the motion of the two harmonic oscillators is neglected, the interaction Hamiltonian takes on a simplified form:

$$\hat{H}_{int} = \frac{1}{2} \int d^3\vec{r} \left[\hat{\gamma}_{00}(\vec{r}) + \frac{1}{2} \hat{\gamma}(\vec{r}) \right] \hat{T}_{00}(\vec{r}). \quad (2.27)$$

By utilizing perturbation theory, we can determine the energy shift of the graviton vacuum. The first-order term vanishes, while the second-order term in perturbation theory yields:

$$\Delta\hat{H}_g \equiv \int d^3\vec{k} \frac{\langle 0 | \hat{H}_{int} | \vec{k} \rangle \langle \vec{k} | \hat{H}_{int} | 0 \rangle}{(E_0 - E_k)}, \quad (2.28)$$

where $|\vec{k}\rangle = (\hat{P}_{00}^\dagger(\vec{k}) + \hat{P}^\dagger(\vec{k}))|0\rangle$ represents the one-particle state formed in the unperturbed vacuum, $E_k = E_0 + \omega_k$ signifies the energy of the one-particle state, and E_0 represents the energy of the vacuum state. The graviton being mediated is now considered off-shell or virtual due to the integration over all possible momenta \vec{k} , and as a result, it does not follow classical equations of motion.

We thus need to compute the term $\langle \vec{k} | \hat{H}_{int} | 0 \rangle$ inside Eq.(2.28). In order to do that, let us expand \hat{H}_{int} as in Eq.(2.27):

$$\langle \vec{k} | \hat{H}_{int} | 0 \rangle = \langle \vec{k} | \left(\frac{1}{2} \int d^3\vec{r} \hat{h}_{00}(\vec{r}) \hat{T}_{00}(\vec{r}) \right) | 0 \rangle = \frac{1}{2} \int d^3\vec{r} \hat{T}_{00}(\vec{r}) \langle \vec{k} | \hat{h}_{00}(\vec{r}) | 0 \rangle. \quad (2.29)$$

We have thus shifted the task to compute $\langle \vec{k} | \hat{h}_{00}(\vec{r}) | 0 \rangle$. Using Eq.(2.19), we have that:

$$\begin{aligned}
\langle \vec{k} | \hat{h}_{00}(\vec{r}) | 0 \rangle &= \langle \vec{k} | \left[A \int d^3 \vec{k}' \sqrt{\frac{\hbar}{(2\pi)^3 2\omega'_k}} \left(\hat{P}_{00}^\dagger(\vec{k}') e^{-i\vec{k}' \cdot \vec{r}} + \hat{P}_{00}(\vec{k}') e^{i\vec{k}' \cdot \vec{r}} \right) \right] | 0 \rangle \\
&= A \int d^3 \vec{k}' \sqrt{\frac{\hbar}{(2\pi)^3 2\omega'_k}} \left(\langle \vec{k}' | \hat{P}_{00}^\dagger(\vec{k}') | 0 \rangle e^{-i\vec{k}' \cdot \vec{r}} + \langle \vec{k}' | \hat{P}_{00}(\vec{k}') | 0 \rangle e^{i\vec{k}' \cdot \vec{r}} \right) \\
&= A \int d^3 \vec{k}' \sqrt{\frac{\hbar}{(2\pi)^3 2\omega'_k}} \left(e^{-i\vec{k}' \cdot \vec{r}} \langle \vec{k} | \vec{k}' \rangle + 0 \right) \\
&= A \int d^3 \vec{k}' \sqrt{\frac{\hbar}{(2\pi)^3 2\omega'_k}} e^{-i\vec{k}' \cdot \vec{r}} \delta^{(3)}(\vec{k} - \vec{k}') = A \sqrt{\frac{\hbar}{(2\pi)^3 2\omega_k}} e^{-i\vec{k} \cdot \vec{r}}.
\end{aligned} \tag{2.30}$$

Plugging it back in Eq.(2.29), one obtains:

$$\langle \vec{k} | \hat{H}_{\text{int}} | 0 \rangle = \frac{A}{2} \sqrt{\frac{\hbar}{2\omega_k}} \hat{T}_{00}(\vec{k}), \tag{2.31}$$

where the Fourier transform definition is employed:

$$\hat{T}_{00}(\vec{k}) = \frac{1}{(2\pi)^{3/2}} \int d^3 \vec{r} e^{-i\vec{k} \cdot \vec{r}} \hat{T}_{00}(\vec{r}). \tag{2.32}$$

From Eq.(2.31), we derive a simple expression:

$$\langle 0 | \hat{H}_{\text{int}} | \vec{k} \rangle \langle \vec{k} | \hat{H}_{\text{int}} | 0 \rangle = \frac{\hbar A^2}{8\omega_k} \hat{T}_{00}^\dagger(\vec{k}) \hat{T}_{00}(\vec{k}). \tag{2.33}$$

which substituted into Eq.(2.28) gives:

$$\Delta \hat{H}_g = -\frac{A^2}{8c^2} \int d^3 \vec{k} \frac{\hat{T}_{00}^\dagger(\vec{k}) \hat{T}_{00}(\vec{k})}{k^2}. \tag{2.34}$$

By performing the momentum integration using spherical coordinates, we arrive at the result:

$$\Delta \hat{H}_g = -\frac{A^2 m^2 c^2}{16\pi |\mathbf{r}_A - \mathbf{r}_B| c^2}, \tag{2.35}$$

where we have excluded the self-energy terms of the individual particles. Finally, inserting $A = \sqrt{\frac{16\pi G}{c^2}}$ into Eq. (29), we obtain Newton's potential:

$$\Delta \hat{H}_g = -\frac{Gm^2}{|\mathbf{x}_A - \mathbf{x}_B|}. \tag{2.36}$$

We can observe that the change in graviton energy, $\Delta \hat{H}_g$, resulting from the interaction between the graviton and matter, is a function that operates on the two matter systems:

$$\Delta\hat{H}_g \equiv f(\hat{x}_A, \hat{x}_B). \quad (2.37)$$

If the two matter systems lack well-defined positions (such as when they are in a spatial superposition or another non-classical state), the change in graviton energy, $\Delta\hat{H}_g$, will not be a real number as expected in classical gravity theory. Instead, it will be an operator-valued quantity, a genuine quantum entity.

Now, our objective is to calculate the excited wave function $|\psi_f\rangle$ of the two harmonic oscillators to establish the connection between entanglement and LOQC discussed in Section III. By employing Eq. (1) and expanding Eq. (30), we find:

$$\Delta\hat{H}_g \approx -\frac{Gm^2}{d} + \frac{Gm^2}{d^2}(\delta\hat{x}_B - \delta\hat{x}_A) - \frac{Gm^2}{d^3}(\delta\hat{x}_B - \delta\hat{x}_A)^2. \quad (2.38)$$

The last term corresponds to the lowest-order matter-matter interaction:

$$\hat{H}_{AB} \equiv \frac{2Gm^2}{d^3}(\delta\hat{x}_A\delta\hat{x}_B). \quad (2.39)$$

It is worth noting that the interaction Hamiltonian \hat{H}_{AB} solely contains the operators of the two harmonic oscillators, $\delta\hat{x}_A$ and $\delta\hat{x}_B$.

However, it is crucial to acknowledge that the term $\delta\hat{x}_A\delta\hat{x}_B$ would not have emerged if we had assumed a real-valued shift in the energy of the gravitational field. In fact, a classical gravitational field is incapable of producing the operator-valued shift in Eq. (30) (and consequently, the quantum interaction potential in Eq. (33)). Therefore, we must conclude that gravitationally induced entanglement is, indeed, a quantum characteristic of the gravitational field.

Next, we will utilize the modes in Eq. (3) to determine:

$$\hat{H}_{AB} \approx \hbar g(\hat{a}_b + \hat{a}^\dagger\hat{b} + \hat{a}\hat{b}^\dagger + \hat{a}^\dagger\hat{b}^\dagger), \quad (2.40)$$

where we define the coupling:

$$g \equiv \frac{Gm}{d^3\omega_m}, \quad (2.41)$$

By employing \hat{H}_{AB} as the interaction Hamiltonian in Eq. (8), we find that the only non-zero coefficient arises from the term $\sim \hat{a}^\dagger\hat{b}^\dagger$ and is given by:

$$C_{11} = -\frac{g}{2\omega_m}, \quad (2.42)$$

We note that the $\hat{a}^\dagger\hat{b}^\dagger$ term generates the first excited states in the harmonic oscillators (with energy $E_1 = E_0 + \hbar\omega_m$). Additionally, we have the term $C_{00} = 1$, which corresponds to the unperturbed state.

Hence, the final state in Eq. (7) simplifies to (up to first order in perturbation theory and setting $\lambda = 1$):

$$|\psi_f\rangle \equiv \frac{1}{\sqrt{1 + \left(\frac{g}{2\omega_m}\right)^2}} [|0\rangle|0\rangle - \frac{g}{2\omega_m} |1\rangle|1\rangle]. \quad (2.43)$$

This state represents entanglement between the ground and first excited states of the two harmonic oscillators. To compute the reduced density matrix, we trace system B (where our notation is $|n\rangle|N\rangle = |n\rangle_A|N\rangle_B$). The concurrence in Eq. (13) reduces to:

$$C \equiv \sqrt{2 \left(1 - \frac{1 + \left(\frac{g}{2\omega_m}\right)^4}{1 + \left(\frac{g}{2\omega_m}\right)^2} \right)} \approx \sqrt{\frac{2g}{\omega_m}}, \quad (2.44)$$

valid for small values of the parameter $\frac{g}{\omega_m} \ll 1$.

Inserting the coupling from Eq. (35), we obtain the concurrence:

$$C = \sqrt{\frac{2Gm}{d^3\omega_m^2}}. \quad (2.45)$$

We thus see that the degree of entanglement grows linearly with the mass of the oscillator and inversely with the distance between the two oscillators (inverse cubic) as well as with the frequency of the harmonic trap (inverse square).

Let us reiterate the key finding. If the underlying gravitational field were classical (specifically, obeying LOCC), then the final state of the matter components, i.e. the two harmonic oscillator states, would have never evolved to the entangled state $|\psi_f\rangle$, but would have rather remained in an unentangled/separable state. Conversely, if the gravitational field is quantized (and hence obeys LOQC) then we have shown that it can give rise to the entangled state $|\psi_f\rangle$.

2.3 QGEM Experiment

The classical theory of general relativity (GR) successfully explains observations on large scales, such as those from solar system tests and gravitational wave detections. However, it falls short when describing phenomena at very small distances and early times, resulting in the prediction of black holes and cosmological singularities where the concept of space-time breaks down.

While a quantum theory of gravity is expected to address these limitations, it remains uncertain whether gravity itself is inherently quantum. Various proposals for a quantum theory of gravity have been put forward. At low energies, the gravitational interaction is believed to be mediated by a massless spin-2 particle called a graviton, which can be quantized within a perturbative quantum theory of gravity. Although this theory faces

challenges like renormalizability at high energies, it provides an effective field theory description of nature at low energies.

Directly detecting the quantum properties of gravitons through momentum transfer is extremely challenging due to the weak strength of the gravitational interaction. Indirect detection methods, such as studying primordial gravitational waves or investigating modifications in the behavior of photons, face difficulties arising from astrophysical and cosmological uncertainties. Additionally, strict constraints on the graviton's mass derived from the propagation of gravitational waves detected by the LIGO observatory suggest no deviations from general relativity in the infrared range.

Given these challenges, the question arises: How can we experimentally test the quantum nature of gravitons at low energies? A recent proposal called quantum gravity-induced entanglement of masses (QGEM) aims to observe entanglement between two quantum superposed test masses as a means of testing the quantum behavior of gravity. The idea involves creating a spatial quantum superposition of these masses and bringing them together in a controlled environment, where their primary interaction is the exchange of gravitons. While implementing such an experiment poses significant hurdles, it offers the potential to validate the QGEM proposal.

In this section we will finally analyze the **QGEM** experiment. It was proposed for the first time in 2017 by two independent works[14, 15].

The main goal of the experiment is to prove the quantum nature of the gravitational interaction. The importance of such an experiment is self evident. In fact, behind all the quantum theories of gravity that have been proposed in the last 50 years, the fundamental question still remains unanswered: is gravity really quantum? Can we actually quantize gravity? If so, what would it be the main evidence of such quantum nature?

2.3.1 LOCC Theorem

One of the primary contribute to the QGEM experiment comes from one of the main principles of Quantum Information Theory:

LOCC Principle: *Any operation performed on an entangled quantum system can be achieved through local operations, meaning operations on individual subsystems, and classical communication between the parties involved.*

The LOCC principle restricts the types of operations that can be applied to maintain the locality of interactions and communication. It ensures that entanglement *cannot* be created or increased by using only local operations and classical communication. This principle provides a framework for understanding the limitations and possibilities of manipulating entangled states using local resources and communication channels.

The main importance of this principle relies in the fact that it is impossible to create entanglement through local and classical operations on two quantum subsystems. That

is because entanglement is the most genuine quantum effects, which is fundamentally *non-local*.

Imagine, therefore, a situation in which there are two massive quantum objects floating in space: because they both have a mass, they will interact through gravitational interaction. Now, from the LOCC principle, we know that only quantum interactions can generate entanglement between the two object we are considering. Therefore, if after the interaction we start to collect data on the two massive objects separately and we observe an entanglement-type correlation between the two sets of measurement, then we can state that gravity has quantum properties. Otherwise, if gravity was a purely classical force, it will be impossible to create entanglement between the two masses.

2.3.2 QGEM Setup

After having outlined the importance of the LOCC theorem in the QGEM experiment, let us analyze the setup proposed in the original paper.

In the proposal, there are two quantum massive object, with masses m_1 and m_2 respectively, both of which are in a spatial superposition (see figure 2.2). In particular, to each of them, we can associate its own Hilbert space \mathcal{H}_1 and \mathcal{H}_2 . Therefore, *before* the interaction (i.e. at $t = 0$), the quantum states associated to the two systems will be given by:

$$\begin{cases} |\Psi\rangle_1 = \frac{1}{\sqrt{2}} (|L\rangle_1 + |R\rangle_1) \\ |\Psi\rangle_2 = \frac{1}{\sqrt{2}} (|L\rangle_2 + |R\rangle_2) \end{cases} . \quad (2.46)$$

If we now consider the composite system $\mathcal{H} = \mathcal{H}_1 \otimes \mathcal{H}_2$, its quantum state at $t = 0$ will be a *separable* state of the following form:

$$|\Psi\rangle = |\Psi\rangle_1 \otimes |\Psi\rangle_2 = \frac{1}{2} [|L\rangle_1 |L\rangle_2 + |L\rangle_1 |R\rangle_2 + |R\rangle_1 |L\rangle_2 + |R\rangle_1 |R\rangle_2] \quad (2.47)$$

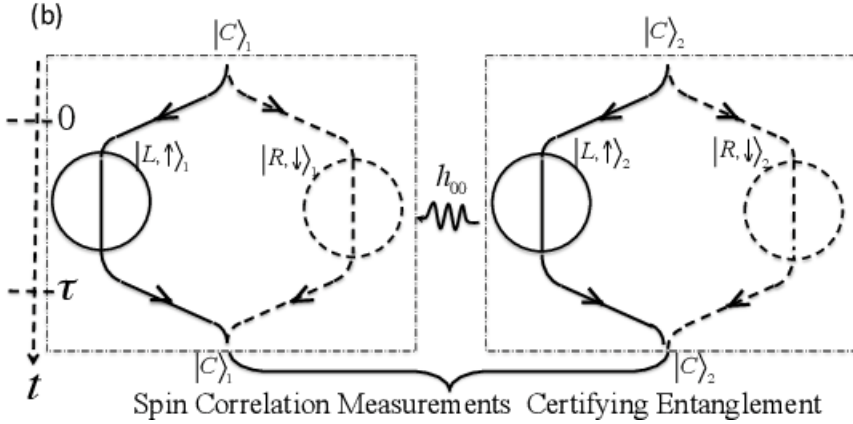


Figure 2.2: Schematic representation of the QGEM setup. Two massive quantum object are posed in spatial superposition through a Stern-Gerlach apparatus. The superposition is kept for a time τ , during which the two masses interact through gravity. In the last step, both the objects are brought back in a well defined position through a refocusing SG apparatus. At this point, it is possible to perform measurement on both systems separately, in order to find evidences for the creation of entanglement.

Thus, the **First Step** of the experiment consists in creating the two spatial superposition. This can be done by a spin dependent spatial splitting of the test mass m_1 and m_2 , performed thanks to a Stern-Gerlach (or SG) apparatus. The state will thus be given more specifically by:

$$|C\rangle_i \frac{1}{\sqrt{2}} (|\uparrow_i\rangle + |\downarrow_i\rangle) \rightarrow \frac{1}{\sqrt{2}} (|L, \uparrow_i\rangle + |R, \downarrow_i\rangle), \quad (2.48)$$

where $|C\rangle_i$ is the *spatially localized* state associated to the m_i particle and the states $|\uparrow_i\rangle$ and $|\downarrow_i\rangle$ are referred to the spin direction of the particle. Moreover, in this setup it is supposed that the spatial superposition created in the first step is the same for both the objects, i.e. $\Delta x_1 = \Delta x_2 \equiv \Delta x$. Finally, the two initial spatially localized states $|C\rangle_1$ and $|C\rangle_2$ are supposed to be separated by a distance d .

The **Second Step** of the experiment consists in holding the superposition created in the previous step for a time $t_{tot} = \tau$, during which the SG apparatus is shut down. Moreover, during this step, it is very important to turn off all the other possible interactions that can be present between, for example, the two massive particles or between one of the particles and the environment. One possibility could be, for example, that both the massive object have some charge impurities, i.e. they posses two charges Q_1 and Q_2 . In this case, the entanglement generated between the two masses at the end of the experiment will be influenced by QED interactions, which can disturb the pure quantum gravitational interaction.

Another source of disturbance that can happen at this stage of the experiment is the

interaction with the environment: for example, it is possible that inside the experimental box in which the experiment is performed there are some air molecules. These objects can possess an electric dipole moment d , which can interact with some dipoles D present inside the massive object in superposition, generating a dipole-dipole interaction of the form $V(r) \sim 1/r^3$. In this case (which will be explicitly analyzed in the next chapters of this work), decoherence effects constitute an important role in the final stage of the experiment, during which will be not possible to *coherently* recompose the initial state $|C\rangle_i$, leading to a disappearance of the interference term of the massive quantum particle, which clearly disturbs the final analysis for the reading of entanglement correlations between the two sets of data.

In particular, these analysis will be performed in the **Third Step** of the experiment, during which both the objects are brought back in a well defined position through a refocusing SG apparatus. At this moment, it becomes viable to independently measure both systems, with the intention of detecting manifestations of entanglement being established. But let us analyze more in detail the final quantum state of the total composite system \mathcal{H} . We know that the time evolution of a system is given by the total Hamiltonian \hat{H} , which in our case is will contain a term like:

$$\hat{H}_{int} = -G \frac{m_1 m_2}{|\vec{x}_1 - \vec{x}_2|} \equiv E(|\vec{x}_1 - \vec{x}_2|), \quad (2.49)$$

where $|\vec{x}_1 - \vec{x}_2|$ represents the distance between the two masses. This means that each term of Eq.(2.47) will have a different phase contribution during the time evolution, given that each branch of the scheme 2.2 will be influenced by different gravitational energies at different distances. In particular, for example, the term $|L\rangle_1 |L\rangle_2$ has a gravitation energy given by $E(d) = -G \frac{m_1 m_2}{d}$, given that the separation distances between the branches L_1 and L_2 is d .

More in detail, the final state $|\Psi(\tau)\rangle$ of the composite system will be given by:

$$\begin{aligned} |\Psi(\tau)\rangle &= \frac{1}{2} [e^{\frac{i}{\hbar} E(d)\tau} |L\rangle_1 |L\rangle_2 + e^{\frac{i}{\hbar} E(d+\Delta x)\tau} |L\rangle_1 |R\rangle_2 + \\ &\quad + e^{\frac{i}{\hbar} E(d-\Delta x)\tau} |R\rangle_1 |L\rangle_2 + e^{\frac{i}{\hbar} E(d)\tau} |R\rangle_1 |R\rangle_2] = \quad (2.50) \\ &= \frac{e^{i\phi}}{2} [|L\rangle_1 |L\rangle_2 + e^{i\Delta\phi_+} |L\rangle_1 |R\rangle_2 + e^{i\Delta\phi_-} |R\rangle_1 |L\rangle_2 + |R\rangle_1 |R\rangle_2], \end{aligned}$$

where in the very last line we have introduced the following phases:

$$\begin{cases} \phi \equiv \frac{E(d)\tau}{\hbar} \\ \Delta\phi_+ \equiv \frac{1}{\hbar} [E(d+\Delta x) - E(d)] \tau \\ \Delta\phi_- \equiv \frac{1}{\hbar} [E(d-\Delta x) - E(d)] \tau \end{cases} . \quad (2.51)$$

We are now able to find the density matrix $\hat{\rho}_1$ associated to the massive quantum system of mass m_1 . In particular, we can define the total density matrix as $\hat{\rho} = |\Psi(\tau)\rangle \langle \Psi(\tau)|$ and then trace out the degrees of freedom of the system m_2 . In order to do that, remember that the actual states associated to the two massive systems contains the spin degrees of freedom, i.e. $|L, \uparrow_i\rangle$ and $|R, \downarrow_i\rangle$. This means that we have an orthonormal basis for the system m_2 , given by $\{|L, \uparrow_i\rangle, |R, \downarrow_i\rangle\}$. In this way, we obtain:

$$\hat{\rho}_1 = \frac{1}{2} \left(|L\rangle_{11} \langle L| + |R\rangle_{11} \langle R| \right) + \frac{1}{4} \left[\left(e^{i\Delta\phi_+} + e^{-i\Delta\phi_-} \right) |L\rangle_{11} \langle R| + H.c. \right], \quad (2.52)$$

where we are continuing to use the notation $\{|L\rangle_i, |R\rangle_i\} \equiv \{|L, \uparrow_i\rangle, |R, \downarrow_i\rangle\}$ for brevity.

Let us focus our attention to the last term of this equation, particularly on the following term:

$$\left(e^{i\Delta\phi_+} + e^{-i\Delta\phi_-} \right) = e^{-i\Delta\phi_-} \left(e^{i(\Delta\phi_+ + \Delta\phi_-)} + 1 \right). \quad (2.53)$$

At this point, we are going to proceed by making the following assumption regarding our setup:

$$d - \Delta x \ll d, \Delta x \quad (2.54)$$

which basically means that, from figure 2.2, the branch R_1 and L_2 are the closest pair of branches of the setup, in which the gravitational interaction is stronger.

Now, because $\phi \sim E(d) \sim 1/d$, we have that:

$$E(d - \Delta x) \gg E(d), E(d + \Delta x) \longrightarrow \Delta\phi_- \gg \phi, \Delta\phi_+. \quad (2.55)$$

This means that we can approximate Eq.(2.52) in the following way:

$$\hat{\rho}_1 \simeq \frac{1}{2} \left(|L\rangle_{11} \langle L| + |R\rangle_{11} \langle R| \right) + \frac{1}{4} \left[e^{-i\Delta\phi_-} \left(e^{-i\Delta\phi_-} + 1 \right) |L\rangle_{11} \langle R| + H.c. \right] \quad (2.56)$$

From Eq.(2.56) it is clear how entanglement is generated: in particular, if the data of the setup are such that $\Delta\phi_- \sim \pi \sim O(1)$, we have that $e^{i\Delta\phi_-} + 1 = 0$, which results in:

$$\hat{\rho}_1 \simeq \frac{1}{2} \left(|L\rangle_{11} \langle L| + |R\rangle_{11} \langle R| \right). \quad (2.57)$$

This expression for $\hat{\rho}_1$ represents a mixed state, where all the off-diagonal terms are suppressed. In this case, the entanglement between the system m_1 and m_2 is maximum. Entanglement has thus been generated between the two masses, only through gravitational interaction.

A final consideration should be made on this result. Remember that the spatial superposition was created through a spin superposition, as can be seen from Eq.(2.48). The actual final state is thus given in terms of the states $|L\rangle_i \rightarrow |L, \uparrow_i\rangle$ and $|R\rangle_i \rightarrow |R, \uparrow_i\rangle$. This is an important distinction to make, because in the very final step of the experiment the massive object will be brought back to a well defined spatial position $|C\rangle_i$. Therefore, only the spin degrees of freedom will be entangled in the end:

$$\begin{aligned} \hat{\rho}_1 &\simeq \frac{1}{2} \left(|L\rangle_{11} \langle L| + |R\rangle_{11} \langle R| \right) \equiv \frac{1}{2} \left(|L, \uparrow_1\rangle \langle L, \uparrow_1| + |R, \downarrow_1\rangle \langle R, \downarrow_1| \right) \rightarrow \\ &\rightarrow |C\rangle_{11} \langle C| \otimes \frac{1}{2} \left(|\uparrow_1\rangle \langle \uparrow_1| + |\downarrow_1\rangle \langle \downarrow_1| \right). \end{aligned} \quad (2.58)$$

Let us now outline some numbers that can be used in a QGEM experiment. In particular, how can we obtain the condition $\Delta\phi_- = \frac{1}{\hbar} [E(d - \Delta x) - E(d)] \tau \sim \pi$ useful to obtain the maximum entangled state of Eq.(2.58)? We can begin by considering particles with the highest achievable masses, specifically $m_1 \approx m_2 \approx 10^{-14} kg$. Realistic proposals have already been put forward to create superpositions of spatially separated states for such particles. Typically, these masses are associated to micro-crystals (such as diamonds) with dimensions given by a radius of $R \sim 10^{-6} m, 10^{-7} m$. As for the distances, it is possible to realize superposition of the order of $\Delta x \sim 10^{-5} m \sim d$, in order to have:

$$\begin{aligned} \Delta\phi_- &\equiv \frac{1}{\hbar} [E(d - \Delta x) - E(d)] \tau \simeq E(d - \Delta x) \frac{\tau}{\hbar} \\ &= \frac{Gm^2\tau}{(d - \Delta x)\hbar} \sim \frac{10^{-11} \cdot (10^{-14})^2 \cdot 1}{10^{-5} 10^{-34}} \sim O(1), \end{aligned} \quad (2.59)$$

where we have considered a time τ of the order of the seconds $\tau \sim 1 s$. Therefore, with this values we are able to obtain a final quantum state of the desired form, like in Eq.(2.58).

Chapter 3

Decoherence due to Electromagnetic interaction

The idea that matter can behave as a wave is key conceptual leap of modern physics, with matterwave interferometry one of the central experimental techniques of quantum mechanics. It is the basis for the notion of quantum superposition [3] and it is building block of quantum entanglement, features that cannot be mimicked by a classical theory [25]. Matter-wave interferometry has been also used in a series of fundamental experiments to demonstrate gravitationally-induced interference with neutrons and atoms. Furthermore, matter-wave interferometers can be excellent quantum sensors [20, 26] and can act as probes of physics beyond the standard model [24].

It was further suggested that the next generation of matter-wave interferometers with nanoparticles will be sensitive enough to probe gravitationally-induced entanglement. Known as a quantum gravity-induced entanglement of masses (QGEM) [14, 15]¹, the scheme shows that if gravity is inherently a quantum entity then the masses of two nearby interferometers will entangle when placed sufficiently close. The key observation is that as long as we follow the standard relativistic quantum mechanics, locality/causality, and general relativity in an effective field theory of quantum gravity the two quantum superposed masses will inevitably entangle each other via the quantum gravitational interaction [14, 28, 23, 29, 30, 31, 32, 33, 34, 35, 16], while classical gravity cannot entangle the two quantum systems as formalized by the local operation and classical communication (LOCC) theorem [36, 14, 28, 23]. Recently, the QGEM protocol was also extended to test the quantum nature of gravity in an optomechanical setup where we can test the quantum gravitational entanglement between matter and photon [37].

However, there are many experimental challenges to be resolved before interferometry with nanoparticles can be implemented. To name a few, creating spatial quantum superpositions [14, 38, 14, 39, 40, 41, 42, 43, 44, 45, 46, 47, 48, 49, 50], ensuring sufficiently

¹The first reporting of the results of the QGEM protocol [14] was in a conference in 2016 [27].

long coherence times [14, 51, 52, 45, 53, 54, 55, 18, 56, 57], and protecting the experiment from external jitters, gravity gradient noise and seismic noise [58].

The aim of this chapter will be to investigate dipole-dipole decoherence in matter-wave interferometry with nanoparticles. Such channel of decoherence is unavoidable and must be taken into account even with a neutral nanocrystals [59, 60]. We will start from the QED lagrangian and obtain the evolution of the density matrix. We will then study the dipole-dipole interaction in a short wavelength and a long wavelength limit. Finally we will apply the obtained formulae to put constraints on the crystal and environmental parameters in the QGEM protocol.

3.1 Hamiltonian construction

We assume that the matter-wave interferometer is in an environment that is large enough and changes slowly enough with respect to the closure of the one-loop interferometer, e.g. we are seeking interaction time $t \ll \tau$, where τ is the time scale of the interferometer.

In particular, we assume that we employ a nano-crystal that is neutral, but it will interact electromagnetically via an interaction term:

$$\mathcal{L} = -e\bar{\psi}\gamma^\mu\psi A_\mu, \quad (3.1)$$

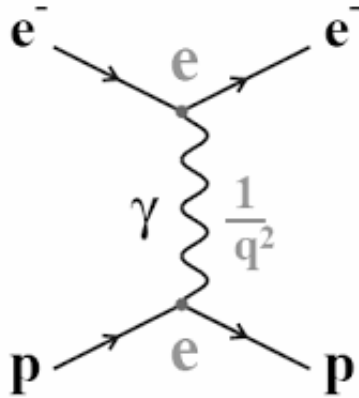


Figure 3.1: Schematic representation of a typical QED interaction between two charged systems e and p at the tree level.

where ψ is the fermion field related to an environmental particle, A_μ is the photon field through which the environment interacts with the crystal, γ^μ represent the Dirac's matrices and e is the electron's charge. Here $\mu = 0, 1, 2, 3$, and we take the signature

(-,+,+,+). The corresponding Hamiltonian interaction is given by:

$$H_{int} = - \int d^3\mathbf{x} \mathcal{L}(\mathbf{x}) = \int d^3\mathbf{x} e^{i\mathbf{p}_f \cdot \mathbf{x}} \bar{\psi} \gamma^\mu \psi A_\mu. \quad (3.2)$$

Let's first evaluate:

$$\bar{\psi} \gamma^\mu \psi = \int \frac{d^3\mathbf{p}_i d^3\mathbf{p}_f}{(2\pi)^6 \sqrt{4E_{p_i} E_{p_f}}} \hat{a}_{p_f}^\dagger \hat{a}_{p_i} e^{-i(\mathbf{p}_i - \mathbf{p}_f) \cdot \mathbf{x}} \bar{u}_{p_f} \gamma^\mu u_{p_i}, \quad (3.3)$$

where \hat{a} (\hat{a}^\dagger) are the destruction (creation) operator of the environmental fermionic field and the u are the spinors. We also assume that there is no anti-particle (e.g. positron) in the on-shell state.

The other quantum field that appears in Eq.(3.1) is a generic EM field $A_\mu(\mathbf{x})$. Now, in our case, this term can be related to the crystal in spatial superposition by considering its fermion current $J_\mu(\mathbf{x})$ associated to the object; in particular, from the Maxwell's equations we have that:

$$A_\mu(\mathbf{x}) = \square^{-1} J_\mu(\mathbf{x}), \quad (3.4)$$

which in the momentum space becomes:

$$\tilde{A}_\mu(\mathbf{q}) = \frac{-i g_{\mu\nu}}{q^2} \tilde{J}^\nu(\mathbf{x}), \quad (3.5)$$

Also add a figure indicating an interferometer and an environmental particle. In doing so, we will be able to find an explicit expression for the matter-matter interaction Hamiltonian in Eq.(3.2) of the environment-system interaction.

The fermion current introduced in Eq.(3.4) can be expressed as:

$$J^\mu(\mathbf{x}) = \bar{\Psi} \gamma^\mu \Psi = \int \frac{d^3\mathbf{k}_i d^3\mathbf{k}_f}{(2\pi)^6 \sqrt{4E_{k_i} E_{k_f}}} \hat{c}_{k_f}^\dagger \hat{c}_{k_i} e^{-i(\mathbf{k}_i - \mathbf{k}_f) \cdot \mathbf{x}} \bar{U}_{k_f} \gamma^\mu U_{k_i} \quad (3.6)$$

where the \hat{c} 's are the creation/destruction operator of the fermion crystal's field and the U 's its spinors.

This leads to:

$$\tilde{J}^\nu(\mathbf{q}) = \int d^3\mathbf{x} e^{i\mathbf{q} \cdot \mathbf{x}} J^\nu(\mathbf{x}) = \int \frac{d^3\mathbf{k}_i d^3\mathbf{k}_f}{(2\pi)^6 \sqrt{4E_{k_i} E_{k_f}}} \hat{c}_{k_f}^\dagger \hat{c}_{k_i} \bar{U}_{k_f} \gamma^\mu U_{k_i} \delta^3(\mathbf{q} + \mathbf{k}_i - \mathbf{k}_f). \quad (3.7)$$

Plugging Eq.(3.7) into Eq.(3.2) through:

$$A_\mu(\mathbf{x}) = \int d^3\mathbf{q} e^{-i\mathbf{q} \cdot \mathbf{x}} \tilde{A}_\mu(\mathbf{q}) = \int d^3\mathbf{q} e^{-i\mathbf{q} \cdot \mathbf{x}} \frac{-i g_{\mu\nu}}{q^2} \tilde{J}^\nu(\mathbf{q}), \quad (3.8)$$

one obtains:

$$\begin{aligned} \hat{H}_{int} = (2\pi)^3 e \int \frac{d^3\mathbf{p}_i d^3\mathbf{p}_f d^3\mathbf{k}_i d^3\mathbf{k}_f}{(2\pi)^{12} \sqrt{16 E_{p_i} E_{p_f} E_{k_i} E_{k_f}}} \hat{a}_{p_f}^\dagger \hat{a}_{p_i} \hat{c}_{k_f}^\dagger \hat{c}_{k_i} \\ \times \delta^3(\mathbf{k}_i + \mathbf{p}_i - \mathbf{k}_f - \mathbf{p}_f) \bar{u}_{p_f} \gamma^\mu u_{p_i} \frac{-i g_{\mu\nu}}{q^2} \bar{U}_{k_f} \gamma^\nu U_{k_i}. \end{aligned} \quad (3.9)$$

Notice that the last term in the RHS is exactly the quantum electrodynamics (QED) matrix element for the fermion-fermion interaction $\mathcal{M}_{p_i, p_f, k_i, k_f}$ [5]:

$$\begin{aligned} \hat{H}_{int} = (2\pi)^3 e \int \frac{d^3\mathbf{p}_i d^3\mathbf{p}_f d^3\mathbf{k}_i d^3\mathbf{k}_f}{(2\pi)^{12} \sqrt{16 E_{p_i} E_{p_f} E_{k_i} E_{k_f}}} \times \\ \hat{a}_{p_f}^\dagger \hat{a}_{p_i} \hat{c}_{k_f}^\dagger \hat{c}_{k_i} \delta^3(\mathbf{k}_i + \mathbf{p}_i - \mathbf{k}_f - \mathbf{p}_f) \mathcal{M}_{p_i, p_f, k_i, k_f}. \end{aligned} \quad (3.10)$$

In particular, one can express the \hat{a} 's (or \hat{c} 's) in terms of one particle states $|\mathbf{k}\rangle$ (or $|\mathbf{p}\rangle$) through the relation $|\mathbf{k}\rangle = \sqrt{2E_k} \hat{a}_k |0\rangle$ (or $|\mathbf{p}\rangle = \sqrt{2E_p} \hat{c}_p |0\rangle$). In particular, the operator $\hat{A} \equiv \hat{a}_{p_f}^\dagger \hat{a}_{p_i}$ *destroys* a particle with momentum \vec{p}_i and *creates* a particles with momentum \vec{p}_f . This means that the action of this operator can be written as:

$$\hat{A} : |\mathbf{p}_i\rangle \longrightarrow |\mathbf{p}_f\rangle. \quad (3.11)$$

Now, we can write the creation operator \hat{a}_k^\dagger (which acts on the vacuum as $|\mathbf{k}\rangle = \sqrt{2E_k} \hat{a}_k |0\rangle$) in the momentum basis representation $\{|\mathbf{k}\rangle\}$ as:

$$\hat{a}_k^\dagger = \frac{1}{\sqrt{2E_k}} |\mathbf{k}\rangle \langle 0|. \quad (3.12)$$

Because of this property, the operator \hat{A} becomes:

$$\hat{A} \equiv \hat{a}_{p_f}^\dagger \hat{a}_{p_i} = \frac{1}{\sqrt{2E_{p_i}} \sqrt{2E_{p_f}}} |\mathbf{p}_f\rangle \langle 0| \langle \mathbf{p}_i| = \frac{1}{\sqrt{2E_{p_i}} \sqrt{2E_{p_f}}} |\mathbf{p}_f\rangle \langle \mathbf{p}_i|, \quad (3.13)$$

which satisfies Eq.(3.11).

This means that Eq.(3.10) gives the following form for the Hamiltonian interaction \hat{H}_{int} :

$$\begin{aligned} \hat{H}_{int} = \int \frac{d^3\mathbf{p}_i d^3\mathbf{p}_f d^3\mathbf{k}_i}{(2\pi)^9 16 E_{p_i} E_{p_f} E_{k_i} E_{k_i+p_i-p_f}} \\ \times \mathcal{M}_{p_i, p_f, k_i, k_i+p_i-p_f} |\mathbf{p}_f\rangle \langle \mathbf{p}_i| e^{i(\mathbf{p}_i - \mathbf{p}_f) \cdot \hat{\mathbf{x}}} |\mathbf{k}_i\rangle \langle \mathbf{k}_i|, \end{aligned} \quad (3.14)$$

²One can indeed verify that the action on the vacuum $|0\rangle$ of this operator is $\frac{1}{\sqrt{2E_k}} |\mathbf{k}\rangle \langle 0| = \frac{1}{\sqrt{2E_k}} |\mathbf{k}\rangle \cdot 1 = \frac{1}{\sqrt{2E_k}} |\mathbf{k}\rangle$, which is exactly the definition of creation operator.

where the Dirac's delta $\delta^3(\mathbf{k}_i + \mathbf{p}_i - \mathbf{k}_f - \mathbf{p}_f)$ has been solved in $d^3\mathbf{k}_f$ and its vector state $|\mathbf{k}_f\rangle \rightarrow |\mathbf{k}_i + \mathbf{p}_i - \mathbf{p}_f\rangle$ has been expressed in terms of the translation operator, which generates translations in the momenta space through the position operator $\hat{\mathbf{x}}$, i.e. $|\mathbf{k}_i + \mathbf{p}_i - \mathbf{p}_f\rangle = e^{i(\mathbf{p}_i - \mathbf{p}_f) \cdot \hat{\mathbf{x}}} |\mathbf{k}_i\rangle$.

We are now able to make some approximations. In fact, in the experiment, the environmental particle's momenta are very low due to the low value of the ambient temperature (e.g., $T \sim 1$ K). This means that $p_i, p_f \ll M$ ³, where M is the nano-crystal's mass. In this way, we have $k_i, k_f \sim 0$ and, in general, $k_i, k_f \ll M$. In other words, we assume the diamond to be stationary initially and much heavier than the environmental particle, so that its momentum does not change. This allows us to approximate the matrix element in Eq.(3.14) as $\mathcal{M}_{p_i, p_f, k_i, k_i + p_i - p_f} \sim \mathcal{M}_{p_i, p_f, 0, 0}$.

Since the nano-crystal is heavy w.r.t. the ambient energy, we can further approximate $2E_{k_i} 2E_{k_i + p_i - p_f} \sim 4ME_{k_i}$. Finally, integrating over k_i and using the identity $\int \frac{d^3\mathbf{k}_i}{(2\pi)^3 2E_{k_i}} |\mathbf{k}_i\rangle \langle \mathbf{k}_i| = \mathbb{I}$, we can obtain the final expression for Eq.(3.2):

$$\hat{H}_{int} = \int \frac{d^3\mathbf{p}_i d^3\mathbf{p}_f}{(2\pi)^6 2E_{p_i} 2E_{p_f}} \frac{\mathcal{M}_{p_i, p_f}}{2M} |\mathbf{p}_f\rangle \langle \mathbf{p}_i| \otimes e^{i(\mathbf{p}_i - \mathbf{p}_f) \cdot \hat{\mathbf{x}}} \mathbb{I}. \quad (3.15)$$

3.2 Born-Markov Master Equation for QED interactions

In order to find the Born-Markov Master Equation for the decoherence of the crystal due to the environment, we start by supposing that the interaction Hamiltonian has the general form [18, 19]:

$$\hat{H}_{int} = \sum_{\alpha} \hat{S}_{\alpha} \otimes \hat{E}_{\alpha}, \quad (3.16)$$

where \hat{S}_{α} and \hat{E}_{α} represent all the degrees of freedom of the matter-wave interferometer and the environment involved in the EM interaction.

From Eq.(3.15) one can find the explicit expression for \hat{S}_{α} and \hat{E}_{α} :

$$\begin{cases} \hat{S}_{\alpha} = \frac{e^{i(\mathbf{p}_i - \mathbf{p}_f) \cdot \hat{\mathbf{x}}}}{2M} \mathbb{I} \\ \hat{E}_{\alpha} = \mathcal{M}_{p_i, p_f} |\mathbf{p}_f\rangle \langle \mathbf{p}_i| \end{cases},$$

which are the same formulas found in [20] for scattering between neutrino and a heavy nucleus mediated by the weak interaction, in which the matrix element \mathcal{M}_{p_i, p_f} is given by:

$$\mathcal{M}_{p_i, p_f} \propto G_F Q_W F(q^2) \bar{u}(p_f) \gamma^{\mu} (1 - \gamma^5) u(p_i) (k_i + k_f)_{\mu}, \quad (3.17)$$

³Here, p_i means $p_i \equiv |\mathbf{p}_i|$. The same applies for k_i later.

where G_F is the Fermi coupling constant, Q_W is the crystal's weak charge, $F(q^2)$ is its form factor, $\bar{u}(p_f)$ and $u(p_i)$ are the environmental particle's spinors and $J_\mu \propto (k_i + k_f)_\mu$ is the crystal's four-current.

Now that we have an expression for \hat{H}_{int} , we can finally use the master equation for the decoherence with the Born-Markov approximation:

$$\frac{d\rho_S}{dt} = -\frac{i}{\hbar} [H_S, \rho_S] - \left\{ \int_0^\infty d\tau \sum_{\alpha\beta} C_{\alpha\beta}(-\tau) [S_\alpha S_\beta(-\tau)\rho_S - S_\beta(-\tau)\rho_S S_\alpha] + \text{H.c.} \right\}, \quad (3.18)$$

where

$$C_{\alpha\beta} = \frac{1}{\hbar^2} \text{Tr} [\rho_E E_\alpha E_\beta(-\tau)] \quad (3.19)$$

and

$$\begin{aligned} S_\beta(-\tau) &= e^{-\frac{iH_S\tau}{\hbar}} S_\beta e^{\frac{iH_S\tau}{\hbar}}, \\ E_\beta(-\tau) &= e^{-\frac{iH_E\tau}{\hbar}} E_\beta e^{\frac{iH_E\tau}{\hbar}}. \end{aligned} \quad (3.20)$$

The basic assumptions of the Born-Markov Master Equation are two: the Born approximation, where the environment is considered to be much larger than the system and the coupling between S and \mathcal{E} is weak enough that it is possible at all times to write the composite $S + \mathcal{E}$ system as a tensorial product:

$$\hat{\rho}_{S+\mathcal{E}}(t) \approx \hat{\rho}_S(t) \otimes \hat{\rho}_\mathcal{E}, \quad (3.21)$$

where $\hat{\rho}_\mathcal{E}$ is approximately constant at all times. The other assumption is the Markov approximation, in which it is supposed that memory effects in the environment are negligible, i.e. any effect that the system has on the environment decays rapidly compared to the evolution of the environment \mathcal{E} itself.

Further, we argue that the COM of the crystal is trapped in a very low frequency trap, so that the time evolution of the operator S_β can be neglected with respect to the correlation time-scale of the environment. Moreover, we will assume that the *unitary* time evolution of the crystal, given by the term $-\frac{i}{\hbar} [H_S, \rho_S]$ of Eq.(3.18), is much slower than the *non-unitary* time evolution given by the second term of the RHS of Eq.(3.18), which corresponds to changes of the system entirely due to the decoherence. This means that the decoherence due to the presence of the environment modifies the state of the system faster than any *free* evolution of the system itself. For this reasons, in the derivation of the decoherence rate below, we will neglect the unitary term $-\frac{i}{\hbar} [H_S, \rho_S]$.

From Eq.(3.19), one can notice that an expression for $\hat{\rho}_E = |\Psi\rangle\langle\Psi|$ is needed. In our case, we will consider the environmental particles to have a (normalized) wave function with a localized momentum \mathbf{p}_0 . Therefore, we will represent it using a Gaussian

wavepacket centered in \mathbf{p}_0 in the momentum space, as follows:

$$|\psi\rangle = \int \frac{d^3\mathbf{p}}{(2\pi)^3\sqrt{2E_p}} \tilde{\psi}(p) |\mathbf{p}\rangle = \int \frac{d^3p}{(2\pi)^3\sqrt{2E_p}} \frac{(2\pi)^{3/2}}{(\pi\tilde{\sigma}^2)^{3/4}} e^{-\frac{|\mathbf{p}-\mathbf{p}_0|^2}{2\tilde{\sigma}^2}} |\mathbf{p}\rangle. \quad (3.22)$$

With this expression for $\hat{\rho}_E$, we are able to compute Eq.(3.19):

$$\begin{aligned} C_{\alpha,\beta} &= Tr[\rho_E E_\alpha E_\beta(-\tau)] = \langle E_\alpha E_\beta(-\tau) \rangle_\psi = (2\pi)^3 \mathcal{M}_{p_i,p_f} \mathcal{M}_{p'_f,p'_i}^* 2E_{p_i} \delta^3(\mathbf{p}_i - \mathbf{p}'_f) \\ &\times \langle \psi | e^{-i\left(E_{p'_i} - E_{p'_f}\right)\tau} | \mathbf{p}_f \rangle \langle \mathbf{p}'_i | \psi \rangle = (2\pi)^9 \pi^{-3/2} \tilde{\sigma}^3 \mathcal{M}_{p_i,p_f} \mathcal{M}_{p'_f,p'_i}^* 2E_{p_i} \delta^3(\mathbf{p}_i - \mathbf{p}'_f) \\ &\times e^{-i\left(E_{p'_i} - E_{p'_f}\right)\tau} 2E_{p'_i} \delta^3(\mathbf{p}_0 - \mathbf{p}_f) \delta^3(\mathbf{p}'_i - \mathbf{p}_0), \end{aligned} \quad (3.23)$$

where we have used the following two properties:

$$\begin{cases} \langle \mathbf{p} | \mathbf{k} \rangle = (2\pi)^3 (2E_p) \delta^3(\mathbf{p} - \mathbf{k}) \\ \delta^3(\mathbf{p}) = \lim_{\tilde{\sigma} \rightarrow 0} \frac{1}{\tilde{\sigma}^3 \pi^{3/2}} e^{-|\mathbf{p}|^2/\tilde{\sigma}^2} \end{cases}, \quad (3.24)$$

the last one meaning that the Gaussian wavepacket of the environmental particle is sharpened enough that can be considered as a Dirac's delta, i.e. the particle has a well defined momentum \mathbf{p}_0 .

Plugging Eq.(3.17) into the second term of the right hand side of Eq.(3.19) (and neglecting the unitary term $-\frac{i}{\hbar} [H_S, \rho_S]$ as specified above), one obtains:

$$\begin{aligned} \frac{d\hat{\rho}_S}{dt} &= -\frac{\pi^{-3/2}\tilde{\sigma}^3}{4M^2} \int d\tau \frac{d^3\mathbf{p}_i d^3\mathbf{p}_f d^3\mathbf{p}'_i d^3\mathbf{p}'_f}{(2\pi)^3 16E_{p_i} E_{p_f} E_{p'_i} E_{p'_f}} 4E_{p_i} E_{p'_i} \mathcal{M}_{p_i,p_f} \mathcal{M}_{p'_i,p'_f}^* \delta^3(\mathbf{p}_i - \mathbf{p}'_f) \\ &\times e^{-i(E_{p'_i} - E_{p'_f})\tau} \delta^3(\mathbf{p}_0 - \mathbf{p}_f) \delta^3(\mathbf{p}'_i - \mathbf{p}_0) \{ -e^{i(\mathbf{p}'_i - \mathbf{p}'_f) \cdot \hat{\mathbf{x}}} \hat{\rho}_S e^{i(\mathbf{p}'_f - \mathbf{p}_f) \cdot \hat{\mathbf{x}}} \\ &\quad + e^{i(\mathbf{p}_i - \mathbf{p}_f) \cdot \hat{\mathbf{x}}} e^{i(\mathbf{p}'_i - \mathbf{p}'_f) \cdot \hat{\mathbf{x}}} \hat{\rho}_S + H.c. \}, \end{aligned} \quad (3.25)$$

which leads to:

$$\begin{aligned} \frac{d\hat{\rho}_S}{dt} &= -\frac{\pi^{-3/2}\tilde{\sigma}^3}{64\pi^2 M^2 E_{p_0}} \int \frac{d^3\mathbf{p}'_f}{E_{p'_f}} |\mathcal{M}_{p_0,p'_f}|^2 \delta(E_{p_0} - E_{p'_f}) \\ &\times \{ -e^{i(\mathbf{p}_0 - \mathbf{p}'_f) \cdot \hat{\mathbf{x}}} \hat{\rho}_S e^{i(\mathbf{p}'_f - \mathbf{p}_0) \cdot \hat{\mathbf{x}}} + e^{i(\mathbf{p}'_f - \mathbf{p}_0) \cdot \hat{\mathbf{x}}} e^{i(\mathbf{p}_0 - \mathbf{p}'_f) \cdot \hat{\mathbf{x}}} \hat{\rho}_S + H.c. \}. \end{aligned} \quad (3.26)$$

Solving $\delta(E_{p_0} - E_{p'_f})$ and using $dp'_f = \frac{E_{p'_f}}{p'_f} dE_{p'_f}$ ⁴ we have:

$$\frac{d\hat{\rho}_S}{dt} = -\frac{\pi^{-3/2}\tilde{\sigma}^3}{64\pi^2 M^2} \frac{p_0}{E_{p_0}} \int d\Omega' |\mathcal{M}_{p_0,p'_f}|^2 \{ -e^{i(\mathbf{p}_0 - \mathbf{p}'_f) \cdot \hat{\mathbf{x}}} \hat{\rho}_S e^{i(\mathbf{p}'_f - \mathbf{p}_0) \cdot \hat{\mathbf{x}}} + \hat{\rho}_S + H.c. \}, \quad (3.27)$$

⁴Again, here $p'_f \equiv |\mathbf{p}'_f|$

where $d\Omega'$ indicates the orientation angle of the final momentum vector $d^3\mathbf{p}_f = d\Omega' dp_f p_f^2$.

Notice that, having now $E_{p_0} = E_{p'_f}$, we have that $|\mathbf{p}_0| = |\mathbf{p}'_f|$ too. This means also that the matrix element \mathcal{M}_{p_0, p'_f} will now depend only on $|\mathbf{p}_0|$ and the angle between \mathbf{p}_0 and \mathbf{p}'_f , i.e. on Ω' . We can also rewrite the $\frac{p_0}{E_{p_0}}$ term as:

$$\frac{p_0}{E_{p_0}} = \frac{\frac{mv_0}{\sqrt{1-v_0^2}}}{\sqrt{p_0^2 + m^2}} = \frac{\frac{mv_0}{\sqrt{1-v_0^2}}}{\sqrt{\frac{m^2 v_0^2}{1-v_0^2} + m^2}} = v_0. \quad (3.28)$$

Notice also that the factor $\mathbf{p}'_f - \mathbf{p}_0$ at the exponent of the right-hand side can be rewritten as $|\mathbf{p}_0|(\hat{n}' - \hat{n}_0)$, where \hat{n}' and \hat{n}_0 are the final and initial direction of the scattered environmental particle (we will express their associated angles with, respectively, Ω' and Ω_0). We can thus rewrite the time evolution equation for ρ_S as:

$$\begin{aligned} \frac{d\hat{\rho}_S}{dt} &= -\frac{\pi^{-3/2}\tilde{\sigma}^3}{64\pi^2 M^2} v_0 \int d\Omega' |\mathcal{M}(\Omega', \Omega_0, E_0)|^2 \\ &\times \{ -e^{-i|\mathbf{p}_0|(\hat{n}' - \hat{n}_0) \cdot \hat{\mathbf{x}}} \hat{\rho}_S e^{i|\mathbf{p}_0|(\hat{n}' - \hat{n}_0) \cdot \hat{\mathbf{x}}} + \hat{\rho}_S + H.c. \}. \end{aligned} \quad (3.29)$$

Now, the factor $\pi^{-3/2}\tilde{\sigma}^3$ it is proportional to the inverse of the volume $1/V$ (see Eq.(A.2)). This means that now will appear, on the right-hand side of Eq.(3.29), a term like $v_0/V = F_1$, which is exactly the flux associated with one environmental particle. This leads us to rewrite Eq.(3.29) as:

$$\begin{aligned} \frac{d\hat{\rho}_S}{dt} &= -\frac{(2\pi)^{3/2}F_1}{64\pi^2 M^2} \int d\Omega' |\mathcal{M}(\Omega', \Omega_0, E_0)|^2 \\ &\times \{ -e^{-i|\mathbf{p}_0|(\hat{n}' - \hat{n}_0) \cdot \hat{\mathbf{x}}} \hat{\rho}_S e^{i|\mathbf{p}_0|(\hat{n}' - \hat{n}_0) \cdot \hat{\mathbf{x}}} + \hat{\rho}_S + H.c. \}, \end{aligned} \quad (3.30)$$

which gives the following expression for the matrix elements of $\hat{\rho}_S$:

$$\begin{aligned} \frac{d\rho_S}{dt}(\mathbf{x}, \mathbf{y}, t) &= -\frac{(2\pi)^{3/2}F_1}{64\pi^2 M^2} \int d\Omega' |\mathcal{M}(\Omega', \Omega_0, E_0)|^2 \\ &\times \{ -e^{-ip_0(\hat{n}' - \hat{n}_0) \cdot (\mathbf{x} - \mathbf{y})} + 1 \} \rho_S(\mathbf{x}, \mathbf{y}, t), \end{aligned} \quad (3.31)$$

where we have defined $\langle \mathbf{x} | \hat{\rho}_S | \mathbf{y} \rangle \equiv \rho_S(\mathbf{x}, \mathbf{y}, t)$.

We can also notice that the term $\frac{1}{64\pi^2 M^2} |\mathcal{M}(\Omega', \Omega_0, E_0)|^2$ is exactly the differential cross section $\frac{d\sigma}{d\Omega'} = \frac{d\sigma}{d\Omega'}(\hat{n}_0, \hat{n}')$ (see (A.1)). Notice that Eq.(3.31) is of the same form of the result found in [20], but with scattering amplitude given by Eq.(3.17).

Eq.(3.31) describes the decoherence due to the interaction between one environmental particle and the nano-crystal. It is easy to generalize it to the case where, instead of having only one, we have N environmental particles. This results in flux as

$$F = n\bar{v} = \frac{N}{V}\bar{v}, \quad (3.32)$$

where \bar{v} is the average velocity of each environmental particle. More in general, if each particle gives a contribution of the type Eq.(3.31) to the decoherence rate, the total contribution will be given by the sum over all possible momenta \mathbf{p}_0 (and velocities \mathbf{v}_0) weighted by a distribution of particles $\mu(\mathbf{p}_0)$ in the momentum space, i.e. a probabilistic distribution such that $\int d^3\mathbf{p}_0 \mu(\mathbf{p}_0) = 1$. It is possible to go even further if we make the assumption that the environment is composed of particles that are *isotropically* distributed:

$$\mu(\mathbf{p}_0)d^3\mathbf{p}_0 = \frac{1}{4\pi}S(p_0)dp_0 d\Omega_0, \quad (3.33)$$

where $\int dp_0 S(p_0) = 1$, in order to have $\int d^3\mathbf{p}_0 \mu(\mathbf{p}_0) = 1$. This gives:

$$\begin{aligned} \frac{d\rho_S}{dt}(\mathbf{x}, \mathbf{y}, t) &= -(2\pi)^{\frac{3}{2}} \int dp_0 S(p_0) nv(p_0) \\ &\times \int \frac{d\Omega_0 d\Omega'}{4\pi} \frac{d\sigma}{d\Omega'} \left\{ -e^{-ip_0(\hat{n}' - \hat{n}_0) \cdot (\mathbf{x} - \mathbf{y})} + 1 \right\} \rho_S(\mathbf{x}, \mathbf{y}, t), \end{aligned} \quad (3.34)$$

from which we can define the so-called Decoherence Rate factor Γ :

$$\Gamma \equiv (2\pi)^{3/2} \int dp_0 S(p_0) nv(p_0) \int \frac{d\Omega_0 d\Omega'}{4\pi} \frac{d\sigma}{d\Omega'} (\hat{n}_0, \hat{n}') \left\{ -e^{-ip_0(\hat{n}' - \hat{n}_0) \cdot (\mathbf{x} - \mathbf{y})} + 1 \right\}, \quad (3.35)$$

In fact, as can be seen from Eq.(3.34), the time evolution of the density matrix will be of the type:

$$\frac{d\rho_S(\mathbf{x}, \mathbf{y}, t)}{dt} = -\Gamma \cdot \rho_S(\mathbf{x}, \mathbf{y}, t) \longrightarrow \rho_S(\mathbf{x}, \mathbf{y}, t) = e^{-\Gamma t} \rho_S(\mathbf{x}, \mathbf{y}, 0). \quad (3.36)$$

This formula shows the role played by the function Γ : it suppresses the off diagonal density matrix elements. In fact, for the elements on the diagonal, we have that $\mathbf{x} = \mathbf{y}$; this means that the contribution from the term $(1 - e^{-ip_0(\hat{n}' - \hat{n}_0) \cdot (\mathbf{x} - \mathbf{y})})$ is 0, resulting in:

$$\frac{d\rho_S(\mathbf{x}, \mathbf{x}, t)}{dt} = 0 \longrightarrow \rho_S(\mathbf{x}, \mathbf{x}, t) = \text{const.} \quad (3.37)$$

This last equation shows that the diagonal elements of ρ_S are not influenced by the environmental interaction, they remain constant over time evolution. Instead, the non diagonal elements are suppressed because of Γ and, in the limit $t \rightarrow +\infty$, they are completely suppressed, i.e. they become asymptotically 0. This means that the density matrix ρ_S becomes diagonal, indicating a mixture. This implies that the environment acquires information from the system, leading to a suppression of non-diagonal terms. The information of the system becomes distributed throughout the environment, requiring an observer to measure both the crystal and environmental data. The crystal is no longer isolated but entangled with the environment, which now possesses information about the system. This results in the formation of a mixture for ρ_S .

3.3 Dipole-Dipole interaction

From Eq.(3.35) we can see that, in order to obtain an explicit expression for the decoherence rate, we have to know the differential cross section related to the type of interaction between the environment and the crystal.

Therefore, let us assume that the environmental particles are gas molecules with a dipole moment. In this case, we will have to consider a dipole-dipole interaction, the potential will be [61]:

$$\begin{aligned} V(\mathbf{r}) &= \frac{1}{4\pi\epsilon_0} \frac{\mathbf{d}_1 \cdot \mathbf{d}_2 - 3(\mathbf{n} \cdot \mathbf{d}_1)(\mathbf{n} \cdot \mathbf{d}_2)}{|\mathbf{r}|^3} \\ &= \frac{d_1 d_2}{4\pi\epsilon_0 r^3} [\cos(\pi - \theta_1 - \theta_2) - 3 \cos(\theta_1)\cos(\theta_2)], \end{aligned} \quad (3.38)$$

where in the first line \mathbf{d}_1 and \mathbf{d}_2 are respectively the electric dipole of the crystal and of the environmental particle, \mathbf{r} represents the distance between the centers of the two dipoles and $\mathbf{n} = \mathbf{r}/|\mathbf{r}|$ is its associated unit vector. In the second line⁵, we have introduced the angles θ_1 and θ_2 between \mathbf{r} and respectively \mathbf{d}_1 and \mathbf{d}_2 , together with the angle $\alpha = \pi - \theta_1 - \theta_2$ between the two dipoles \mathbf{d}_1 and \mathbf{d}_2 .

In particular, the function inside the squared brackets in the last line of Eq.(3.65) oscillates between the values 4 and -4 . The worst case scenario will therefore be represented by the maximum value for this function (i.e. 4), which will give also the maximum value for the potential energy $V(\mathbf{r})$. In fact, in this case, the interaction will be stronger, resulting in a bigger decoherence rate Γ (see Eq.(3.35)).

This means that the form for the potential energy of the dipole-dipole interaction that we will consider in this work will be:

$$V(r) = \frac{d_1 d_2}{\pi\epsilon_0 r^3} \quad (3.39)$$

Our goal is to compute the differential cross section for this type of potential. A very useful tool for this purpose is the so-called Born approximation⁶, which expresses the differential cross section $\frac{d\sigma}{d\Omega}$ in terms of the Fourier Transform $\tilde{V}(q)$ of the potential $V(\mathbf{r})$:

$$\frac{d\sigma}{d\Omega} = \frac{m^2}{4\pi^2 \hbar^4} |\tilde{V}(q)|^2. \quad (3.40)$$

The validity of this approximation is in the weak interaction regime, i.e. it can be applied when the kinetic energy E_k of the COM is bigger compared to the potential energy $V(r)$ (see [62] for further details). We will verify below the validity of this approximation.

⁵We have also introduced $d_i \equiv |\mathbf{d}_i|$ and $r \equiv |\mathbf{r}|$.

⁶Notice that this approximation is formally different from the homonym one used in the previous section for the derivation of the Master Equation.

In our case, we should thus have:

$$E_k \gg \frac{d_1 d_2}{\pi \epsilon_0 r^3}, \quad (3.41)$$

Notice also that, if we consider the environment to be a thermal bath of equilibrium temperature T , the average kinetic energy of each environmental particle will be given by $\bar{E}_k \sim k_B T$. We can therefore numerically evaluate the LHS of Eq.(3.41) by using this expression for \bar{E}_k . In a QGEM setup, the temperature is of the order of $T \sim 1$ K. This leads to $\bar{E}_k \sim 10^{-23}$ J.

Now, in order to numerically verify the RHS of Eq. (3.41) we need to know what values for the dipoles d_1 and d_2 we have to use. Respectively, d_1 and d_2 are the dipole of the crystal and of the environmental particle. Physically we can thus consider the environment to be composed of atomic dipoles, given for example by Helium molecules. This means that we can consider d_2 to be [22]:

$$d_2 \sim e \cdot R_a \sim (1.602 \times 10^{-19} \text{C}) \times (10^{-10} \text{m}) \sim 10^{-29} \text{C} \cdot \text{m} = 3 \text{ D}, \quad (3.42)$$

where $R_a \sim 10^{-10} \text{m}$ represents the average atomic radius and e is the electron charge. Here we have used as a unit for the dipole the Debye, which in standard units is $1 \text{ D} = 3.336 \times 10^{-30} \text{ C} \cdot \text{m}$.

Notice also that, as it is clear from Eq.(3.39), we need also to associate a number to the interaction distance r in order to estimate the magnitude of the potential. For this purpose, we can use $r = R \sim 10^{-6} \text{m}$ ⁷ as the radius of the crystal considered in the QGEM proposal [24], which is the minimum possible distance of interaction (the environmental particles are not energetic enough to penetrate the material) and therefore corresponds to the *maximum* value for $V(r)$, i.e. the worst case scenario.

Now, with these values for d_2 and $r \sim R$, we can use Eq.(3.41) to *constrain* the maximum value that d_1 can have in order to apply the Born approximation:

$$d_1 \ll \pi \epsilon_0 \frac{R^3}{d_2} \bar{E}_k \longrightarrow d_1 \ll 10^{-23} \text{C} \cdot \text{m}. \quad (3.43)$$

If all these numerical conditions hold, we can derive the differential cross section $d\sigma/d\Omega$ using the Born approximation. The Fourier transform of (3.39) will give:

$$\begin{aligned} \tilde{V}(q) &= \int d^3 \vec{x} e^{\frac{i}{\hbar} \vec{q} \cdot \vec{x}} (-1) \frac{d_1 d_2}{\pi \epsilon_0 r^3} \\ &= -\frac{d_1 d_2}{\pi \epsilon_0} 2\pi \int_{-1}^1 d(\cos(\theta)) \int_0^{+\infty} dr r^2 \frac{e^{\frac{i}{\hbar} q r \cos(\theta)}}{r^3} = -\frac{4\hbar d_1 d_2}{\epsilon_0 q} \int_0^{+\infty} dr \frac{\sin(\frac{q}{\hbar} r)}{r^2}, \end{aligned} \quad (3.44)$$

⁷Knowing that the crystal's density is $\rho \sim 3.5 \times 10^3 \frac{\text{kg}}{\text{m}^3}$ (e.g., a nano-crystal), with this value of the radius R we will have a mass of $m = \frac{4}{3} \pi R^3 \rho \sim 10^{-14} \text{kg}$.

where $\vec{q} = \vec{p}_{fin} - \vec{p}_0$ is the transferred momentum of the scattered particle.

As we can see, this integral is divergent when $r \rightarrow 0$. This means that the differential cross-section is defined above a minimum interaction distance. In a QGEM setup, we are considering our nano-crystal to have a finite size [24], i.e. to be a sphere of radius $R \sim 10^{-6}$ m and, hence gives a lower limit for the above integral:

$$\tilde{V}(q) = -\frac{4\hbar d_1 d_2}{\epsilon_0 q} \int_R^{+\infty} dr \frac{\sin(\frac{q}{\hbar} r)}{r^2}, \quad (3.45)$$

The integral in the RHS can be solved analytically

$$\tilde{V}(q) = -\frac{4\hbar d_1 d_2}{\epsilon_0 q} \left(\frac{\sin(\frac{q}{\hbar} R)}{R} - \frac{q}{\hbar} Ci\left(\frac{q}{\hbar} R\right) \right), \quad (3.46)$$

where the function $Ci(z)$ is defined as:

$$Ci(z) = -\int_z^{+\infty} dt \frac{\cos(t)}{t}. \quad (3.47)$$

One of the main properties of this function is that:

$$\lim_{z \rightarrow +\infty} Ci(z) = 0. \quad (3.48)$$

This means that we should be able to get rid of the $Ci(\frac{q}{\hbar} R)$ term if its argument is big enough.

Let us thus try to numerically evaluate $\frac{q}{\hbar} R$. We know that q is the transferred momentum $\vec{q} = \vec{p}'_f - \vec{p}_0$. But we also know that the environmental particle is much lighter than the crystal (which is our target particle) and we have also supposed that the environmental dipole has low energy with respect to the mass energy of the crystal. These are approximations that we have already made in the previous section 3; in particular, as can be seen from Eq.(3.26), these assumption led to the conservation of energy through a Dirac's delta $\delta(E_{p'_f} - E_{p_0})$. This means that $E_{p'_f} = E_{p_0}$ and therefore $p'_f = p_0$, i.e. the *modulus* of the momentum of the environmental particle is the same before and after the scattering process. Only the *direction* of the final momentum is different from the initial one.

This means that the transferred momentum q will have the following expression:

$$\begin{aligned} q &= \sqrt{p'^2_f + p_0^2 - 2\vec{p}'_f \cdot \vec{p}_0} = \sqrt{2p_0^2 - 2p_0^2 \cos(\theta')} \\ &= p_0 \sqrt{2(1 - \cos(\theta'))} = 2p_0 \sin(\theta'/2), \end{aligned} \quad (3.49)$$

where in the second to last but one equality we have used the trigonometric property $\cos(\theta') = 1 - 2 \sin^2(\theta'/2)$.

Eq. (3.49) tells us that, numerically, q is of the same order of the initial momentum p_0 . Now, we can consider the environment to be a thermal bath of particles at equilibrium temperature T . This means that the *average* momentum of one environmental particle will be $p_0 = \sqrt{2mk_B T}$. Therefore, considering a temperature of $T \sim 1$ K, a mass for the environmental dipole to be of the order of the proton mass $m \sim 10^{-27}$ kg (e.g. an Helium molecule⁸) and considering $R \sim 10^{-6}$ m, we have:

$$\frac{q}{\hbar} R \sim \frac{\sqrt{2mk_B T}}{\hbar} R \sim 10^3 \gg 1. \quad (3.50)$$

Because of Eq.(3.50) and Eq.(3.48), we will approximate the RHS of the Fourier transformation given by Eq.(3.67) in the following way: $\frac{\sin(\frac{q}{\hbar}R)}{R} - \frac{q}{\hbar} Ci\left(\frac{q}{\hbar}R\right) \sim \frac{\sin(\frac{q}{\hbar}R)}{R}$. In this way, as we will see below, it will be possible to compute analytically the integral for the total cross section, i.e. $\sigma_{CM} = \int d\Omega' \frac{d\sigma}{d\Omega'}$. The validity of such an approximation can be verified *a posteriori*, as it is shown in the Appendix A.3.

The Fourier transformation of the potential will thus give:

$$\tilde{V}(q) \simeq -\frac{4\hbar d_1 d_2}{\epsilon_0 R} \frac{\sin\left(\frac{q}{\hbar}R\right)}{q}. \quad (3.51)$$

From the Born approximation (see Eq.(3.40)), we finally obtain the value for the differential cross section:

$$\frac{d\sigma}{d\Omega} = \frac{4m^2 d_1^2 d_2^2}{\pi^2 \epsilon_0^2 \hbar^2 R^2} \frac{\sin^2\left(\frac{q}{\hbar}R\right)}{q^2}. \quad (3.52)$$

3.3.1 Short-wavelength limit approximation

We are now ready to make some approximation in order to apply Eq.(3.35) to the case of dipole-dipole interaction.

We know that the de Broglie wavelength associated to the environmental ions is $\lambda_0 = \frac{2\pi\hbar}{p_0}$. If we consider the particles to be inside a box of temperature T , the average momenta of one ion will be $p_0 = \sqrt{2mk_B T}$, which gives:

$$\lambda_0 = \frac{2\pi\hbar}{\sqrt{2mk_B T}} \sim 10^{-9} \text{m}, \quad (3.53)$$

where, for the numerical value, we have used $m \sim 10^{-27}$ kg and $T \sim 1$ K.

We can ask now if it is possible to consider the short-wavelength limit, i.e. the limit where $\lambda_0 \ll \Delta x$, where Δx is the superposition distance of the crystal. Using a

⁸The Helium's molar mass is $M_{He} = 0.004 \frac{\text{kg}}{\text{mol}}$; this means that its mass is $m_{He} = \frac{M_{He}}{N_A} = \frac{0.004 \frac{\text{kg}}{\text{mol}}}{6.022 \times 10^{23} \text{mol}^{-1}} \sim 10^{-27} \text{kg}$.

superposition size of $\Delta x \sim 10^{-5}\text{m}$ and a mass for the ion similar to the one of the proton $m \sim 10^{-27}\text{kg}$, we have that the short-wavelength limit is satisfied everytime:

$$\lambda_0 = \frac{2\pi\hbar}{\sqrt{2mk_B T}} \ll \Delta x \longrightarrow T \gg \frac{4\pi^2\hbar^2}{2mk_B\Delta x^2} \sim 10^{-7}\text{K}, \quad (3.54)$$

which is always satisfied in a QGEM setup, considering that $T \sim 1\text{K}$.

But, if the short-wavelength limit holds, $\lambda_0 \ll \Delta x$ implies that $p_0\Delta x \gg 1$. This means that the phase exponential $e^{-ip_0(\hat{n}'-\hat{n}_0)\cdot(\vec{x}-\vec{y})}$, when is integrated over all possible p_0 's (as in 3.35), oscillates very fast and in the end its contribution will be negligible. This gives us the expression for the decoherence rate in the short-wavelength limit:

$$\Gamma_S = (2\pi)^{3/2} \int dp_0 S(p_0) nv(p_0) \sigma_{CM}(p_0), \quad (3.55)$$

where $\sigma_{CM} = \int \frac{d\Omega_0 d\Omega'}{4\pi} \frac{d\sigma}{d\Omega'}(\hat{n}_0, \hat{n}')$ is the total cross section and the subscript S in Γ_S stands for "Short", indicating that we are computing the decoherence rate in the short-wavelength limit.

Let us thus compute σ_{CM} . Using Eq.(3.68), we have that:

$$\begin{aligned} \sigma_{CM} &= \int \frac{d\Omega_0}{4\pi} \int d\Omega' \frac{4m^2 d_1^2 d_2^2}{\pi^2 \epsilon_0^2 \hbar^2 R^2} \frac{\sin^2\left(\frac{q}{\hbar} R\right)}{q^2} \\ &= \frac{4m^2 d_1^2 d_2^2}{\pi^2 \epsilon_0^2 \hbar^2 R^2} \int d\Omega' \frac{\sin^2\left(\frac{2p_0}{\hbar} \sin(\theta'/2) R\right)}{(2p_0 \sin(\theta'/2))^2} \\ &= \frac{8m^2 d_1^2 d_2^2}{\pi \epsilon_0^2 \hbar^2 R^2} \int_{-1}^1 d[\cos(\theta')] \frac{\sin^2\left(\frac{2p_0}{\hbar} \sin(\theta'/2) R\right)}{(2p_0 \sin(\theta'/2))^2} \\ &= \frac{2m^2 d_1^2 d_2^2}{\pi \epsilon_0^2 \hbar^2 R^2 p_0^2} \int_0^1 dx \ 4x \frac{\sin^2\left(\frac{2p_0}{\hbar} R x\right)}{x^2} = \frac{8m^2 d_1^2 d_2^2}{\pi \epsilon_0^2 \hbar^2 R^2 p_0^2} \int_0^1 dx \frac{\sin^2\left(\frac{2p_0}{\hbar} R x\right)}{x}, \end{aligned} \quad (3.56)$$

where we have used the fact that the transferred momentum q is $q = 2p_0 \sin(\theta'/2)$ and in the last but one line we have defined $x \equiv \sin(\theta'/2)$, in order to make the following substitution:

$$\int_{-1}^1 d[\cos(\theta')] = \int_{-1}^1 d[1 - 2x^2] = \int_1^0 dx (-2)2x = \int_0^1 dx 4x. \quad (3.57)$$

The integral that appears in the final line of Eq.(3.69) can be solved analytically:

$$\int_0^1 dx \frac{\sin^2\left(\frac{2p_0}{\hbar} R x\right)}{x} = \frac{1}{2} \left[\gamma - Ci\left(4\frac{p_0}{\hbar} R\right) + \ln\left(4\frac{p_0}{\hbar} R\right) \right], \quad (3.58)$$

where $Ci(z)$ is the function defined in Eq.(3.47).

The total cross section is thus given by:

$$\sigma = \frac{8m^2 d_1^2 d_2^2}{\pi \epsilon_0^2 \hbar^2 L^2 p_0^2} \frac{1}{2} \left[\gamma - Ci \left(4 \frac{L}{\hbar} p_0 \right) + \ln \left(4 \frac{L}{\hbar} p_0 \right) \right], \quad (3.59)$$

It is worth noting that this expression for the total cross section is well behaved for very small temperatures. In particular, for the limit where $p_0 \rightarrow 0$ (i.e. $T \rightarrow 0$ K if one considers $p_0 = \sqrt{2mk_B T}$), we have:

$$\lim_{p_0 \rightarrow 0} \left[\gamma - Ci \left(4 \frac{L}{\hbar} p_0 \right) + \ln \left(4 \frac{L}{\hbar} p_0 \right) \right] = 0.^9 \quad (3.60)$$

This means that $\lim_{T \rightarrow 0} \sigma = 0$, which leads to the following behaviour for the decoherence rate at very low temperatures:

$$\lim_{T \rightarrow 0} \Gamma_S = 0, \quad (3.61)$$

as can be seen from Eq.(3.90).

Not only this result is finite, but it is also physical: in fact, at $T = 0$ K, there is no energy for the environmental dipoles and without energy there is no interaction with the crystal, i.e. no decoherence.

Also in this case, we can consider the contribution of $Ci(z)$ to be negligible w.r.t. the other terms: in fact, using the fact that $\frac{p_0}{\hbar} R \sim \frac{\sqrt{2mk_B T}}{\hbar} R \sim 10^3 \gg 1$ at $T = 1$ K, we can use again the property Eq.(3.48). Moreover, we have that $\ln \left(4 \frac{p_0}{\hbar} R \right) \sim \ln(4 \cdot 10^3) \sim 8 \gg \gamma \simeq 0.577$, which allows us to write:

$$\sigma_{CM} \simeq \frac{4m^2 d_1^2 d_2^2}{\pi \epsilon_0^2 \hbar^2 R^2 p_0^2} \ln \left(4 \frac{p_0}{\hbar} R \right). \quad (3.62)$$

The last step we need to take in order to compute Γ_S using Eq.(3.90) is to pick a distribution $S(p_0)$ for the environmental particles. Now, because we suppose that the environmental dipoles form a thermal bath of temperature $T = 1$ K, the average energy of one environmental particle will thus be $\bar{E} \sim k_B T$, which leads to an average momentum of $\bar{p} \sim \sqrt{2mk_B T}$. Therefore, a suitable candidate for $S(p_0)$ is the Maxwell-Boltzmann distribution:

$$S(p_0) = 4\pi p_0^2 \left(2\pi m k_B T \right)^{-3/2} e^{-\frac{p_0^2}{2mk_B T}}, \quad (3.63)$$

⁹This can be easily seen from the expansion of $Ci(x) = \gamma + \ln(x) + \sum_{n=1}^{+\infty} \frac{(-x^2)^n}{2n(2n)!} = \gamma + \ln(x) - \frac{x^2}{2 \cdot 2!} + \frac{x^4}{4 \cdot 4!} + \dots$. For $x \rightarrow 0$, one can see that the only terms in the expansion that survive are $\gamma + \ln(x)$, i.e. for small x we have that $Ci(x) - \ln(x) \sim \gamma$, which is the reason why the overall limit is 0.

which satisfies the requirement $\int dp_0 S(p_0) = 1$. Furthermore, one can notice that, for very small temperatures (i.e. $T \leq 1$ K) Eq.(3.63) is strongly peaked around its mean value $\bar{p} = \sqrt{2mk_B T}$. That is because Eq.(3.63) is a Gaussian function of the type $S(p_0) \sim e^{-\frac{p_0^2}{\sigma}}$, where σ represents the standard deviation, which intuitively tells us how much the distribution is spread over the momentum space. Now, in our case we have $\sigma \propto mk_B T \sim 10^{-25} \text{kg} \frac{\text{m}}{\text{s}} \ll 1$ and therefore a very narrow distribution centered around $\bar{p} = \sqrt{2mk_B T}$.

We can thus consider all the particles to have approximately the same momentum \bar{p} , i.e. we can consider $S(p_0) = \delta(p_0 - \bar{p})$. This distribution satisfies also the requirement given by Eq.(3.33), i.e. $\int dp_0 S(p_0) = \int dp_0 \delta(p_0 - \bar{p}) = 1$.

We are now ready to compute the decoherence rate Γ_S in the short-wavelength limit. Plugging the expression for the total cross section given by Eq.(3.62) inside Eq.(3.90), we find that:

$$\begin{aligned} \Gamma_S &= (2\pi)^{\frac{3}{2}} \int dp_0 \delta(p_0 - \bar{p}) n \frac{p_0}{m} \frac{4m^2 d_1^2 d_2^2}{\pi \epsilon_0^2 \hbar^2 R^2 p_0^2} \times \\ &\times \ln \left(4 \frac{p_0}{\hbar} R \right) = 8\sqrt{\pi} \frac{m d_1^2 d_2^2 n}{\epsilon_0^2 \hbar^2 R^2} \frac{\ln \left(4 \frac{R}{\hbar} \sqrt{2mk_B T} \right)}{\sqrt{mk_B T}}. \end{aligned} \quad (3.64)$$

The case for non-approximated potential

The same procedure developed in this last subsection can be applied also to the case where the potential of Eq.(3.65) is considered in the computation for the differential cross section, i.e. we will now not make the "worst case scenario" approximation made in Eq.(3.39), in order to have a more complete and precise discussion about the dipole-dipole interaction. Because the original potential 3.65 has a more complicated form compared to 3.39 given its angular dependence, the explicit calculations are not easy to perform analytically. Nonetheless they can still be performed thanks to the use of computational methods, such as Mathematica.

From Eq.(3.35) we can see that, in order to obtain an explicit expression for the decoherence rate, we have to know the differential cross section related to the type of interaction between the environment and the crystal.

In this case the potential will be given by [61]:

$$\begin{aligned} V(\mathbf{r}) &= \frac{1}{4\pi\epsilon_0} \frac{\mathbf{d}_1 \cdot \mathbf{d}_2 - 3(\mathbf{n} \cdot \mathbf{d}_1)(\mathbf{n} \cdot \mathbf{d}_2)}{|\mathbf{r}|^3} \\ &= \frac{d_1 d_2}{4\pi\epsilon_0 r^3} [\cos(\pi - \theta_1 - \theta_2) - 3 \cos(\theta_1) \cos(\theta_2)]. \end{aligned} \quad (3.65)$$

Let us thus compute the Fourier transform of (3.65), i.e. $\tilde{V}(\mathbf{q}) = \int d^3\mathbf{x} e^{i\mathbf{q}\cdot\mathbf{x}}V(\mathbf{r})$. In particular, defining the vectorial components for $\mathbf{d}_1 = (0, 0, d_1)$, $\mathbf{d}_2 = (d_{2x}, d_{2y}, d_{2z})$ and $\mathbf{n} = (\sin(\bar{\theta})\cos(\bar{\phi}), \sin(\bar{\theta})\sin(\bar{\phi}), \cos(\bar{\theta}))$ ¹⁰, we can perform the angular integral over $d\bar{\Omega} = d\bar{\phi}d\bar{\theta} \sin(\bar{\theta})$ first:

$$\begin{aligned} & \int d\bar{\phi}d\bar{\theta} \sin(\bar{\theta}) e^{i\frac{r}{\hbar}qr \cos(\bar{\theta})} \frac{1}{4\pi\epsilon_0} \frac{\mathbf{d}_1 \cdot \mathbf{d}_2 - 3(\mathbf{n} \cdot \mathbf{d}_1)(\mathbf{n} \cdot \mathbf{d}_2)}{r^3} \\ &= -\frac{2d_1d_{2z}}{\epsilon_0} \frac{1}{\frac{q^3}{\hbar^3}r^6} \left(\left(\frac{r^2}{\hbar^2}q^2 - 3 \right) \sin\left(\frac{r}{\hbar}q\right) + 3\frac{r}{\hbar}q \cos\left(\frac{r}{\hbar}q\right) \right) \end{aligned} \quad (3.66)$$

where $\mathbf{q} = \mathbf{p}_{fin} - \mathbf{p}_0$ is the transferred momentum of the scattered particle.

Eq.(3.66) should now be integrated over $\int_0^{+\infty} dr r^2$. The problem is that now this integral is divergent when $r \rightarrow 0$. This means that the differential cross-section is defined above a minimum interaction distance. In a QGEM setup, we are considering our nanocrystal to have a finite size [24], i.e. to be a sphere of radius $R \sim 10^{-6}\text{m}$ and hence gives a lower limit for the integral:

$$\begin{aligned} \tilde{V}(q) &= -\frac{2d_1d_{2z}\hbar^3}{\epsilon_0q^3} \int_R^{+\infty} dr r^2 \frac{1}{r^6} \left(\left(\frac{r^2}{\hbar^2}q^2 - 3 \right) \sin\left(\frac{r}{\hbar}q\right) + 3\frac{r}{\hbar}q \cos\left(\frac{r}{\hbar}q\right) \right) \\ &= \frac{2d_1d_{2z}\hbar^3}{\epsilon_0R^3q^3} \left(\sin\left(\frac{R}{\hbar}q\right) - \frac{R}{\hbar}q \cos\left(\frac{R}{\hbar}q\right) \right). \end{aligned} \quad (3.67)$$

Eq.(3.67) can be inserted inside the Born formula in order to find the differential cross section $\frac{d\sigma}{d\Omega}$. From Eq.(3.40), we can see that we need to compute the modulus squared of the Fourier transform (3.67). After doing that, we can average the final result over the orientation of the environmental dipole d_2 , which in Eq.(3.67) appears with the term $d_{2z} = d_2\cos(\theta_2)$. We can schematically summarize these operations as: $\tilde{V}(q) \rightarrow |\tilde{V}(q)|^2 \rightarrow \int d\phi_2d\theta_2 \sin(\theta_2)|\tilde{V}(q)|^2$.

The final expression for the differential cross section will thus be given by:

$$\frac{d\sigma}{d\Omega} = \frac{4\hbar^2m^2d_1^2d_2^2}{3\pi\epsilon_0^2R^6q^6} \left(\sin\left(\frac{R}{\hbar}q\right) - \frac{R}{\hbar}q \cos\left(\frac{R}{\hbar}q\right) \right)^2. \quad (3.68)$$

Let us thus compute σ_{CM} . Using Eq.(3.68), we have that:

¹⁰Here, $\bar{\theta} \in (0, \pi)$ and $\bar{\phi} \in (0, 2\pi)$

$$\begin{aligned}
\sigma_{CM} &= \int \frac{d\Omega_0}{4\pi} \int d\Omega' \frac{4\hbar^2 m^2 d_1^2 d_2^2}{3\pi\epsilon_0^2 R^6 q^6} \left(\sin\left(\frac{R}{\hbar}q\right) - \frac{R}{\hbar}q \cos\left(\frac{R}{\hbar}q\right) \right)^2 \\
&= \frac{\hbar^2 m^2 d_1^2 d_2^2}{48\pi\epsilon_0^2 R^6 p_0^6} 2\pi \int_0^\pi d\theta' \sin(\theta') \frac{1}{\sin^6(\theta'/2)} \\
&\times \left(\sin\left(2\frac{R}{\hbar}p_0 \sin(\theta'/2)\right) - 2\frac{R}{\hbar}p_0 \sin(\theta'/2) \cos\left(2\frac{R}{\hbar}p_0 \sin(\theta'/2)\right) \right)^2 \quad (3.69) \\
&= \frac{m^2 d_1^2 d_2^2 \hbar^2}{48\epsilon_0^2 R^6 p_0^6} \left[-1 - 8 \left(\frac{R}{\hbar}p_0\right)^2 + 32 \left(\frac{R}{\hbar}p_0\right)^4 \right. \\
&\quad \left. + \cos\left(4\frac{R}{\hbar}p_0\right) + 4\frac{R}{\hbar}p_0 \sin\left(4\frac{R}{\hbar}p_0\right) \right].
\end{aligned}$$

where we have used the fact that the transferred momentum q is $q = 2p_0 \sin(\theta'/2)$.

Moreover, we can consider again all the particles to have approximately the same momentum \bar{p} , i.e. we can consider $S(p_0) = \delta(p_0 - \bar{p})$.

We are now ready to compute the decoherence rate Γ_S in the short-wavelength limit. Plugging the expression for the total cross section given by Eq.(3.69) inside Eq.(3.90), we find that:

$$\begin{aligned}
\Gamma_S &= (2\pi)^{\frac{3}{2}} \int dp_0 \delta(p_0 - \bar{p}) n \frac{p_0}{m} \frac{m^2 d_1^2 d_2^2 \hbar^2}{48\epsilon_0^2 R^6 p_0^6} \left[-1 - 8 \left(\frac{R}{\hbar}p_0\right)^2 + 32 \left(\frac{R}{\hbar}p_0\right)^4 \right. \\
&\quad \left. + \cos\left(4\frac{R}{\hbar}p_0\right) + 4\frac{R}{\hbar}p_0 \sin\left(4\frac{R}{\hbar}p_0\right) \right] = \quad (3.70) \\
&= \frac{\hbar^2 m d_1^2 d_2^2 n}{48\epsilon_0^2 R^6 \bar{p}^5} \left[-1 - 8 \left(\frac{R}{\hbar}\bar{p}\right)^2 + 32 \left(\frac{R}{\hbar}\bar{p}\right)^4 + \cos\left(4\frac{R}{\hbar}\bar{p}\right) + 4\frac{R}{\hbar}\bar{p} \sin\left(4\frac{R}{\hbar}\bar{p}\right) \right]
\end{aligned}$$

This equation represents a more precise expression for the decoherence rate given in the approximated case by Eq.(3.64). Anyway we can perform a numerical evaluation of the term $\frac{R}{\hbar}\bar{p}$ in order to spot the actual differences between Eq.(3.64) and Eq.(3.70). In fact, in a QGEM setup, we have that $R \sim 10^{-6}\text{m}$ and $\bar{p} \sim 10^{-25}\text{kg}\frac{\text{m}}{\text{s}}$, giving $\frac{R}{\hbar}\bar{p} \sim 10^3 \gg 1$. This means that, in the final expression for Eq.(3.70) the dominant term inside the parenthesis is $\left(\frac{R}{\hbar}\bar{p}\right)^4$, while the others can be considered to be negligible to this one. This gives the following approximation for Eq.(3.70):

$$\Gamma_S \simeq \frac{2m d_1^2 d_2^2 n}{3\epsilon_0^2 \hbar^2 R^2 \bar{p}}. \quad (3.71)$$

Comparing this expression with Eq.(3.64), we can see that the approximation made by the choice of the potential (3.39) can be considered to be a suitable one: in fact, the

only extra contribution is given by the factor $\ln\left(4\frac{R}{\hbar p}\right) \sim 7$, which does not represent a big overestimate for the order of magnitude for the decoherence rate, given that we are looking for values for Γ_S of $\Gamma_S \sim 10^{-2}\text{Hz}$, as we will see in the next sections.

3.3.2 Long-wavelength approximation

Let us now study the opposite limit case of Eq.(3.35). In particular, we will consider the case where the wavelength associated to the environmental particle is much bigger than the superposition size, i.e. $\lambda_0 \gg \Delta x$. This means that, because $\lambda_0 \sim \frac{1}{p_0}$, we have that $ip_0(\hat{n}' - \hat{n}_0) \cdot (\vec{x} - \vec{y}) \ll 1$.

In this way, we can expand the exponential that appears in the RHS of Eq.(3.35) to obtain:

$$\frac{i}{\hbar} p_0 (\hat{n}' - \hat{n}_0) \cdot (\vec{x} - \vec{y}) + \frac{1}{2\hbar^2} p_0^2 [(\hat{n}' - \hat{n}_0) \cdot (\vec{x} - \vec{y})]^2. \quad (3.72)$$

The first term gives an integral of an odd function, due to the fact that $\hat{n}' - \hat{n}_0$ is antisymmetric in the exchange of \hat{n} and \hat{n}' , while $\frac{d\sigma}{d\Omega}(\hat{n}_0, \hat{n}')$ is symmetric, giving a total odd function. The second term gives instead a non-null contribution. Moreover, it can be further simplified: in fact, we can assume that the particular direction $\vec{x} - \vec{y} = |\vec{x} - \vec{y}| \hat{s} = \Delta x \hat{s}$ of the scattering center (i.e. of the crystal) does not depend on the direction \hat{s} . We can thus average this term over all possible directions \hat{s} , obtaining:

$$\begin{aligned} (\Delta x)^2 \frac{1}{3} \sum_{s=x,y,z} [\hat{s} \cdot (\hat{n}' - \hat{n}_0)]^2 &= \frac{1}{3} (\Delta x)^2 |\hat{n}' - \hat{n}_0|^2 \\ &= \frac{2}{3} (\Delta x)^2 |1 - \hat{n}' \cdot \hat{n}_0| = \frac{2}{3} (\Delta x)^2 (1 - \cos(\theta')). \end{aligned} \quad (3.73)$$

where θ' is the scattering angle.

This means that, in the expression for Γ , the angular integral will become:

$$\begin{aligned} &\int d\Omega' \frac{d\sigma}{d\Omega'}(\hat{n}_0, \hat{n}') \frac{2}{3} (1 - \cos(\theta')) \\ &= \frac{2\pi}{3} \int d(\cos(\theta')) (1 - \cos(\theta')) \frac{d\sigma}{d\Omega'}(\hat{n}_0, \hat{n}') \equiv \sigma_{eff}, \end{aligned} \quad (3.74)$$

where we have integrated over the azimuthal angle $\int_0^{2\pi} d\phi = 2\pi$ and we have defined the effective cross section σ_{eff} . This means that, using Eq.(3.35), the final expression for the decoherence rate Γ in the long-wavelength limit is:

$$\Gamma_L = (2\pi)^{3/2} \Delta x^2 \int dp_0 S(p_0) n \frac{p_0}{m} \sigma_{eff}(p_0) \frac{p_0^2}{\hbar^2}. \quad (3.75)$$

which is an expression that can also be found in the literature [18, 19]. As in Eq.(3.90), now the subscript L stands for "Long", considering that we are computing the decoherence rate in the long-wavelength limit.

Comparing Eq.(3.75) and Eq.(3.90) we notice that we can obtain the long-wavelength limit expression by substituting $\sigma_{tot} \rightarrow \sigma_{eff}$ inside the short-wavelength limit formula and by multiplying it by the term $\Delta x^2 \frac{p_0^2}{\hbar^2}$. In particular, we can notice that σ_{eff} will be numerically of the same order of σ_{tot} , given that the only difference between the two is a purely geometrical factor $(1 - \cos(\theta'))$ inside Eq.(3.74). Therefore, the main difference between the two expressions is entirely encoded inside the term $\Delta x^2 \frac{p_0^2}{\hbar^2}$.

Now, when the *physical* situation is the short-wavelength limit, this term will be $\Delta x^2 \frac{p_0^2}{\hbar^2} \gg 1$, given that $\lambda_0 \sim \frac{\hbar}{p_0} \ll \Delta x$. This means that, when we have physically a short wavelength for the environmental particle compared to the superposition size, the following inequality holds:

$$\frac{\Gamma_S}{\Gamma_L} \sim \frac{1}{\Delta x^2 \frac{p_0^2}{\hbar^2}} \ll 1, \quad (3.76)$$

which leads to:

$$\Gamma_S \ll \Gamma_L. \quad (3.77)$$

This means that, when the physical limit is the short-wavelength limit, Eq.(3.75) will thus be an **upper bound** to the decoherence rate. Therefore, if we use Eq.(3.75) to compute the decoherence rate when $\lambda_0 \ll \Delta x$, we will obtain a superior limit which will be never exceeded by the physical decoherence rate given by Eq.(3.90).

We are now able to compute σ_{eff} for the dipole-dipole interaction case. In particular, plugging Eq.(3.68) inside Eq.(3.74), we obtain:

$$\begin{aligned} \sigma_{eff} &= \frac{16m^2 d_1^2 d_2^2}{3\pi \epsilon_0^2 \hbar^2 R^2 p_0^2} \int_0^1 dx x \sin^2\left(\frac{2R}{\hbar} p_0 x\right) \\ &= \frac{16m^2 d_1^2 d_2^2}{3\pi \epsilon_0^2 \hbar^2 R^2 p_0^2} \frac{1}{8\left(\frac{2R}{\hbar} p_0\right)^2} \left[1 + 2\left(\frac{2R}{\hbar} p_0\right)^2 \right. \\ &\quad \left. - \cos\left(\frac{4R}{\hbar} p_0\right) - \frac{4R}{\hbar} p_0 \sin\left(\frac{4R}{\hbar} p_0\right) \right], \end{aligned} \quad (3.78)$$

where we have again used the substitution given by Eq.(3.57) in the computation of the integral.

We can notice that, also in this case, its limit for $p \rightarrow 0$ is finite¹¹; in particular:

$$\lim_{p \rightarrow 0} \sigma_{eff}(p) = \frac{16m^2 d_1^2 d_2^2}{3\pi \epsilon_0^2 \hbar^4}. \quad (3.79)$$

¹¹This limit can be easily computed using de l'Hopital's method.

This means that, because $p_0 \propto T$, we will have a final result that has good behavior for very small temperatures, i.e. $T \ll 1$ K. Therefore, as can be seen from Eq.(3.75), we have that:

$$\lim_{T \rightarrow 0} \Gamma_L \sim \lim_{T \rightarrow 0} p_0^3 \sigma_{eff}(p_0) = 0, \quad (3.80)$$

which is the same behaviour for the decoherence rate found in the previous section (see Eq.(3.61)).

Let us thus compute explicitly Eq.(3.75). In our case, we can consider the environmental dipoles to be confined within the walls of the experimental box to all have energy given by the temperature, i.e. $\bar{p} = \sqrt{2mk_B T} \sim 10^{-25} \text{kg} \frac{\text{m}}{\text{s}}$. This is equivalent to considering a momentum distribution like $S(p_0) = \delta(p_0 - \bar{p})$. Moreover, using again the fact that $Rp_0/\hbar \gg 1$, we can approximate σ_{eff} as (see Eq.(3.78)):

$$\sigma_{eff}(p) \simeq \frac{16m^2 d_1^2 d_2^2}{3\pi\epsilon_0^2 \hbar^2 R^2 p^2} \frac{2(2\frac{R}{\hbar})^2}{8(2\frac{R}{\hbar})^2} = \frac{4m^2 d_1^2 d_2^2}{3\pi\epsilon_0^2 \hbar^2 R^2 p^2}. \quad (3.81)$$

Using this expression for $\sigma_{eff}(p)$ inside Eq.(3.75), we obtain:

$$\Gamma_L = \frac{16md_1^2 d_2^2 n}{3\epsilon_0^2 \hbar^4 R^2} \Delta x^2 \sqrt{\pi m k_B T}. \quad (3.82)$$

3.3.3 Applications to the QGEM experiment

In this section, we are going to explore the consequences that the dipole-dipole interaction can have on the QGEM experiment. In particular, following the original proposal [14], it is very important to keep the spatial superposition of the masses for a time $\tau \sim 1$ s, in order to allow the masses to interact gravitationally and generate entanglement that can be measured at the end of the various steps of the experiment. For this reason, it is very important to keep track of all the possible sources of decoherence, i.e. everything that can lead to a destruction of the spatial superposition.

One of the unavoidable sources of decoherence during the experiment arises from electromagnetic interactions. Specifically, despite creating a vacuum with extremely low pressure inside the experimental box [58], there is still a possibility that some random air molecules may inadvertently persist within the box. Such molecules are neutral objects and can therefore possess an electric dipole d_2 of the order of $d_2 \sim 1$ D [22]. This means that the interaction between an environmental particle and the crystal in superposition is possible: in fact, it can happen that the neutral crystal has a dipole d_1 too [63, 21].

Crystal's dipole induced by the environment

What should thus be the value for the crystal's dipole d_1 ? The first case that we are going to analyze is when d_1 is induced by the environment. In fact, being a dielectric

material, the crystal has a polarizability α when subjected to an external electric field E_{ext} , which inside the crystal is perceived as a local field $E_{loc} = E_{ext}/\epsilon_r$, with $\epsilon_r \sim 5.7$ being the relative dielectric constant of the crystal. In particular, in isotropic media, the external field will create a local dipole in each atom of the crystal's lattice [61]:

$$d_1 = \alpha E_{loc}. \quad (3.83)$$

This means that the total contribution will be given by the sum over all N' atoms of the lattice:

$$d_1 = N' \alpha E_{loc}. \quad (3.84)$$

So, in order to find an explicit expression for d_1 , we need the expressions for α and E_{loc} . For α we have the Classius-Mossotti relation:

$$\frac{n' \alpha}{3\epsilon_0} = \frac{\epsilon_r - 1}{\epsilon_r + 2}, \quad (3.85)$$

where $n' = \frac{N'}{V}$ is the atomic density inside the crystal, the volume is given by $V \sim R^3 \sim (10^{-6}\text{m})^3$.

In this case, the induced electric field will be thus generated by the environmental dipole d_2 [61]:

$$E_{loc} = \frac{d_2}{\pi \epsilon_0 \epsilon_r \bar{r}^3}, \quad (3.86)$$

where \bar{r} represents the average interaction distance between an environmental particle (which lies inside an experimental box of side's size $L \sim 10^{-2}\text{m}$ [58]) and the nano-crystal. In the worst case scenario, this average distance is given by $\bar{r} \simeq R \sim 10^{-6}\text{m}$, which is the closest possible distance between d_1 and d_2 .

With this expression for E_{loc} , Eq.s(3.84), (3.85) and (3.86) give the following value for d_1 :

$$d_1 = \frac{3d_2}{\pi \epsilon_r} \left(\frac{\epsilon_r - 1}{\epsilon_r + 2} \right) \sim 10^{-30} \text{ C} \cdot \text{m}, \quad (3.87)$$

where we have used the same value for d_2 used in Eq.(3.42), i.e. $d_2 \sim 10^{-29}\text{C} \cdot \text{m}$.

Let us finally get some numerical result for the decoherence rate Γ_S found in Eq.(3.64). For example, we can consider the two dipoles d_1 and d_2 to have the values that we have found above in Eq.(3.87) and Eq.(3.42). These values correspond to the physical situation where the environmental dipole d_2 induces a dipole d_1 inside the crystal because of its dielectric properties. For the other data that appear in Eq.(3.64) we can use $m \sim 10^{-27}\text{kg}$ (e.g. Helium molecule), $T \sim 1 \text{ K}$, $\Delta x \sim 10^{-5}\text{m}$, $R \sim 10^{-6}\text{m}$ and $n \sim 10^8\text{m}^{-3}$. This last value can be related also to the pressure p , which is the actual parameter that is controlled in a QGEM setup proposal; in particular, we can consider n and p to be

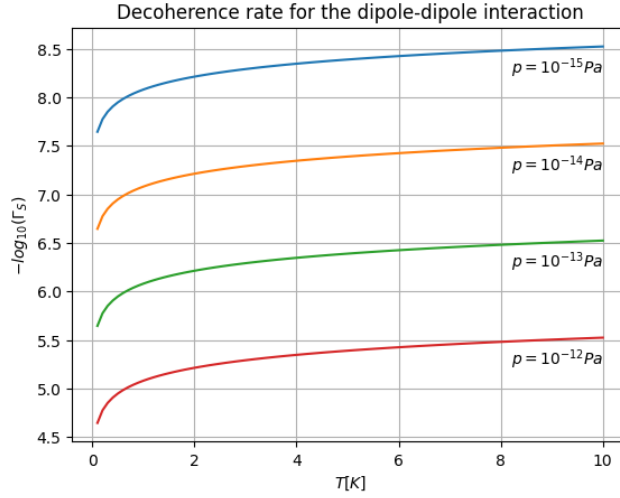


Figure 3.2: Behaviour for the decoherence rate Γ_S computed in the short-wavelength limit as a function of the temperature T . The graph shows that, for a range of temperatures $T \in \{10^{-1}\text{K}, 10\text{ K}\}$, α will lie in the interval $\alpha \in \{4, 9\}$ and the range for the decoherence rate will be $\Gamma_S \in \{10^{-9}\text{Hz}, 10^{-4}\text{Hz}\}$. The various plots correspond to different values for the pressure $p \in \{10^{-15}\text{Pa}, 10^{-12}\text{Pa}\}$.

correlated through the perfect gas law $p = nk_B T$, which gives a value for the pressure of the order of $p \sim 10^{-15}$ Pa.

Therefore, using all these values for the variables that appear in the final decoherence rate, Eq.(3.64) gives:

$$\Gamma_S \sim 10^{-8} \text{ Hz}. \quad (3.88)$$

The physical meaning of this value is clear from Eq.(3.34), which can be expressed and solved in terms of Γ_S in the following way:

$$\frac{d\rho_S(\mathbf{x}, \mathbf{y}, t)}{dt} = -\Gamma_S \cdot \rho_S(\mathbf{x}, \mathbf{y}, t) \longrightarrow \rho_S(\mathbf{x}, \mathbf{y}, t) = e^{-\Gamma_S t} \rho_S(\mathbf{x}, \mathbf{y}, 0). \quad (3.89)$$

This means that, if the value for Γ_S found in Eq.(3.88) holds, the off-diagonal elements of ρ_S will be suppressed in a time t_{supp} of the order of $t_{supp} \sim 10^8$ s. This is a very high value, especially compared to the time $\tau \sim 2$ s during which the crystal is kept in superposition in the QGEM proposal. Therefore, assuming that the environmental dipole d_2 generates a crystal's dipole d_1 given by Eq.(3.87), the dipole-dipole interaction analyzed in this work should not give problems for the realization of the experiment.

The general behaviour of the decoherence rate it is shown in figure 3.2. In particular, we describe the decoherence rate Γ_S in terms of its powers $\Gamma_S = 10^{-\alpha}\text{Hz}$, which leads

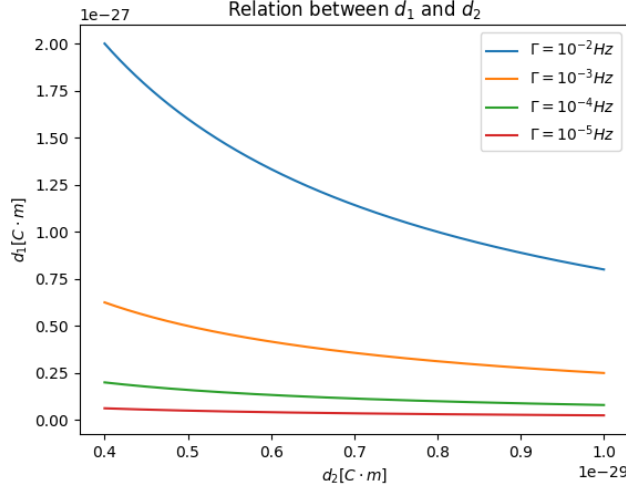


Figure 3.3: Relation between the crystal's dipole d_1 and the environmental particle's one d_2 . In this plot, it is shown how the different values of d_1 change in function of d_2 with different orders of magnitude considered for Γ_S . In particular, considering a range for Γ_S of $\Gamma_S \in \{10^{-5} Hz, 10^{-2} Hz\}$ and a value for d_2 of the order of $d_2 \sim 1D = 3.336 \times 10^{-30} C \cdot m$, the crystal's dipole will be of the order of $d_1 \sim 10^3 D \simeq 10^{-27} C \cdot m$.

to $\alpha = -\log_{10}(\frac{\Gamma_S}{Hz})$. In figure 3.2, it is represented the behaviour of α in terms of the temperature T , where the different plots correspond to different values for the pressure $p \in \{10^{-15} Pa, 10^{-12} Pa\}$ (or, equivalently, for the number density n). As it is clear from the graph, if we consider a range of temperatures $T \in \{10^{-1} K, 10 K\}$, α will lie in the interval $\alpha \in \{4, 9\}$, which corresponds to the following range for the decoherence rate: $\Gamma_S \in \{10^{-9} Hz, 10^{-4} Hz\}$.

Constraint for the crystal's dipole

Eq.(3.64) can also be used to constrain all the possible values that the crystal's dipole d_1 can have. In particular, we can require the decoherence rate Γ_S to be smaller than $10^{-2} Hz$. This maximum value for the decoherence rate is chosen because, one of the main challenges of the QGEM setup, is to keep the crystal in spatial superposition for at least $\tau \sim 2$ s. This means that, with $\Gamma_S \sim 10^{-2} Hz$, the superposition will be destroyed in a time of $t_{supp} \sim 100$ s $\gg \tau$ and should therefore not represent a problem for the QGEM experiment.

In figure 3.3 it is represented the relation between the numerical values of the crystal's dipole d_1 and the environmental particle d_2 for different orders of magnitude of the decoherence rate $\Gamma_S \in \{10^{-5} Hz, 10^{-2} Hz\}$. In particular, as was already discussed in Eq.(3.42), the environmental dipole should be associated in a realistic experiment to molecules present, for example, in the air. The values for the electric dipole of this

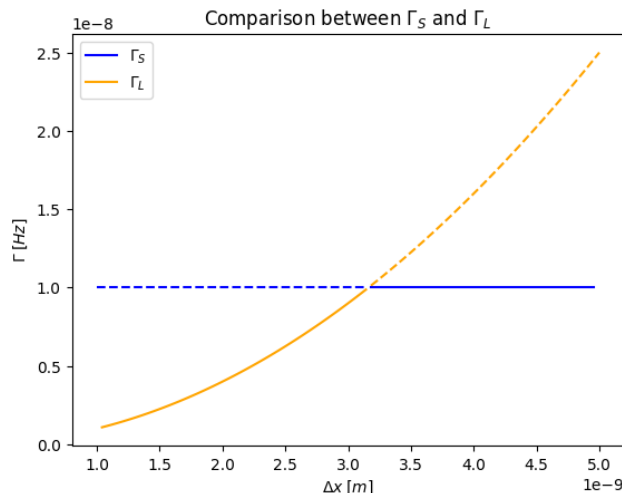


Figure 3.4: Comparison between Γ_S and Γ_L as functions of the superposition distance Δx . For $\Delta x \sim 10^{-9}m$, Γ_S and Γ_L become comparable, because $\Delta x \sim \lambda_0$. Instead, in the region where $\Delta x \gg \lambda_0$, Γ_L represents an overestimate of the decoherence rate, as it was already discussed in Eq.(3.76). Finally, in the $\Delta x \ll \lambda_0$ region, $\Gamma_S \gg \Gamma_L$, because in this case the environmental particle is not able to fully resolve the superposition distance of the crystal and now the is Γ_S to be an overestimate of the decoherence rate.

type of molecules center around $d_2 \sim 1 \text{ D} \simeq 3.336 \times 10^{-30} \text{ C} \cdot \text{m}$ [22]. With this order for magnitude of d_2 , figure 3.3 shows that the possible range for the crystal's dipole d_1 should be of $d_1 \sim 10^{-27} \text{ C} \cdot \text{m} = 10^{-2} e \cdot \mu\text{m} \simeq 10^3 \text{ D}$. It is also worth noting that with this value for d_1 the Born approximation (Eq.(3.40)) is still valid, as it is clear from the condition found with Eq.(3.43) in section 3.3.

Comparison between short and long-wavelength limit

One final discussion should be made for the decoherence rate computed in the long-wavelength limit. In fact, it is worth noting that Eq.(3.82) is much bigger than the value computed in the short-wavelength limit, as can be seen from Eq.(3.88). In particular, substituting the same numerical values used in Eq(3.88) inside Eq.(3.82), we have that $\frac{\Gamma_S}{\Gamma_L} \sim 10^{-7} \ll 1$, exactly as it was predicted from theoretical considerations in Eq.(3.76). Figure 3.4 compares the functions Γ_S and Γ_L in terms of the superposition distance Δx . In the short-wavelength limit, Γ_S is independent of Δx because the environmental particle already has complete information about the superposition distance.

In contrast, in the long-wavelength limit, Γ_L depends on Δx , following a quadratic relationship $\Gamma_L \propto \Delta x^2$. This is because the particle cannot resolve the superposition distance when λ_0 is smaller than Δx . Consequently, as Δx increases and becomes comparable to λ_0 , the environmental particle gains more information about the crystal's

position, leading to faster decoherence.

The behavior of Γ_S and Γ_L is evident in figure 3.4. Around $\Delta x \sim 10^{-9}\text{m}$, which is the same order as λ_0 at $T \sim 1\text{ K}$, both functions have similar values. For larger values of Δx in the physical region of the QGEM setup ($\Delta x \sim 10^{-5}\text{m} \gg \lambda_0 \sim 10^{-9}\text{m}$), Γ_L exceeds Γ_S , consistent with the theoretical prediction.

In the region where $\Delta x \ll 10^{-9}\text{m}$, Γ_S greatly surpasses Γ_L , aligning with the fact that the environmental particle cannot resolve the superposition distance when λ_0 is large compared to Δx . In this case, the short-wavelength limit overestimates the decoherence rate, and Γ_L provides a more accurate approximation. However, this situation is not physically relevant in a QGEM-like setup, as discussed in section (3.3.1).

3.4 Application to others QED interactions

In this section, we are going to apply the decoherence formalism analyzed until now to long range EM interactions, such as the Coulomb interaction and the ion-dipole one. As we will see, the models used for computing the decoherence rate in this work will give serious problems in the application to such interactions.

3.4.1 Charge-charge interaction in the short wavelength limit

The expression for the decoherence rate in the short-wavelength limit:

$$\Gamma = (2\pi)^{3/2} \int_0^{+\infty} dp_0 S(p_0) n v(p_0) \sigma_{CM}(p_0), \quad (3.90)$$

where $\sigma_{CM} = \int d\Omega \frac{d\sigma}{d\Omega}$ is the total cross section.

Let's now compute the total cross section σ_{CM} . We know that, from the Born approximation, the differential cross section is given by:

$$\frac{d\sigma}{d\Omega} = \frac{m^2 e^4}{64\pi^2 \epsilon_0^2 p_0^4 \sin^4(\theta/2)}. \quad (3.91)$$

This differential cross section diverges at small angles. This means that we need an IR cutoff for the angle θ . This can be done through the use of the impact parameter b . It is known, in fact, that it is related to the cross section through $\sigma = \pi b^2$. This means that:

$$\frac{d\sigma}{d\Omega} = \frac{2\pi b db}{2\pi \sin(\theta) d\theta} = \frac{b db}{\sin(\theta) d\theta}, \quad (3.92)$$

which leads to:

$$b db = \frac{m^2 e^4}{32\pi^2 \epsilon_0^2 p_0^4} \frac{\cos(\theta/2)}{\sin^3(\theta/2)} d\theta. \quad (3.93)$$

After integrating out, we obtain:

$$b(\theta) = \frac{me^2}{4\pi\epsilon_0 p_0^2} \cotan(\theta/2). \quad (3.94)$$

From this expression, it is clear that θ decreases with b . The key point is that, if our ions are confined in a box of side L , then b will have a maximum value $b_{max} = L/2$. This correspond to a *minimum* value for θ :

$$\theta_{min} = 2 \arctan\left(\frac{me^2}{2\pi\epsilon_0 p_0^2 L}\right). \quad (3.95)$$

The total cross section will thus be given by:

$$\begin{aligned} \sigma_{TOT}(p_0) &= \int d\Omega \frac{d\sigma}{d\Omega} = 8\pi \frac{m^2 e^4}{64\pi^2 \epsilon_0^2 p_0^4} \int_{\theta_{min}}^1 \frac{d(\sin(\theta/2))}{\sin^3(\theta/2)} \\ &= 8\pi \frac{m^2 e^4}{64\pi^2 \epsilon_0^2 p_0^4} \left(-\frac{1}{2}\right) (1 - \operatorname{cosec}^2(\theta_{min}/2)) \\ &= 4\pi \frac{m^2 e^4}{64\pi^2 \epsilon_0^2 p_0^4} \cotan^2(\theta_{min}/2) \\ &= \pi \left(\frac{me^2}{4\pi\epsilon_0 p_0^2} \cotan(\theta_{min}/2) \right)^2 = \frac{\pi}{4} L^2, \end{aligned} \quad (3.96)$$

where in the very last step we have used [3.95](#).

The last step before computing the decoherence rate is to find a distribution for the environmental ions. We will consider them to be a perfect gas at the thermal equilibrium. In particular, they can be described by a Maxwell-Boltzmann distribution:

$$S(p_0) = 4\pi p_0^2 (2\pi m k_B T)^{-3/2} e^{-\frac{p_0^2}{2mk_B T}}, \quad (3.97)$$

such that $\int_0^{+\infty} dp_0 S(p_0) = 1$.

We are now ready to compute the decoherence rate:

$$\Gamma = (2\pi)^{3/2} \int_0^{+\infty} 4\pi p_0^2 (2\pi m k_B T)^{-3/2} e^{-\frac{p_0^2}{2mk_B T}} \frac{p_0}{m} \frac{\pi}{4} L^2. \quad (3.98)$$

Using the formula for the gaussian integral:

$$\int_0^{+\infty} q^{2n+1} e^{-\frac{q^2}{a^2}} dq = \frac{n!}{2} a^{2n+2}, \quad (3.99)$$

we finally obtain:

$$\Gamma_{ion-ion} = \sqrt{2}\pi^2 \frac{n}{m} L^2 \sqrt{2mk_B T}. \quad (3.100)$$

Considering the environment to be composed of free charged ions, with mass m given approximately by the proton's mass (i.e. $m \sim 10^{-27} \text{ kg}$), temperature $T \sim 1\text{K}$, experimental box of size $L \sim 10^{-3}m$ and a number density $n \sim 10^{10}m^{-3}$ (which, through the relation $p = nk_B T$, corresponds to $p \sim 10^{-13} \text{ Pa}$) we have:

$$\Gamma_{ion-ion} \sim 10^6 \text{ Hz}. \quad (3.101)$$

3.4.2 Charge-charge interaction in the long wavelength limit

The decoherence rate in the long-wavelength limit:

$$\Gamma = \Delta x^2 \int dp_0 S(p_0) n v(p_0) \frac{p_0^2}{\hbar^2} \sigma_{eff}(p_0), \quad (3.102)$$

where σ_{eff} is given by:

$$\sigma_{eff} = \frac{2\pi}{3} \int_{-1}^1 d(\cos(\theta)) [1 - \cos(\theta)] \frac{d\sigma}{d\Omega}. \quad (3.103)$$

Using the differential cross section for the charge-charge scattering as in Eq.(3.91) and considering the minimum angle as in Eq.(3.95), we obtain:

$$\begin{aligned} \sigma_{eff} &= \frac{2\pi}{3} \int_{-1}^{\cos(\theta_{min})} d(\cos(\theta)) [1 - \cos(\theta)] \frac{m^2 e^4}{64\pi^2 \epsilon_0^2 p_0^4 \sin^4(\theta/2)} \\ &= \frac{m^2 e^4}{96\pi \epsilon_0^2 p_0^4} \int_s^1 dx \ 4x \ 2x^2 \frac{1}{x^4} = \frac{m^2 e^4}{12\pi \epsilon_0^2 p_0^4} \int_s^1 dx \frac{1}{x} = \frac{m^2 e^4}{96\pi \epsilon_0^2 p_0^4} \ln\left(\frac{1}{s}\right), \end{aligned} \quad (3.104)$$

where in the second line we have changed variable of integration:

$$d(\cos(\theta)) \rightarrow d\left(1 - 2 \sin^2\left(\frac{\theta}{2}\right)\right) \equiv d(1 - 2x^2) = -2 \ 2x \ dx = -4x \ dx, \quad (3.105)$$

and defined $s \equiv \sin\left(\frac{\theta_{min}}{2}\right)$.

Let us analyze more in detail s . In particular, from Eq.(3.95), we know that:

$$\sin\left(\frac{\theta_{min}}{2}\right) = \sin\left[\arctan\left(\frac{me^2}{2\pi\epsilon_0 p_0^2 L}\right)\right] \equiv \sin[\arctan(\alpha)]. \quad (3.106)$$

Using the fact that:

$$\alpha = \tan(\beta) = \frac{\sin(\beta)}{\cos(\beta)} = \frac{\sin(\beta)}{\sqrt{1 - \sin^2(\beta)}}, \quad (3.107)$$

we obtain:

$$s \equiv \sin\left(\frac{\theta_{min}}{2}\right) = \frac{\alpha}{\sqrt{1+\alpha^2}}. \quad (3.108)$$

the effective action will be thus given by:

$$\begin{aligned} \sigma_{eff} &= \frac{m^2 e^4}{96\pi\epsilon_0^2 p_0^4} \ln\left(\frac{\sqrt{1 + \left(\frac{me^2}{2\pi\epsilon_0 p_0^2 L}\right)^2}}{\frac{me^2}{2\pi\epsilon_0 p_0^2 L}}\right) \\ &= \frac{m^2 e^4}{96\pi\epsilon_0^2 p_0^4} \ln\left(\frac{2\pi\epsilon_0 p_0^2 L}{me^2} \sqrt{1 + \left(\frac{me^2}{2\pi\epsilon_0 p_0^2 L}\right)^2}\right). \end{aligned} \quad (3.109)$$

Let us now compute the final decoherence rate Γ , which is given by Eq.(3.102). In particular, we can define a statistical distribution $S(p_0)$ for the environmental particles given by a Dirac's delta $\delta(p_0 - \bar{p})$, with $\bar{p} = \sqrt{2mk_B T}$. In fact, for temperatures T near to 0 K, as in the QGEM setup, the Maxwell Boltzmann is strongly peaked around the value $p = \bar{p} = \sqrt{2mk_B T}$. This means that we can use a delta-like distribution, i.e. $S(p_0) = \delta(p_0 - \bar{p})$, instead of a Maxwell-Boltzmann.

In thus way, the final decoherence rate is:

$$\begin{aligned} \Gamma &= \Delta x^2 \int_0^{+\infty} dp_0 \delta(p_0 - \bar{p}) n \frac{p_0 p_0^2}{m \hbar^2} \frac{m^2 e^4}{96\pi\epsilon_0^2 p_0^4} \ln\left(\frac{2\pi\epsilon_0 p_0^2 L}{me^2} \sqrt{1 + \left(\frac{me^2}{2\pi\epsilon_0 p_0^2 L}\right)^2}\right) \\ &= \frac{me^4 \Delta x^2 n}{96\pi\epsilon_0^2 \hbar^2 \bar{p}} \ln\left(\frac{2\pi\epsilon_0 \bar{p}^2 L}{me^2} \sqrt{1 + \left(\frac{me^2}{2\pi\epsilon_0 \bar{p}^2 L}\right)^2}\right) \end{aligned} \quad (3.110)$$

Notice that the numerical value of the term $\frac{me^2}{2\pi\epsilon_0 p_0^2 L}$ inside the squared root is negligible, i.e. considering $m \sim 10^{-27} kg$, $\bar{p} = \sqrt{2mk_B T} \sim 10^{-25} kg \frac{m}{s}$ and $L \sim 10^{-3} m$, we have that:

$$\frac{me^2}{2\pi\epsilon_0 \bar{p}^2 L} \sim 4.6 \times 10^{-2} \ll 1, \quad (3.111)$$

which leads to:

$$\Gamma \simeq \frac{me^4 \Delta x^2 n}{96\pi\epsilon_0^2 \hbar^2 \bar{p}} \ln\left(\frac{2\pi\epsilon_0 \bar{p}^2 L}{me^2}\right). \quad (3.112)$$

Let us compute its numerical value. Using, as always, $m \sim 10^{-27} kg$, $T \sim 1 K$, $n \sim 10^{10} m^{-3}$ and $\Delta x \sim 10^{-5} m$, we obtain:

$$\Gamma \sim 10^{10} Hz. \quad (3.113)$$

3.4.3 Charge-dipole interaction in the short wavelength limit

In this case, we will consider the case where the diamond used in the QGEM experiment is neutral, i.e. with total charge equal to 0. But, also in this case, there can be decoherence due to EM interaction, because the crystal can have a dipole moment \vec{d} .

We can use in this case the same model that we used for the charged case. The only difference is in the cross section, because now the potential between the environmental particle and the crystal is:

$$V(r, \phi) = \frac{1}{4\pi\epsilon_0} \frac{Qd}{r^2} \cos(\phi), \quad (3.114)$$

where Q is the environmental particle's charge, $d = |\vec{d}|$ is the dipole moment of the crystal and ϕ is the angle between \vec{d} and the vector $\hat{r} = \frac{\vec{r}}{r}$ that connects the environmental particle and the COM of the crystal.

We can use again the Born approximation to find the differential cross section for this potential. Let's start with the Fourier transform:

$$\begin{aligned} \tilde{V}(q) &= \int_0^{2\pi} d\psi \int_0^\pi d\phi \sin(\phi) \int_0^{+\infty} dr r^2 \frac{1}{4\pi\epsilon_0} \frac{Qd}{r^2} \cos(\phi) \\ &= \frac{Qd}{2\epsilon_0} \int_0^{+\infty} dr \int_{-1}^1 d(\cos(\phi)) \cos(\phi) e^{iqr \cos(\phi)} \\ &= \frac{Qd}{2\epsilon_0} \int_0^{+\infty} dr 2i \frac{\sin(qr) - qr \cos(qr)}{(qr)^2} \\ &= i \frac{Qd}{\epsilon_0 q} \int_0^{+\infty} dx \frac{\sin(x) - x \cos(x)}{x^2} = i \frac{Qd}{\epsilon_0 q}. \end{aligned} \quad (3.115)$$

Plugging this into the Born approximation formula, after substituting $q \rightarrow q/\hbar$ in order to obtain the right SI units, we have:

$$\frac{d\sigma}{d\Omega} = \frac{m^2}{4\pi^2\hbar^4} |\tilde{V}(q)|^2 = \frac{m^2 Q^2 d^2}{16\pi^2 \epsilon_0^2 \hbar^2} \frac{1}{p^2 \sin^2(\theta/2)}, \quad (3.116)$$

where $\vec{q} = \vec{p}_f - \vec{p}_i$ is considered to be the transferred momentum, i.e. $|\vec{q}| = q = \sqrt{p_i^2 + p_f^2 - 2\vec{p}_i \cdot \vec{p}_f} = 2p \sin(\theta/2)$, where we have used the fact that, for this case where the target crystal is much heavier than the projectile environmental particle, we have $|\vec{p}_i| = |\vec{p}_f| = p$.

As we can see from 3.133, also in this case we have a singularity for small angles $\theta \sim 0$. This means that, in order to compute the differential cross section, we have to find a minimum angle θ_{min} , which corresponds to a maximum value for the impact parameter b , i.e. a cutoff for b . Knowing that $\sigma = \pi b^2$, we can find a relation between b and θ :

$$\begin{aligned} \frac{d\sigma}{d\Omega} &= \frac{2\pi b db}{2\pi \sin(\theta) d\theta} = \frac{b}{\sin(\theta)} \frac{db}{d\theta} \\ &= \frac{m^2}{4\pi^2 \hbar^4} |\tilde{V}(q)|^2 = \frac{m^2 Q^2 d^2}{16\pi^2 \epsilon_0^2 \hbar^2 p^2 \sin^2(\theta/2)}. \end{aligned} \quad (3.117)$$

Integrating out θ , we obtain:

$$\frac{b^2}{2} = 4 \frac{m^2 Q^2 d^2}{16\pi^2 \epsilon_0^2 \hbar^2 p^2} \ln \left[\frac{1}{\sin(\theta/2)} \right]. \quad (3.118)$$

It is clear from this relation that b decreases as θ increases, which mean that θ_{min} will correspond to $b_{max} = L/2$. Their relation is:

$$L^2 = \frac{2m^2 Q^2 d^2}{\pi^2 \epsilon_0^2 \hbar^2 p^2} \ln \left[\frac{1}{\sin(\theta_{min}/2)} \right]. \quad (3.119)$$

Let's use this expression for θ_{min} for computing the total cross section:

$$\begin{aligned} \sigma &= \int d\Omega \frac{m^2 Q^2 d^2}{16\pi^2 \epsilon_0^2 \hbar^2 p^2 \sin^2(\theta/2)} \\ &= \frac{m^2 Q^2 d^2}{16\pi^2 \epsilon_0^2 \hbar^2 p^2} 2\pi \int_{-1}^{\cos(\theta_{min})} d(\cos(\theta)) \frac{1}{\sin^2(\theta/2)} \\ &= \frac{m^2 Q^2 d^2}{16\pi^2 \epsilon_0^2 \hbar^2 p^2} 8\pi \ln \left[\frac{1}{\sin(\theta_{min}/2)} \right] \\ &= \frac{\pi}{4} \frac{2m^2 Q^2 d^2}{\pi^2 \epsilon_0^2 \hbar^2 p^2} \ln \left[\frac{1}{\sin(\theta_{min}/2)} \right] = \frac{\pi}{4} L^2, \end{aligned} \quad (3.120)$$

where in the very last step we have used [3.119](#).

With this cross section and considering the distribution for the environmental particles to be $S(p_0) = 4\pi p_0^2 (2\pi m k_B T)^{-3/2} e^{-\frac{p_0^2}{2mk_B T}}$ as before, we obtain a final decoherence rate:

$$\begin{aligned} \Gamma_{ion-dipole} &= (2\pi)^{3/2} \int_0^{+\infty} 4\pi p_0^2 (2\pi m k_B T)^{-3/2} \times \\ &\times e^{-\frac{p_0^2}{2mk_B T}} \frac{p_0}{m} \frac{\pi}{4} L^2 = \sqrt{2\pi^2} \frac{n}{m} L^2 \sqrt{2mk_B T}. \end{aligned} \quad (3.121)$$

This result is exactly the same of the charge-charge interaction in the short-wavelength limit. This means that also in this case we should obtain $\Gamma \sim 10^6 \text{Hz}$ if we use the same parameters used in Eq.([3.101](#)).

3.4.4 Charge-dipole interaction in the long wavelength limit

Being a dielectric material, the crystal has a polarizability α when subjected to an external electric field E_{ext} , which inside the crystal is perceived as a local field E_{loc} . In particular, in isotropic media, the external field will create a local dipole in each atom of the crystal's lattice:

$$d = \alpha E_{loc}. \quad (3.122)$$

This means that the total contribution will be given by the sum over all N' atoms of the lattice:

$$d = N' \alpha E_{loc}. \quad (3.123)$$

So, in order to find an explicit expression for d , we need the expressions for α and E_{loc} . For α we have the **Classius-Mossotti relation**:

$$\frac{n' \alpha}{3\epsilon_0} = \frac{\epsilon_r - 1}{\epsilon_r + 2}, \quad (3.124)$$

where $n' = \frac{N'}{V}$ is the atomic density inside the crystal and the volume is given by $V \sim R^3 \sim (10^{-7}m)^3$.

For the local field, in our case it is simply generated by the charged environmental particle:

$$E_{ext} = \frac{e}{4\pi\epsilon_0\epsilon_r \bar{r}^2}, \quad (3.125)$$

where \bar{r} is the average distance between the environmental particle and the crystal. In this case, considering that all the events happen in an experimental box of size $L \sim 10^{-3}m$, the average ion-crystal distance will increase with the size of the box. This means that we can consider:

$$\bar{r} \sim L. \quad (3.126)$$

We are now able to find an explicit expression for d :

$$d = N' \frac{3\epsilon_0}{n'} \left(\frac{\epsilon_r - 1}{\epsilon_r + 2} \right) \frac{e}{4\pi\epsilon_0\epsilon_r} \frac{1}{L^2} = \frac{3eR}{4\pi\epsilon_r} \left(\frac{\epsilon_r - 1}{\epsilon_r + 2} \right) \left(\frac{R}{L} \right)^2. \quad (3.127)$$

The numerical value for this dipole, using $R \sim 10^{-7}m$, $L \sim 10^{-3}m$ and $\epsilon_r \sim 5.7$, is:

$$d \sim 4.1 \times 10^{-36} \text{ C} \cdot \text{m}. \quad (3.128)$$

The final formula for the decoherence rate, in the long-wavelength limit, is:

$$\Gamma = \Delta x^2 \int_0^{+\infty} dp \rho(p) v(p) \frac{p^2}{\hbar^2} \sigma_{eff}(p), \quad (3.129)$$

where Δx^2 is the superposition distance, $\rho(p)$ is the momentum distribution of the N environmental particles (e.g. a Maxwell-Boltzman distribution), $v(p) = \frac{p}{m}$ is the velocity of the environmental particle and:

$$\sigma_{eff} = \frac{2\pi}{3} \int_{-1}^1 d(\cos(\theta)) [1 - \cos(\theta)] \frac{d\sigma}{d\Omega} \quad (3.130)$$

is the efficient cross-section.

In order to find σ_{eff} , we first need to find the differential cross section $\frac{d\sigma}{d\Omega}$. The potential between the environmental particle and the crystal is:

$$V(r, \phi) = \frac{1}{4\pi\epsilon_0} \frac{Qd}{r^2} \cos(\phi), \quad (3.131)$$

where Q is the environmental particle's charge, $d = |\vec{d}|$ is the dipole moment of the crystal and ϕ is the angle between \vec{d} and the vector $\hat{r} = \frac{\vec{r}}{r}$ that connects the environmental particle and the COM of the crystal.

We can use again the Born approximation to find the differential cross section for this potential. Let's start with the Fourier transform:

$$\begin{aligned} \tilde{V}(q) &= \int_0^{2\pi} d\psi \int_0^\pi d\phi \sin(\phi) \int_0^{+\infty} dr r^2 \frac{1}{4\pi\epsilon_0} \frac{Qd}{r^2} \cos(\phi) \\ &= \frac{Qd}{2\epsilon_0} \int_0^{+\infty} dr \int_{-1}^1 d(\cos(\phi)) \cos(\phi) e^{iqr \cos(\phi)} \\ &= \frac{Qd}{2\epsilon_0} \int_0^{+\infty} dr 2i \frac{\sin(qr) - qr \cos(qr)}{(qr)^2} \\ &= i \frac{Qd}{\epsilon_0 q} \int_0^{+\infty} dx \frac{\sin(x) - x \cos(x)}{x^2} = i \frac{Qd}{\epsilon_0 q}. \end{aligned} \quad (3.132)$$

Plugging this into the Born approximation formula, after substituting $q \rightarrow q/\hbar$ in order to obtain the right SI units, we have:

$$\frac{d\sigma}{d\Omega} = \frac{m^2}{4\pi^2 \hbar^4} |\tilde{V}(q)|^2 = \frac{m^2 Q^2 d^2}{16\pi^2 \epsilon_0^2 \hbar^2} \frac{1}{p^2 \sin^2(\theta/2)}, \quad (3.133)$$

where $\vec{q} = \vec{p}_f - \vec{p}_i$ is considered to be the transferred momentum, i.e. $|\vec{q}| = q = \sqrt{p_i^2 + p_f^2 - 2\vec{p}_i \cdot \vec{p}_f} = 2p \sin(\theta/2)$, where we have used the fact that, for this case where the target crystal is much heavier than the projectile environmental particle, we have $|\vec{p}_i| = |\vec{p}_f| = p$.

Using [3.133](#), we can compute $\sigma_{eff}(p)$:

$$\begin{aligned}
\sigma_{eff}(p) &= \frac{2\pi}{3} \int_{-1}^1 d(\cos(\theta)) [1 - \cos(\theta)] \frac{m^2 Q^2 d^2}{16\pi^2 \epsilon_0^2 \hbar^2 p^2} \frac{1}{\sin^2(\theta)} \\
&= \frac{m^2 Q^2 d^2}{24\pi \epsilon_0^2 \hbar^2 p^2} \int_0^1 d[\sin(\theta/2)] \cdot 4 \sin(\theta/2) \cdot 2 \sin^2(\theta/2) \frac{1}{\sin^2(\theta/2)} \\
&= \frac{m^2 Q^2 d^2}{3\pi \epsilon_0^2 \hbar^2 p^2} \int_0^1 d[\sin(\theta/2)] \cdot \sin(\theta/2) = \frac{m^2 Q^2 d^2}{6\pi \epsilon_0^2 \hbar^2 p^2}.
\end{aligned} \tag{3.134}$$

We are now ready to compute the final decoherence rate. In particular, using $\rho(q) = 4\pi n p^2 (2\pi m k_B T)^{-3/2} e^{-\frac{p^2}{2mk_B T}}$, with $n = \frac{N}{L^3}$ being the environmental particle number density, we obtain:

$$\begin{aligned}
\Gamma &= \Delta x^2 \int_0^{+\infty} dp 4\pi n p^2 (2\pi m k_B T)^{-3/2} e^{-\frac{p^2}{2mk_B T}} \frac{p}{m} \frac{p^2}{\hbar^2} \frac{m^2 Q^2 d^2}{6\pi \epsilon_0^2 \hbar^2 p^2} = \\
&= \frac{2m Q^2 d^2}{3\pi^{3/2} \epsilon_0^2 \hbar^4} \Delta x^2 n (2mk_B T)^{-3/2} \int_0^{+\infty} dp p^3 e^{-\frac{p^2}{2mk_B T}}.
\end{aligned} \tag{3.135}$$

Using:

$$\int_0^{+\infty} dp p^{2l+1} e^{-\frac{p^2}{2mk_B T}} = \frac{l!}{2} (2mk_B T)^{l+1}, \tag{3.136}$$

we obtain the final decoherence rate:

$$\Gamma = \frac{m Q^2 d^2}{3\pi^{3/2} \epsilon_0^2 \hbar^4} \Delta x^2 n \sqrt{2mk_B T}. \tag{3.137}$$

Finally, we can compute its numerical value. In particular, using $m \sim 10^{-27} kg$ (i.e. proton mass for the environmental particle), $Q = e \sim 1.602 \times 10^{-19} C$, $\Delta x \sim 10^{-5} m$, $T \sim 1 K$ and the value for $d \sim 4.1 \times 10^{-36} C \cdot m$ found in the previous section, we obtain:

$$\Gamma_{ion-dipole}^{(long)} \sim (2.7 \times 10^{-14} n) Hz, \tag{3.138}$$

where n represents now only the *numerical* value of the environmental particle density: its units have already been absorbed in the final result in Hz .

We can show now how this result represents a physical value. In fact, in order to have a final decoherence rate of the order of $\Gamma \sim 10^{-2} Hz$, we need n to be:

$$n \sim 10^{12} \frac{particles}{m^3}. \tag{3.139}$$

In terms of the pressure $p = nk_B T$, using $T \sim 1 K$, we have:

$$p \sim 10^{-11} Pa, \tag{3.140}$$

which represents a physical value that can be performed in the QGEM experiment.

3.5 Decoherence due to acceleration

3.5.1 Charged case

Decoherence due to the acceleration happens because the photons emitted by the accelerated charged particle brings with them information about the system. So, at this point, in order to obtain any type of information about the particle, it is not sufficient to perform measurements on the particle alone, because the information is shared with the photons emitted; i.e. the particle is entangled with the photons.

This means that, during the acceleration process, the state of our system is:

$$|\Psi\rangle = \frac{1}{\sqrt{2}}(|L\rangle_{part} |\Psi_1\rangle_{rad} + |R\rangle_{part} |\Psi_2\rangle_{rad}), \quad (3.141)$$

where $|\Psi_{1,2}\rangle_{rad}$ are the states associated to the emitted radiation, respectively, to the left and the right branch of the particle.

As Eq.(1.19) shows [18], the decoherence factor is encoded in the scalar product of the two final states of the environment, i.e.:

$$\rho(x, x', t = 0) \longrightarrow \rho(x, x', t = 0) \langle \Psi_1 | \Psi_2 \rangle. \quad (3.142)$$

We thus need to find an expression for $|\Psi_{1,2}\rangle$. We can start by choosing them to be coherent states [64]:

$$|\alpha\rangle = e^{-\frac{|\alpha|^2}{2}} \sum_n \frac{\alpha^n}{\sqrt{n!}} |n\rangle, \quad (3.143)$$

where $\alpha = |\alpha|e^{i\phi}$ is a complex number that characterizes the radiation emitted. In particular, it is known that they are related to the expectation value of the EM field emitted [65]:

$$\langle \alpha | \hat{E}(x) | \alpha \rangle \sim |\alpha| \sin(k \cdot x - \phi) \vec{e}, \quad (3.144)$$

where \vec{e} is the direction of the electric field. This means that $|\alpha|$ is related to the intensity of the field and ϕ is its phase.

In our case, the difference between the two coherent states $|\alpha_L\rangle$ and $|\alpha_R\rangle$ it's only in the phase: in fact, being the superposition setup symmetric between the two brunches L and R (see figure 2.2), the intensity of the radiation emitted will be the same. The only difference is in the position where the radiation is emitted, whether if the crystal is in L or R ; this differences has an influence only in the phase of the EM field: in fact, as can be seen from 3.144, if we perform a translation $x \longrightarrow x + \Delta x$, the extra Δx factor will enter as an extra phase.

This means that:

$$\begin{cases} |\alpha_L| = |\alpha_R| \\ \phi_L \neq \phi_R \end{cases}. \quad (3.145)$$

The scalar product will thus give:

$$\begin{aligned} \langle \alpha_L | \alpha_R \rangle &= \left(e^{-\frac{|\alpha|^2}{2}} \sum_m \frac{\alpha_L^{m*}}{\sqrt{m!}} \langle m | \right) \left(e^{-\frac{|\alpha|^2}{2}} \sum_n \frac{\alpha_R^n}{\sqrt{n!}} |n\rangle \right) = \\ &= e^{-|\alpha|^2} \sum_{m,n} \frac{|\alpha|^{n+m}}{\sqrt{m!} n!} e^{i(n\phi_R - m\phi_L)} \langle m | n \rangle = \\ &= e^{-\langle N \rangle} \sum_n \frac{\langle N \rangle^n}{n!} e^{in(\phi_L - \phi_R)} = e^{-\langle N \rangle} e^{\langle N \rangle e^{i(\phi_L - \phi_R)}} = e^{-\langle N \rangle (1 - e^{i(\phi_L - \phi_R)})}, \end{aligned} \quad (3.146)$$

where we have used the known property of the coherent states $\langle N \rangle = |\alpha|^2 =$ average number of photons in the state $|\alpha\rangle$.

From Eq.(3.146) it is clear that, in order to find an explicit expression for the decoherence rate, we first need to find an expression for $\langle N \rangle = |\alpha|^2$. This can be done by starting from the **Larmor's formula**, which gives the power $P(t)$ emitted by an accelerating charged particle:

$$P(t) = \frac{dU}{dt} = \frac{Q^2 a^2(t)}{6\pi\epsilon_0 c^3}, \quad (3.147)$$

where U represents the energy emitted, Q is the total charge of the accelerating particle and $a(t)$ is the acceleration function.

In order to find the total energy emitted U_{tot} , we can integrate out P in time t by considering the following acceleration $a(t)$:

$$\begin{cases} a = const. & \text{if } t \in [0, t_0] \\ 0 & \text{otherwise} \end{cases}, \quad (3.148)$$

where t_0 is the total time during when the particle is accelerated. This gives:

$$U_{tot} = \frac{Q^2 a^2 t_0}{6\pi\epsilon_0 c^3}. \quad (3.149)$$

Assuming now that each photon contributes with an energy $E = \hbar\omega \sim \frac{2\pi\hbar}{t_0}$, dividing U_{tot} with E will give us the total number of photons emitted $\langle N \rangle$:

$$\langle N \rangle \sim \frac{Q^2 a^2 t_0^2}{12\pi^2 \epsilon_0 c^3 \hbar}. \quad (3.150)$$

An alternative expression for $\langle N \rangle$ can be found in terms of the superposition distance Δx : in fact, we can simply use the classical equations of motion for an accelerated system $x = x_0 + v_0 t + \frac{1}{2} a(t) t^2$. In our case, we have a constant acceleration a for a finite amount of time t_0 , during which the particle travels a distance $d = \frac{\Delta x}{2}$. This leads to:

$$\frac{\Delta x}{2} = \frac{1}{2} a t_0^2, \quad (3.151)$$

which can be used to find an explicit expression for a , i.e. $a = \frac{\Delta x}{t_0^2}$. Substituting this inside 3.150, we obtain (in SI units):

$$\langle N \rangle \sim \frac{Q^2 \Delta x^2}{12 \pi^2 \epsilon_0 c^3 \hbar t_0^2}. \quad (3.152)$$

Notice that 3.152 is the same result used in [35].

Let's now check the numerical dimensions of $\langle N \rangle$ for a QGEM setup. Considering $Q \sim e = \text{electron's charge}$, $\Delta x \sim 10^{-5} m$ and a total acceleration time of the order $t_0 \sim 1 s$, we obtain:

$$\langle N \rangle \sim 8.6 \times 10^{-31}. \quad (3.153)$$

We can see that $\langle N \rangle$ is the dominant factor in the exponential of the expression for the scalar product 3.146. In particular, the term $1 - e^{i(\phi_L - \phi_R)}$ will only contribute to make the scalar product smaller and will not contribute to increasing the order of $\langle N \rangle$, given that $0 \leq |1 - e^{i(\phi_L - \phi_R)}| \leq 2$. This means that the term at the exponent of 3.146 is of the order of $\langle N \rangle$, which is very small, i.e. $\langle N \rangle \ll 1$. Therefore, the scalar product in Eq.(3.146) can be rewritten as:

$$\langle \alpha_L | \alpha_R \rangle \simeq e^{-\langle N \rangle(t_0)}, \quad (3.154)$$

where we made explicit the t_0 dependence of $\langle N \rangle$.

Considering now that the matrix element evolves according to equation 3.142, we can find a time evolution for the matrix element w.r.t. to time t , in order to obtain the decoherence rate Γ . In particular:

$$\rho(x, x', t) = \rho(x, x', 0) \langle \alpha_L | \alpha_R \rangle \simeq \rho(x, x', 0) e^{-\langle N \rangle(t)} \quad (3.155)$$

where in the very last step we have used Eq.(3.154) and generalized it to a generic time t instead of the total one t_0 .

Finally, it is useful to remember that the decoherence rate Γ is defined as the *rate* at which the off-diagonal elements of the density matrix are suppressed, i.e. how fast the suppression term $e^{-\langle N \rangle(t)}$ goes to 0. This allows us to find the following expression for Γ :

$$\Gamma = \frac{d\langle N \rangle(t)}{dt} = \frac{d}{dt} \left[\frac{Q^2 a^2 t^2}{12\pi^2 \epsilon_0 c^3 \hbar} \right] = \frac{Q^2 a^2 t}{6\pi^2 \epsilon_0 c^3 \hbar} = \frac{U(t)}{\hbar}, \quad (3.156)$$

where we have used the expression for $\langle N \rangle$ given by Eq.(3.150) and used Eq.(3.149) for the energy emitted at a generic instant of time t .

Notice that Eq.(3.156) will give a numerical value of the same order of $\langle N \rangle$, as can be seen by comparing it with Eq.(3.153). This means that, during the **Third Step** of the QGEM proposal, the electromagnetic phenomena analyzed in this case should not represent a relevant source of noise for the realisation of the experiment.

3.5.2 Dipole case

In this subsection, we are going to consider the same process analyzed in the previous one, but now the accelerated crystal is neutral and the only EM property that can lead to decoherence is its own dipole d .

The only difference with the charged case is that the power emitted will be different. In particular, the Larmor formula for an accelerating dipole gives:

$$P = \frac{\ddot{d}(t)^2}{6\pi\epsilon_0 c^3}, \quad (3.157)$$

which gives the energy emitted per unit of time.

Let's find out how to compute explicitly $\ddot{d}(t)$. We can express the dipole as:

$$\mathbf{d}(t) = \int_V d^3\mathbf{x}' \mathbf{x}' \rho(\mathbf{x}', t), \quad (3.158)$$

where $\rho(\mathbf{x}', t)$ is the charge density.

Therefore, as can be seen from Eq.(3.157), it is worth studying the cases where $\dot{\mathbf{d}}(t) \neq 0$ and $\ddot{\mathbf{d}}(t) \neq 0$. In particular, any change in time of $\mathbf{d}(t)$ is strictly correlated to the time dependence of $\rho(\mathbf{x}', t)$ inside the integral of the RHS of Eq.(3.158).

In particular, we are going to analyze the case when the neutral dipole \mathbf{d} undergoes a *translational* acceleration, i.e. when the system *rigidly* translates and the trajectory of its center of mass is a uniform acceleration motion. This is exactly the case for the **Third Step** of the QGEM experiment studied in section 2.3.2, where the superposition of the nano-crystal is brought back to the initial state and the system undergoes thus an acceleration.

In this case, the only time dependence in Eq.(3.158) is inside the argument of $\rho(\mathbf{x}', t) = \rho(\mathbf{x}'(t))$: that is because the only property of the dipole that changes over time is its position in space. In particular, the equations of motion of its center of mass are dictated by the following transformation: $\mathbf{x}' \rightarrow \mathbf{x}' + \frac{1}{2}\mathbf{a}t^2$, which is the case of a *uniform* accelerating motion with constant acceleration \mathbf{a} . This results in the following time evolution for the dipole moment \mathbf{d} :

$$\mathbf{d}(0) \longrightarrow \mathbf{d}(t) = \int_V d^3\mathbf{x}' \mathbf{x}' \rho\left(\mathbf{x}' + \frac{1}{2}\mathbf{a}t^2\right) = \int_{V'} d^3\mathbf{x} \left(\mathbf{x} - \frac{1}{2}\mathbf{a}t^2\right) \rho(\mathbf{x}), \quad (3.159)$$

where we have performed the following change of variable: $\mathbf{x} = \mathbf{x}' + \frac{1}{2}\mathbf{a}t^2$. In particular, this substitution changes also the finite volume $V \rightarrow V'$ over which $\rho(\mathbf{x})$ is integrated. Now, if we consider V to be much bigger than the volume of our nano-crystal V_C , i.e. if all the charge distribution is contained inside V , any shift of the volume V' will not influence the result of the integration, because the charge distribution will still be entirely contained inside V' . This allows us to write $\int_{V'}(\dots) = \int_V(\dots)$ and Eq.(3.159) can be rewrite as:

$$\begin{aligned} \mathbf{d}(t) &= \int_V d^3\mathbf{x} \left(\mathbf{x} - \frac{1}{2}\mathbf{a}t^2\right) \rho(\mathbf{x}) = \\ &\int_V d^3\mathbf{x} \mathbf{x} \rho(\mathbf{x}) - \frac{1}{2}\mathbf{a}t^2 \int_V d^3\mathbf{x} \rho(\mathbf{x}) = \mathbf{d}(0) + 0 = \mathbf{d}(0), \end{aligned} \quad (3.160)$$

where we have used the fact that the dipole is a neutral object and has therefore a total charge of $\int_V d^3\mathbf{x} \rho(\mathbf{x}) = 0$.

Eq.(3.160) is very important for our analysis, because it shows that \mathbf{d} is translational invariant and, in the case of translational acceleration, there is **no** change in the dipole, i.e. $\dot{\mathbf{d}}(t) = 0 = \ddot{\mathbf{d}}(t)$. Therefore, from Eq.(3.157), we have that in this case the power emitted is $P = 0$ and no radiation is emitted by the dipole. But, we also know that if there is no emission of radiation, there is no creation of photons in the environment and therefore no information about the quantum properties of the superposed nano-crystal is spread over the environment. This leads to the final conclusion that, in the case for translational acceleration, there is **no** decoherence. The **Third Step** of the QGEM setup does not represent a problem for the realization of the experiment if the nano-crystal possesses an electric dipole.

Conclusion

In this comprehensive study, we have extensively analyzed two distinct models for decoherence, namely the Scattering Model and the Born-Markov Master Equation. These models have provided us with insights into the dynamics of decoherence phenomena, shedding light on the interplay between quantum systems and their surrounding environments.

The Scattering Model, a widely employed framework, delves into the computation of the decoherence rate by rigorously examining the scalar product between the final states of the scattered environmental particle. By employing the S-matrix and its corresponding formalism, this model enables us to precisely determine the final decoherence rate, drawing upon the differential cross section that characterizes the interaction between the system and the environment.

Simultaneously, we have analyzed the Born-Markov Master Equation, a powerful tool for investigating the dynamics of quantum systems within a large environment. This model provides a valuable means of deriving a dynamical equation for the density matrix of a quantum system that finds itself immersed in an environment of large scale. By employing the Born approximation, which accounts for the disparity in size between the system and the environment, and incorporating the Markovian assumption, which disregards memory effects within the environment after its interaction with the system, we acquire a non-unitary time evolution equation for the system's density matrix. Through this, we gain insights into the temporal behavior and evolution of the quantum system under the influence of its surrounding environment.

In this thesis project, we have delved further into the application of these models, focusing on a generic QED interaction Hamiltonian between two fermions within the framework of the Born-Markov master equation. This Hamiltonian, constructed in terms of operators for both the system and the environment, has provided us with a foundation for applying the Born-Markov equation. Remarkably, by assuming the system to be significantly heavier than the environmental particle, we have derived a final formula for the decoherence rate that mirrors the form (up to a constant factor) found within the Scattering Model.

Expanding upon these findings, we have directed the focus towards exploring the dipole-dipole interactions, a compelling area of study within the context of decoherence.

By deriving the differential cross section for such interactions, we have successfully obtained an explicit expression for the decoherence rate, utilizing the parameters employed within the QGEM experiment, such as temperature, pressure, and the dipole of the nano-crystal. This comprehensive numerical evaluation has enabled us to ascertain an upper bound for the crystal's dipole, ensuring a decoherence rate smaller than 0.01 Hz. This requirement arises from the necessity of preserving the spatial superposition of the massive particle for a minimum duration of 1 second, accordingly to the QGEM proposal. By guaranteeing a decoherence rate of 0.01 Hz or less, we can confidently ensure the preservation of the crucial superposition throughout the experiment. Remarkably, the upper bound for the crystal's dipole determined through this work is on the order of $d_1 = 10^3 \text{D}$, which represents a relatively small value when compared to certain measurements conducted within laboratory settings [66]. Therefore, this final result shows the importance of studying this type of decoherence source for the realization of the QGEM experiment: in fact, the interaction analyzed can in principle represent a real life physical situation in a lab, where the superposed nano-crystal can be surrounded by a non negligible number of environmental air molecules. In particular, for typical thermodynamical values of the QGEM proposal (i.e. $T \sim 1 \text{ K}$ and $p \sim 10^{-13} \text{ Pa}$), we obtain a non-null number density for the environmental particles $n = \frac{p}{k_B T} \sim 10^{10} \text{ m}^{-3}$. Moreover, these particles can be represented by air molecules in real life situations, which inevitably possess a non-null electric dipole moment $d_2 \sim 1 \text{ D}$ [22].

Furthermore, we have extended our investigation to other types of electromagnetic interactions, such as Coulomb interaction and ion-dipole interaction. These interactions, characterized by their infinite range of action, present unique challenges within the Scattering Model framework due to their infinite total cross sections. In fact, as it is clear from Eq.(1.39), the decoherence rate Γ_S is defined only when the total cross section σ_{tot} is finite. Consequently, the Scattering Model cannot be directly applied to analyze these interactions, as the final results heavily depend on a cutoff parameter L , representing the maximum impact parameter of an environmental particle, as can be seen from Eq.(3.96). Such a cutoff parameter causes the final results to lose information on the specific nature of the interaction, such as the elementary charge, as it is clear from Eq.(3.100) and Eq.(3.121).

Another result that shows clearly how the decoherence models analyzed and used in this work are not suitable for long-range interactions is Eq.(3.138). In fact, if we consider in this equation a number density of $n \sim 10^{10} \text{ m}^{-3}$, the final decoherence rate computed in the long-wavelength limit will be of $\Gamma_{ion-dipole}^{(long)} \sim 10^{-4} \text{ Hz}$. In particular, the problem with this result lies in the fact that it is much smaller than the value of $\Gamma_{ion-dipole} \sim 10^6 \text{ Hz}$ given by Eq.(3.138); this clearly contradicts the analysis made in Eq.(1.46) with the comparison between the short and the long-wavelength limit, where it was shown that in this case the long-wavelength approximation gives an upper bound for the final decoherence rate. Such a theoretical consideration is instead satisfied in the dipole-dipole case, which is an interaction with a finite and well-defined total cross

section, as it was already widely discussed in section (3.3).

The reason behind this type of behaviour for long range interactions can be some of the fundamental approximation that we have used in the derivation for the Born-markov master equation. In particular, it is possible that the Born approximation described in Eq.(1.53) cannot hold for long range interactions: in fact, it is impossible in this case to separate the environment and the system, because as soon as an environmental particle enters the experimental box it will immediately feel the, for example, Coulomb potential, which has an infinite range of influence. Anyway, the reasons behind the evident failure of the Born-Markov master equation and the Scattering Model in the application to the long range interactions is a topic that still needs a more complete and detailed discussion, which represents one of the possible future questions and developments started by this thesis.

More in general, this work has shown how important is to keep track of the electromagnetic sources of decoherence in a QGEM experiment. In fact, the weakest interaction analyzed (i.e. dipole-dipole with $V(r) \sim \frac{1}{r^3}$) has already given a strong constraint on the maximum possible electric dipole possessed by the nano-crystal, as we just discussed above. This implies that the remaining two interactions, namely Coulomb interaction with $V(r) \sim \frac{1}{r}$ and ion-dipole interaction with $V(r) \sim \frac{1}{r^2}$, which are stronger than the first interaction, may also impose significant constraints on the electromagnetic parameters of the QGEM proposal. That is why it is important to find a model that works for decoherence rate induced by long range interactions.

Finally, in the very last section 3.5 we have analyzed the possible influences that different EM sources (such as charge and dipole) can have on the QGEM experiment in the **Third Step** of the proposal. In particular, we have shown how the decoherence rate induced by the emission of radiations of an accelerating charged nano-crystal will be negligible for the realization of the experiment, given that $\Gamma_{acc}^{charge} \sim 10^{-30}$ Hz. Moreover, if the nano-crystal possesses a dipole moment instead of an electric charge, it has been shown that the radiation emitted in this case should be null (see Eq.(3.160)): therefore, in this step of the proposal, an electric dipole should not represent a problem for the realization of the experiment.

To summarize, the QGEM experiment represents a pioneering and highly promising proposal aimed at unraveling the nature of Quantum Gravity. Through its studies and consequences, we aim to tackle the fundamental question of whether gravity can be described within a quantum framework. By probing the quantum behavior of gravity and exploring various quantum theories of gravity that accurately depict reality, we embark on an unprecedented exploration of the fundamental principles that govern our universe. The QGEM experiment revolutionizes our understanding of Quantum Gravity, giving us crucial insights into how gravity behaves at the smallest scales. It opens up the way for exciting breakthroughs in our knowledge of the fundamental laws of nature.

Appendix A

Appendix

In this appendix we are going to show the details of some QED calculations. In particular, we are going to find the expression for the matrix element $|\mathcal{M}|^2$ of the ion-crystal interaction (which is completely analogue to the electron-proton scattering, i.e. the Rutherford's scattering) and its relation with the differential cross section.

A.1 Differential cross section for a $2 \rightarrow 2$ process

Let us start from the definition of cross section:

$$d\sigma = \frac{1}{T\Phi} dP, \quad (\text{A.1})$$

where T is the total time during which interactions happen, Φ is the flux of particles (e.g. if we are in the LAB frame then Φ is the flux of the incoming projectile particles) and dP is the (quantum) probability that one interaction happens.

If we consider the COM frame, the flux Φ will be given by:

$$\Phi = \frac{|\vec{v}_1 - \vec{v}_2|}{V}, \quad (\text{A.2})$$

where \vec{v}_1 and \vec{v}_2 are the velocities of the two initial particles; the minus sign is because they run into each other during the collision.

Let us now compute dP . During scattering processes, the operator involved is the Scattering matrix \hat{S} and its matrix elements give us the transition probability from an initial state $|i\rangle$ to a final one $|f\rangle$:

$$dP = \frac{|\langle f | \hat{S} | i \rangle|^2}{\langle i | \langle f |} \prod_j \frac{V}{(2\pi)^3} d^3 p_j. \quad (\text{A.3})$$

This formula represents the probability of the interaction inside an infinitesimal volume of the momentum space $d\Pi = \prod_j \frac{V}{(2\pi)^3} d^3p_j$, where j represents the number of final states.

Because in QFT we have $|p\rangle = \sqrt{2E_p} \hat{a}_p^\dagger |0\rangle$, the inner products in the denominator of (A.3) gives:

$$\langle i \rangle = \prod_i (2\pi)^3 2E_i \delta^{(3)}(0). \quad (\text{A.4})$$

In a finite volume, we have:

$$(2\pi)^3 \delta^{(3)}(\vec{p} = 0) = \int_V d^3x e^{i\vec{p}\cdot\vec{x}} = \int_V d^3x = V. \quad (\text{A.5})$$

Similarly in 4D:

$$\delta^{(4)}(0) = \frac{TV}{(2\pi)^4}. \quad (\text{A.6})$$

This means that:

$$\begin{cases} \langle i \rangle = (2E_1 V)(2E_2 V) \\ \langle f \rangle = \prod_j 2E_j V \end{cases}. \quad (\text{A.7})$$

Now, the transferred matrix \mathcal{T} is related to S through:

$$S = \mathbf{1} + i\mathcal{T} = \mathbf{1} + i(2\pi)^4 \delta^{(4)}(\Sigma p) \mathcal{M}. \quad (\text{A.8})$$

Thus the non-trivial part of the \hat{S} matrix element is:

$$|\langle f | \hat{S} | i \rangle|^2 = \delta^{(4)}(0) \delta^{(4)}(\Sigma p) (2\pi)^8 |\langle f | \mathcal{M} | i \rangle|^2 = TV \delta^{(4)}(\Sigma p) (2\pi)^4 |\mathcal{M}|^2. \quad (\text{A.9})$$

Plugging everything back in (A.3), we obtain:

$$dP = \frac{T}{V} \frac{1}{2E_1 2E_2} |\mathcal{M}|^2 \prod_j \frac{d^3p_j}{(2\pi)^3 2E_j} (2\pi)^4 \delta^{(4)}(\Sigma p). \quad (\text{A.10})$$

Finally, we have an expression for the cross section in the COM:

$$d\sigma = \frac{1}{2E_1 2E_2 |\vec{v}_1 - \vec{v}_2|} |\mathcal{M}|^2 d\Pi_{lips}, \quad (\text{A.11})$$

where $d\Pi_{lips} = \prod_j \frac{d^3p_j}{(2\pi)^3 2E_j} (2\pi)^4 \delta^{(4)}(\Sigma p)$.

In the special case where we have 2 final states, such that $\vec{p}_1 = -\vec{p}_2$, $\vec{p}_3 = -\vec{p}_4$ and $E_1 + E_1 = E_3 + E_4 = E_{CM}$, $d\Pi_{lips}$ becomes:

$$d\Pi_{lips} = \frac{d^3 p_3}{(2\pi)^3 2E_3} \frac{d^3 p_4}{(2\pi)^3 2E_4} (2\pi)^4 \delta^{(4)}(\Sigma p). \quad (\text{A.12})$$

Integrating over \vec{p}_4 we obtain:

$$d\Pi_{lips} = \frac{1}{16\pi^2} d\Omega \int dp_f \frac{p_f^2}{E_3 E_4} \delta(E_3 + E_4 - E_{CM}) = \frac{1}{16\pi^2} d\Omega \frac{p_f}{E_{CM}} \theta(E_{CM} - m_3 - m_4), \quad (\text{A.13})$$

where $p_f = |\vec{p}_3| = |\vec{p}_4|$ and $p_i = |\vec{p}_1| = |\vec{p}_2|$.

We can now rewrite $|\vec{v}_1 - \vec{v}_2|$ as:

$$\left| \frac{p_i}{E_1} + \frac{p_i}{E_2} \right| = p_i \frac{E_{CM}}{E_1 E_2}, \quad (\text{A.14})$$

in order to obtain the final expression for the differential cross section:

$$\frac{d\sigma}{d\Omega} = \frac{1}{64\pi^2 E_{CM}^2} \frac{p_f}{p_i} |\mathcal{M}|^2 \theta(E_{CM} - m_3 - m_4). \quad (\text{A.15})$$

Applying (A.15) in the case where the target is much heavier than the projectile ($M \gg m$), we can write $nE_{CM} \simeq M^2$ and also $p_i = p_f$. In this way, considering the case where $E_{CM} > m_3 + m_4$, we obtain the final expression for the differential cross section:

$$\frac{d\sigma}{d\Omega} = \frac{1}{64\pi^2 E_{CM}^2} |\mathcal{M}|^2. \quad (\text{A.16})$$

A.2 Number density factor

In this Appendix, we will give meaning to the factor $\pi^{-3/2} \tilde{\sigma}^3$. In particular, let us see the connection between $\tilde{\sigma}$ and the uncertainty in space along one direction $\sigma_x = \sqrt{\langle x^2 \rangle_\psi - \langle x \rangle_\psi^2}$ (i.e. along x), with $\psi(x)$ being the wave-function in physical space. From (3.22), we can see that:

$$\begin{aligned} \psi(x) &= \int_{-\infty}^{+\infty} dp_x e^{-ip_x x} \tilde{\psi}_{p_x}(p) \\ &= \int_{-\infty}^{+\infty} dp_x e^{-ip_x x} \frac{(2\pi)^{1/2}}{(\pi \tilde{\sigma}^2)^{1/4}} e^{-\frac{p_x^2}{2\tilde{\sigma}^2}} \\ &= 2\pi^{3/4} \tilde{\sigma}^{1/2} e^{-\frac{\tilde{\sigma}^2}{2} x^2}. \end{aligned} \quad (\text{A.17})$$

Now we can compute σ_x :

$$\begin{aligned}
\sigma_x &= \sqrt{\langle x^2 \rangle_\psi - \langle x \rangle_\psi^2} \\
&= \int_{-\infty}^{+\infty} dx x^2 |\psi(x)|^2 = \frac{\sqrt{2}\pi}{\tilde{\sigma}}.
\end{aligned} \tag{A.18}$$

But we know also that the uncertainty in space is physically due to the fact that the environmental particles, as all the other particles involved in the experiment, are confined in a volume $V = L^3$. This means that:

$$V = L^3 = \sigma_x^3 = \frac{2^{3/2}\pi^3}{\tilde{\sigma}^3}, \tag{A.19}$$

which leads finally to:

$$\pi^{-3/2}\tilde{\sigma}^3 = \frac{(2\pi)^{3/2}}{V}. \tag{A.20}$$

A.3 Validity for the approximation of the $Ci(z)$ function

The main goal of this appendix is to show the validity of the approximation made in section 3.3 for the Fourier transformation of the dipole-dipole potential $\tilde{V}(q)$ given by Eq.(3.51). In particular, we are going to verify this assumption by computing *numerically* the integral for the total cross section $\sigma_{CM} = \int d\Omega' \frac{d\sigma}{d\Omega'}$ and comparing the resulting decoherence rate Γ_S with the one found in Eq.(3.64).

Let us start by considering the *complete* Fourier transformation $\tilde{V}(q)$:

$$\tilde{V}(q) = -\frac{4\hbar d_1 d_2}{\epsilon_0 q} \left(\frac{\sin\left(\frac{q}{\hbar}R\right)}{R} - \frac{q}{\hbar} Ci\left(\frac{q}{\hbar}R\right) \right). \tag{A.21}$$

In this way, using the Born approximation formula, the differential cross section will be:

$$\frac{d\sigma}{d\Omega'} = \frac{4m^2 d_1^2 d_2^2}{\pi^2 \epsilon_0^2 \hbar^2 q^2} \left[\frac{\sin\left(\frac{q}{\hbar}R\right)}{R} - \frac{q}{\hbar} Ci\left(\frac{q}{\hbar}R\right) \right]^2, \tag{A.22}$$

which integrated gives the total cross section σ_{CM} :

$$\begin{aligned}
\sigma_{CM} &= \int d\Omega' \frac{d\sigma}{d\Omega'} = \int d\Omega' \frac{4m^2 d_1^2 d_2^2}{\pi^2 \epsilon_0^2 \hbar^2 q^2} \left[\frac{\sin\left(\frac{q}{\hbar} R\right)}{R} - \frac{q}{\hbar} Ci\left(\frac{q}{\hbar} R\right) \right]^2 \\
&= \alpha \int d\Omega' \frac{1}{(2p_0 \sin(\theta'/2))^2} \left[\frac{\sin\left(\frac{2p_0 \sin(\theta'/2)}{\hbar} R\right)}{R} - \frac{2p_0 \sin(\theta'/2)}{\hbar} Ci\left(\frac{2p_0 \sin(\theta'/2)}{\hbar} R\right) \right]^2 \\
&= 2\pi\alpha \int_{-1}^1 d(\cos(\theta')) \frac{1}{4p_0^2 \sin^2(\theta'/2)} \left[\frac{\sin\left(2\frac{p_0}{\hbar} \sin(\theta'/2) R\right)}{R} - 2\frac{p_0}{\hbar} \sin(\theta'/2) Ci\left(2\frac{p_0}{\hbar} \sin(\theta'/2) R\right) \right]^2 \\
&= \frac{2\pi\alpha}{4p_0^2} \int_0^1 dx \, 4x \frac{1}{x^2} \left[\frac{\sin(ax)}{R} - \frac{a}{R} x Ci(ax) \right]^2 \\
&= \frac{2\pi\alpha}{p_0^2 R^2} \int_0^1 dx \frac{[\sin(ax) - ax Ci(ax)]^2}{x},
\end{aligned} \tag{A.23}$$

where we have defined $\alpha \equiv \frac{4m^2 d_1^2 d_2^2}{\pi^2 \epsilon_0^2 \hbar^2}$, $a \equiv 2\frac{p_0}{\hbar} R$ and performed the change of variable inside the integral already defined in Eq.(3.57) (see subsection 3.3.1).

Now, the integral appearing in the very last equality of Eq.(A.23) it is very hard to solve analytically, but nonetheless it is possible to solve it numerically. In particular, if we consider the density distribution for the environmental particles to be $S(p_0) = \delta(p_0 - \bar{p})$ (as already discussed below Eq.(3.63)), with $\bar{p} = \sqrt{2mk_B T} \sim 10^{-25} \text{kg} \frac{\text{m}}{\text{s}}$ being the average momentum, we can associate a numerical value to a , i.e. $a \equiv 2\frac{p_0}{\hbar} R \sim 10^{31}$.

In this way, we have that $\int_0^1 dx \frac{[\sin(ax) - ax Ci(ax)]^2}{x} \simeq 0.7$ and the total cross section can be written as:

$$\sigma_{CM} \simeq 1.4 \times \frac{\pi\alpha}{p_0^2 R^2} \sim 5.6 \times \frac{m^2 d_1^2 d_2^2}{\pi \epsilon_0^2 \hbar^2 R^2 p_0^2}, \tag{A.24}$$

where we have used $\alpha \equiv \frac{4m^2 d_1^2 d_2^2}{\pi^2 \epsilon_0^2 \hbar^2}$.

It is worth notice that this expression for σ_{CM} does *not* contain the correct momentum dependence $\sigma_{CM}(p_0)$, because also the integral $\int_0^1 dx \frac{[\sin(ax) - ax Ci(ax)]^2}{x}$ depends on p_0 through the parameter a . We have left the explicit p_0 dependence outside the integral in

¹Remember that R is considered to be $R \sim 10^{-6} \text{m}$.

order to compare the total cross section given by Eq.(A.24) with the one given in section 3.3.1 by Eq.(3.62). In particular, the only difference between this two expressions for σ_{CM} lies in the factor 5.6 in the numerator of Eq.(A.24) and the factor $4 \ln \left(4 \frac{p_0}{\hbar} R\right)$ in the numerator of Eq.(3.62). Numerically, we have that $4 \ln \left(4 \frac{p_0}{\hbar} R\right) \sim 33$, which is only ~ 6 times bigger with respect to the term appearing in Eq.(A.24).

Now, because, $\Gamma_S \propto \sigma_{CM}$, the approximation made in section 3.3 will give a numerical value for the decoherence rate only ~ 6 times bigger than the non-approximated value, which does *not* influence the order of magnitude for Γ_S . Therefore, we have just proven the validity of such an approximation.

Bibliography

- [1] A. Einstein, “The foundation of the general theory of relativity,” 1916.
- [2] P. A. M. Dirac, *The principles of quantum mechanics*. Oxford, 4 ed., 1930.
- [3] E. Schrodinger, “Die gegenwartige Situation in der Quantenmechanik,” *Naturwiss.*, vol. 23, pp. 807–812, 1935.
- [4] C. Rovelli, *Quantum Gravity*. Cambridge Monographs on Mathematical Physics, Cambridge University Press, 2004.
- [5] M. D. Schwartz, *Quantum Field Theory and the Standard Model*. Cambridge University Press, 3 2014.
- [6] A. Einstein, B. Podolsky, and N. Rosen, “Can quantum-mechanical description of physical reality be considered complete?,” *Phys. Rev.*, vol. 47, pp. 777–780, May 1935.
- [7] M. F. Pusey, J. Barrett, and T. Rudolph, “On the reality of the quantum state,” *Nature Physics*, vol. 8, pp. 475–478, may 2012.
- [8] N. Birrell and P. Davies, *Quantum Fields in Curved Space*. Cambridge Monographs on Mathematical Physics, Cambridge University Press, 1984.
- [9] S. Hawking and R. Penrose, *The Nature of Space and Time*. Isaac Newton Institute series of lectures, Princeton University Press, 2000.
- [10] V. A. Rubakov and D. S. Gorbunov, *Introduction to the Theory of the Early Universe: Hot big bang theory*. Singapore: World Scientific, 2017.
- [11] J. Polchinski, *String Theory*. String Theory 2 Volume Hardback Set, Cambridge University Press, 2001.
- [12] G. Brightwell and M. Luczak, “The mathematics of causal sets,” 2015.
- [13] E. P. Verlinde, “Emergent gravity and the dark universe,” *SciPost Physics*, vol. 2, may 2017.

- [14] S. Bose, A. Mazumdar, G. W. Morley, H. Ulbricht, M. Toroš, M. Paternostro, A. Geraci, P. Barker, M. S. Kim, and G. Milburn, “Spin Entanglement Witness for Quantum Gravity,” *Phys. Rev. Lett.*, vol. 119, no. 24, p. 240401, 2017.
- [15] C. Marletto and V. Vedral, “Gravitationally-induced entanglement between two massive particles is sufficient evidence of quantum effects in gravity,” *Phys. Rev. Lett.*, vol. 119, no. 24, p. 240402, 2017.
- [16] M. Christodoulou *et al.*, “Locally mediated entanglement through gravity from first principles,” 2022.
- [17] M. Christodoulou, A. D. Biagio, R. Howl, and C. Rovelli, “Gravity entanglement, quantum reference systems, degrees of freedom,” *Classical and Quantum Gravity*, vol. 40, p. 047001, jan 2023.
- [18] M. Schlosshauer, “The quantum-to-classical transition and decoherence,” 4 2014.
- [19] E. Joos, *Decoherence and the Appearance of a Classical World in Quantum Theory*. Physics and astronomy online library, Springer, 2003.
- [20] E. Kilian, M. Toroš, F. F. Deppisch, R. Saakyan, and S. Bose, “Requirements on quantum superpositions of macro-objects for sensing neutrinos,” *Phys. Rev. Res.*, vol. 5, no. 2, p. 023012, 2023.
- [21] G. Afek, F. Monteiro, B. Siegel, J. Wang, S. Dickson, J. Recoaro, M. Watts, and D. C. Moore, “Control and measurement of electric dipole moments in levitated optomechanics,” *Phys. Rev. A*, vol. 104, p. 053512, Nov 2021.
- [22] J. Woodall, M. Agúndez, A. Markwick-Kemper, and T. Millar, “The umist database for astrochemistry 2006,” <http://dx.doi.org/10.1051/0004-6361:20064981>, vol. 466, 05 2007.
- [23] S. Bose, A. Mazumdar, M. Schut, and M. Toroš, “Mechanism for the quantum natured gravitons to entangle masses,” *Phys. Rev. D*, vol. 105, no. 10, p. 106028, 2022.
- [24] P. F. Barker, S. Bose, R. J. Marshman, and A. Mazumdar, “Entanglement based tomography to probe new macroscopic forces,” *Phys. Rev. D*, vol. 106, no. 4, p. L041901, 2022.
- [25] R. Horodecki, P. Horodecki, M. Horodecki, and K. Horodecki, “Quantum entanglement,” *Rev. Mod. Phys.*, vol. 81, pp. 865–942, 2009.
- [26] M.-Z. Wu, M. Toroš, S. Bose, and A. Mazumdar, “Quantum gravitational sensor for space debris,” *Phys. Rev. D*, vol. 107, no. 10, p. 104053, 2023.

- [27] https://www.youtube.com/watch?v=0Fv-0k13s_k, 2016. Accessed 1/11/22.
- [28] R. J. Marshman, A. Mazumdar, and S. Bose, “Locality and entanglement in tabletop testing of the quantum nature of linearized gravity,” *Phys. Rev. A*, vol. 101, no. 5, p. 052110, 2020.
- [29] F. Gunnink, A. Mazumdar, M. Schut, and M. Toroš, “Gravitational decoherence by the apparatus in the quantum-gravity induced entanglement of masses,” 10 2022.
- [30] S. G. Elahi and A. Mazumdar, “Probing massless and massive gravitons via entanglement in a warped extra dimension,” 3 2023.
- [31] U. K. B. Vinckers, A. de la Cruz-Dombriz, and A. Mazumdar, “Quantum entanglement of masses with non-local gravitational interaction,” 3 2023.
- [32] D. Carney, P. C. E. Stamp, and J. M. Taylor, “Tabletop experiments for quantum gravity: a user’s manual,” *Class. Quant. Grav.*, vol. 36, p. 034001, 2019.
- [33] A. Belenchia *et al.*, “Quantum Superposition of Massive Objects and the Quantization of Gravity,” *Phys. Rev. D*, vol. 98, p. 126009, 2018.
- [34] D. Carney, “Newton, entanglement, and the graviton,” *Phys. Rev. D*, vol. 105, no. 2, p. 024029, 2022.
- [35] D. L. Danielson, G. Satishchandran, and R. M. Wald, “Gravitationally mediated entanglement: Newtonian field versus gravitons,” *Phys. Rev. D*, vol. 105, p. 086001, 2022.
- [36] C. H. Bennett, D. P. DiVincenzo, J. A. Smolin, and W. K. Wootters, “Mixed state entanglement and quantum error correction,” *Phys. Rev. A*, vol. 54, pp. 3824–3851, 1996.
- [37] D. Biswas, S. Bose, A. Mazumdar, and M. Toroš, “Gravitational Optomechanics: Photon-Matter Entanglement via Graviton Exchange,” 9 2022.
- [38] T. W. van de Kamp, R. J. Marshman, S. Bose, and A. Mazumdar, “Quantum Gravity Witness via Entanglement of Masses: Casimir Screening,” *Phys. Rev. A*, vol. 102, no. 6, p. 062807, 2020.
- [39] M. Scala, M. S. Kim, G. W. Morley, P. F. Barker, and S. Bose, “Matter-wave interferometry of a levitated thermal nano-oscillator induced and probed by a spin,” *Phys. Rev. Lett.*, vol. 111, p. 180403, Oct 2013.

- [40] C. Wan, M. Scala, G. W. Morley, A. A. Rahman, H. Ulbricht, J. Bateman, P. F. Barker, S. Bose, and M. S. Kim, “Free nano-object ramsey interferometry for large quantum superpositions,” *Phys. Rev. Lett.*, vol. 117, p. 143003, Sep 2016.
- [41] Y. Margalit *et al.*, “Realization of a complete Stern-Gerlach interferometer: Towards a test of quantum gravity,” 11 2020.
- [42] R. J. Marshman, A. Mazumdar, R. Folman, and S. Bose, “Constructing nano-object quantum superpositions with a Stern-Gerlach interferometer,” *Phys. Rev. Res.*, vol. 4, no. 2, p. 023087, 2022.
- [43] S. Machluf, Y. Japha, and R. Folman, “Coherent stern–gerlach momentum splitting on an atom chip,” *Nature Communications*, vol. 4, p. 2424, 09 2013.
- [44] O. Amit, Y. Margalit, O. Dobkowski, Z. Zhou, Y. Japha, M. Zimmermann, M. A. Efremov, F. A. Narducci, E. M. Rasel, W. P. Schleich, and R. Folman, “ T^3 stern-gerlach matter-wave interferometer,” *Phys. Rev. Lett.*, vol. 123, p. 083601, Aug 2019.
- [45] J. S. Pedernales, G. W. Morley, and M. B. Plenio, “Motional dynamical decoupling for interferometry with macroscopic particles,” *Phys. Rev. Lett.*, vol. 125, p. 023602, Jul 2020.
- [46] Y. Margalit, Z. Zhou, O. Dobkowski, Y. Japha, D. Rohrlich, S. Moukouri, and R. Folman, “Realization of a complete stern-gerlach interferometer,” *arXiv preprint arXiv:1801.02708*, 2018.
- [47] R. Zhou, R. J. Marshman, S. Bose, and A. Mazumdar, “Catapulting towards massive and large spatial quantum superposition,” *Phys. Rev. Res.*, vol. 4, no. 4, p. 043157, 2022.
- [48] R. Zhou, R. J. Marshman, S. Bose, and A. Mazumdar, “Mass-independent scheme for enhancing spatial quantum superpositions,” *Phys. Rev. A*, vol. 107, no. 3, p. 032212, 2023.
- [49] R. Zhou, R. J. Marshman, S. Bose, and A. Mazumdar, “Gravito-diamagnetic forces for mass independent large spatial quantum superpositions,” 11 2022.
- [50] R. J. Marshman, S. Bose, A. Geraci, and A. Mazumdar, “Entanglement of Magnetically Levitated Massive Schrödinger Cat States by Induced Dipole Interaction,” 4 2023.
- [51] M. Schut, J. Tilly, R. J. Marshman, S. Bose, and A. Mazumdar, “Improving resilience of quantum-gravity-induced entanglement of masses to decoherence using three superpositions,” *Phys. Rev. A*, vol. 105, no. 3, p. 032411, 2022.

- [52] J. Tilly, R. J. Marshman, A. Mazumdar, and S. Bose, “Qudits for witnessing quantum-gravity-induced entanglement of masses under decoherence,” *Phys. Rev. A*, vol. 104, no. 5, p. 052416, 2021.
- [53] S. Rijavec, M. Carlesso, A. Bassi, V. Vedral, and C. Marletto, “Decoherence effects in non-classicality tests of gravity,” *New J. Phys.*, vol. 23, no. 4, p. 043040, 2021.
- [54] O. Romero-Isart, A. C. Pflanzer, F. Blaser, R. Kaltenbaek, N. Kiesel, M. Aspelmeyer, and J. I. Cirac, “Large quantum superpositions and interference of massive nanometer-sized objects,” *Physical review letters*, vol. 107 2, p. 020405, 2011.
- [55] D. E. Chang, C. A. Regal, S. B. Papp, D. J. Wilson, J. Ye, O. Painter, H. J. Kimble, and P. Zoller, “Cavity opto-mechanics using an optically levitated nanosphere,” *Proceedings of the National Academy of Sciences*, vol. 107, pp. 1005–1010, dec 2009.
- [56] A. Bassi, K. Lochan, S. Satin, T. P. Singh, and H. Ulbricht, “Models of wave-function collapse, underlying theories, and experimental tests,” *Reviews of Modern Physics*, vol. 85, no. 2, p. 471, 2013.
- [57] M. Toroš, A. Mazumdar, and S. Bose, “Loss of coherence of matter-wave interferometer from fluctuating graviton bath,” 8 2020.
- [58] M. Toroš, T. W. Van De Kamp, R. J. Marshman, M. S. Kim, A. Mazumdar, and S. Bose, “Relative acceleration noise mitigation for nanocrystal matter-wave interferometry: Applications to entangling masses via quantum gravity,” *Phys. Rev. Res.*, vol. 3, no. 2, p. 023178, 2021.
- [59] H. B. G. Casimir and D. Polder, “The Influence of retardation on the London-van der Waals forces,” *Phys. Rev.*, vol. 73, pp. 360–372, 1948.
- [60] H. B. G. Casimir, “On the Attraction Between Two Perfectly Conducting Plates,” *Indag. Math.*, vol. 10, pp. 261–263, 1948.
- [61] J. D. Jackson, *Classical electrodynamics*. New York, NY: Wiley, 3rd ed. ed., 1999.
- [62] R. Newton, *Scattering Theory of Waves and Particles*. International series in pure and applied physics, McGraw-Hill, 1966.
- [63] M. Abdulsattar, “Electronic and structural properties of nitrogen-vacancy center in diamond nanocrystals: A theoretical study,” *Karbala International Journal of Modern Science*, vol. 1, 10 2015.

- [64] E. Wang, J. Xiao, and H. Zhang, “Bremsstrahlung radiation as a coherent state in thermal QED,” *Journal of Physics G: Nuclear and Particle Physics*, vol. 27, pp. 2379–2387, nov 2001.
- [65] A. L. Fetter and J. D. Walecka, *Quantum Theory of Many-Particle Systems*. Boston: McGraw-Hill, 1971.
- [66] G. Afek, F. Monteiro, B. Siegel, J. Wang, S. Dickson, J. Recoaro, M. Watts, and D. C. Moore, “Control and measurement of electric dipole moments in levitated optomechanics,” *Phys. Rev. A*, vol. 104, no. 5, p. 053512, 2021.
- [67] B. Hensen *et al.*, “Loophole-free Bell inequality violation using electron spins separated by 1.3 kilometres,” *Nature*, vol. 526, pp. 682–686, 2015.
- [68] A. Großardt, “Acceleration noise constraints on gravity induced entanglement,” *Phys. Rev. A*, vol. 102, no. 4, p. 040202, 2020.
- [69] K. Sinha and P. W. Milonni, “Dipoles in blackbody radiation: momentum fluctuations, decoherence, and drag force,” *J. Phys. B*, vol. 55, no. 20, p. 204002, 2022.
- [70] A. Peres, “Finite violation of a bell inequality for arbitrarily large spin,” *Phys. Rev. A*, vol. 46, pp. 4413–4414, Oct 1992.
- [71] N. Gisin and A. Peres, “Maximal violation of bell’s inequality for arbitrarily large spin,” *Physics Letters A*, vol. 162, no. 1, pp. 15–17, 1992.
- [72] O. Romero-Isart, “Quantum superposition of massive objects and collapse models,” *Physical Review A*, vol. 84, nov 2011.
- [73] O. Amit, Y. Margalit, O. Dobkowski, Z. Zhou, Y. Japha, M. Zimmermann, M. A. Efremov, F. A. Narducci, E. M. Rasel, W. P. Schleich, and R. Folman, “ T^3 stern-gerlach matter-wave interferometer,” *Phys. Rev. Lett.*, vol. 123, p. 083601, Aug 2019.
- [74] S. Machluf, Y. Japha, and R. Folman, “Coherent stern-gerlach momentum splitting on an atom chip,” *Nature communications*, vol. 4, p. 2424, 09 2013.
- [75] H. Chevalier, A. J. Paige, and M. S. Kim, “Witnessing the nonclassical nature of gravity in the presence of unknown interactions,” *Phys. Rev. A*, vol. 102, no. 2, p. 022428, 2020.
- [76] H. C. Nguyen and F. Bernards, “Entanglement dynamics of two mesoscopic objects with gravitational interaction,” *The European Physical Journal D*, vol. 74, pp. 1–5, 6 2020.

- [77] J. F. Barry, J. M. Schloss, E. Bauch, M. J. Turner, C. A. Hart, L. M. Pham, and R. L. Walsworth, “Sensitivity Optimization for NV-Diamond Magnetometry,” *Rev. Mod. Phys.*, vol. 92, no. 1, p. 015004, 2020.
- [78] A. Gali, “\emph {Ab initio} theory of nitrogen-vacancy center in diamond,” *arXiv preprint arXiv:1906.00047*, 2019.
- [79] P. Griffiths and J. Harris, *Principles of algebraic geometry*. John Wiley & Sons, 2014.
- [80] L. H. Ford, “Casimir force between a dielectric sphere and a wall: A model for amplification of vacuum fluctuations,” *Phys. Rev. A*, vol. 58, pp. 4279–4286, Dec 1998.
- [81] H. Ye, H. Yan, and R. B. Jackman, “Dielectric properties of single crystal diamond,” *Semiconductor science and technology*, vol. 20, no. 3, p. 296, 2005.
- [82] J.-M. L. Floch, R. Bara, J. G. Hartnett, M. E. Tobar, D. Mouneyrac, D. Passerieux, D. Cros, J. Krupka, P. Goy, and S. Caroopen, “Electromagnetic properties of polycrystalline diamond from 35 k to room temperature and microwave to terahertz frequencies,” *Journal of Applied Physics*, vol. 109, no. 9, p. 094103, 2011.
- [83] T. Biswas, E. Gerwick, T. Koivisto, and A. Mazumdar, “Towards singularity and ghost free theories of gravity,” *Phys. Rev. Lett.*, vol. 108, p. 031101, 2012.
- [84] T. Biswas, A. Mazumdar, and W. Siegel, “Bouncing universes in string-inspired gravity,” *JCAP*, vol. 03, p. 009, 2006.
- [85] S. Abel, L. Buoninfante, and A. Mazumdar, “Nonlocal gravity with worldline inversion symmetry,” *JHEP*, vol. 01, p. 003, 2020.
- [86] E. Witten, “Noncommutative Geometry and String Field Theory,” *Nucl. Phys. B*, vol. 268, pp. 253–294, 1986.
- [87] A. Ibarra, M. Gonzalez, R. Vila, and J. Molla, “Wide frequency dielectric properties of cvd diamond,” *Diamond and Related Materials*, vol. 6, no. 5-7, pp. 856–859, 1997.
- [88] A. D. Rider, D. C. Moore, C. P. Blakemore, M. Louis, M. Lu, and G. Gratta, “Search for Screened Interactions Associated with Dark Energy Below the 100 μm Length Scale,” *Phys. Rev. Lett.*, vol. 117, no. 10, p. 101101, 2016.
- [89] C. Subramaniam, T. Yamada, K. Kobashi, A. Sekiguchi, D. N. Futaba, M. Yumura, and K. Hata, “One hundred fold increase in current carrying capacity in a carbon nanotube–copper composite,” *Nature communications*, vol. 4, no. 1, p. 2202, 2013.

- [90] R. J. Marshman, A. Mazumdar, G. W. Morley, P. F. Barker, S. Hoekstra, and S. Bose, “Mesoscopic Interference for Metric and Curvature (MIMAC) & Gravitational Wave Detection,” *New J. Phys.*, vol. 22, no. 8, p. 083012, 2020.
- [91] A. F. . P. Association and A. W. Council, *Beam Design Formulas with Shear and Moment Diagrams: Design Aid No. 6*. American Forest & Paper Association, Incorporated, 2007.
- [92] J.-F. Hsu, P. Ji, C. W. Lewandowski, and B. D’Urso, “Cooling the motion of diamond nanocrystals in a magneto-gravitational trap in high vacuum,” *Scientific reports*, vol. 6, no. 1, p. 30125, 2016.
- [93] P. Hyllus, O. Gühne, D. Bruß, and M. Lewenstein, “Relations between entanglement witnesses and bell inequalities,” *Phys. Rev. A*, vol. 72, p. 012321, Jul 2005.
- [94] M. Schlosshauer, “Quantum Decoherence,” *Phys. Rept.*, vol. 831, pp. 1–57, 2019.
- [95] D. J. Griffiths, “Introduction to electrodynamics,” 2005.
- [96] R. Feynman, R. Leighton, and M. Sands, “Feynman lectures on physics. vol. 2: Mainly electromagnetism and matter, 592 pp,” 1963.
- [97] A. T. Pérez and R. Fernández-Mateo, “Electric force between a dielectric sphere and a dielectric plane,” *Journal of Electrostatics*, vol. 112, p. 103601, 2021.
- [98] H. Wyld, *Mathematical Methods For Physics*. CRC Press, 1999.
- [99] J. A. Stratton, *Electromagnetic theory*, vol. 33. John Wiley & Sons, 2007.
- [100] Y. Margalit, O. Dobkowski, Z. Zhou, O. Amit, Y. Japha, S. Moukouri, D. Rohrlich, A. Mazumdar, S. Bose, C. Henkel, and R. Folman, “Realization of a complete stern-gerlach interferometer: Toward a test of quantum gravity,” *Science Advances*, vol. 7, no. 22, p. eabg2879, 2021.
- [101] T. D. Galley, F. Giacomini, and J. H. Selby, “A no-go theorem on the nature of the gravitational field beyond quantum theory,” *Quantum*, vol. 6, p. 779, aug 2022.